Proceedings of 3nd Agria Conference on Innovative Pneumatic Vehicles – ACIPV 2019

May 09, 2019 Eger, Hungary

EMERSON

Proceedings

of the

3th Agria Conference on Innovative Pneumatic Vehicles – ACIPV 2019

May 09, 2019
Eger, Hungary

Edited by
László Pokorádi

Published by
Óbuda University, Institute of Mechatronics and Vehicle Engineering

ISBN 978-963-449-149-1

Technical Sponsor:
Aventics Hungary Kft.

Organizer:
Óbuda University, Institute of Mechatronics and Vehicle Engineering

Honorary Chairs:
László Palkovics, BUTE, Budapest
Mihály Réger, Óbuda University, Budapest

Honorary Committee:
I. Gödri, Aventics Hungary Kft., Eger
Z. Rajnai, Óbuda University, Budapest

Conference Founding Chair:
L. Pokorádi, Óbuda University, Budapest

Scientific Program Committee:
János Bihari, University of Miskolc
Zsolt Farkas, Budapest University of Technology and Economics
Lucian Fechete, Technical University of Cluj-Napoca
Wieslaw Fiebig, Wroclaw University of Science and Technology
Dénes Fodor, University of Pannonia
Zoltán Forgó, Sapientia Hungarian University of Transylvania
György Juhász, University of Debrecen
Gábor Kátai-Urbán, Neumann János Egyetem
László Kelemen, University of Miskolc
Tomáš Kroutil, Brno University of Technology
János Líska, Neumann János Egyetem
Marten Madissoo, Estonian University of Life Sciences
Ghinea Mihai, University POLITEHNICA of Bucharest
Vilnis Pirs, Latvian University of Agriculture
Krzysztof Psiuk, Silesian University of Technology
Mihai Simon, Universitatea Petru Maior
István Péter Szabó, Szegedi Tudományegyetem
Janis Rudzitis, Riga Technical University
Tibor Szabó, Budapest University of Technology and Economics
Pawel Sliwinski, Gdańsk University of Technology
Tibor István Tóth, University of Szeged
Tibor Vesselenyi, University of Oradea

Organizing Committee Chair:
E. Tamás, Aventics Hungary Kft., Eger

Organizing Committee:
Enikő Pekk, Aventics Kft., Eger
Ferenc Bolyki, Aventics Kft., Eger

CONTENTS

Program of ACIPV 2019

Time: May 09. 2019. Thursday.
Locale: Aventics Hungary Kft, 3300 Eger, Bánki Donát u. 3.

13:00-13:15 Transfer by bus from the Érsekkert (Sports hall) to Aventics,
13:15-13:45 buffet lunch.

Plenary Section	
Room Bánki Donát	
Chair: Pokorádi, László	
13:45	Gödri, István Opening speech Director Operations, Managing Director at AVENTICS Hungary Kft.
13:50	Gerecke, Wolf Director Strategic Product Management at Aventics GmbH FROM INNOVATIVE PRODUCTS TO AN INNOVATIVE COMPANY
14:05	Kolonicsné Szlávik, Tímea Plant Manager at Emerson Process Management Hungary Ltd. WOMEN IN STEM AT EMERSON

14: 20-14: 30 Pause

	Section A	**Section B**
	Room Bánki Donát	Room John von Neumann
	Chair: Dr. Szakács, Tamás	Chair: Dr. Szabó, József Zoltán
14:30	László Pokorádi, Tamás Szakács *GRAPH MODELLING OF PNEUMATIC VEHICLE CONTROL SYSTEM*	Pintér, Péter *AUTONOMUS SOLUTIONS FOR A PNEUMOBILE*
14:45	Juhász, György etal. *PNEUMOBILE TELEMETRY SYSTEM WITH NI DEVICES AND EVALUATION OF MEASURED DATA*	Demeter, László; Forgó, Zoltán *ADAPTIVE PNEUMATIC SUSPENSION USING LINEAR QUADRATIC CONTROL*
15:00	Szakács, Tamás *MODELLING AND VALIDATION OF A PNEUMOBIL*	Przemysław Kałucki et.al: *OPTIMISATION OF THE COMPRESSED AIR DRIVE SYSTEM*
15:15	Tóth, István Tibor *DRIVE ALTERNATIVES. IS THE FUTURE SURELY IN THE ELECTRIC DRIVE?*	Madissoo, Marten et.al.: *OPTIMIZED 3D PRINTED PNEUMATIC CYLINDER END CAPS*

Poster section:

Farmos, Rudolf; Forgó, Zoltán DETERMINATION OF THECOEFFICIENT OFFRICTION OF PNEUMATIC SYSTEMS	Szabó, István Péter; Horváth, Gábor *DESIGNING A SUSPENSION OF THE AIRRARI PNEUMOBILE*

16:00-17: 00 Plant tour
17:10-17: 30 Transfer by bus to the Érsekkert (Sports hall)
18:00-18: 30 Technical opening – Érsekkert (Sports hall)

Optimisation of the compressed air drive system

Przemysław KAŁUCKI*, Michał SOBOTA, Krzysztof PSIUK***, Sebastian RZYDZIK*****

**Silesian University of Technology, Gliwice, 44-100,*
(phone:+48 722 317 367, kalucki.przemyslaw@gmail.com).
*** Silesian University of Technology, Gliwice, 44-100*
(e-mail: michal.sobota.pl@gmail.com)
**** Silesian University of Technology, Gliwice, 44-100*
(e-mail: krzysztof.psiuk@polsl.pl, sebastian.rzydzik@polsl.p)

Abstract: This document shows the optimization process of the compressed air drive system. Drive system has been designed to drive a vehicle, which takes part in Aventics Pneumobil competition. The main part of the project was to compare the performance of the best variants in terms of maximum speed, acceleration and air consumption. It was simulated to run in a qualifying race in which the travel time, average speed and used air were compared. Mechanical resistance, rolling resistance, air resistance, moment of inertia and terrain from the GPS system were taken into simulation. After the analysis, the drive system has been selected. The document shows in a simplified way the design process and presents the basic problems solved in the optimization process. it can be used as an aid in the design and optimization process of similar drive system, but it should also pay attention to the problem of the control system with the pneumatic system, which was not included in this process..

1. INTRODUCTION

The content of the document is based on the diploma project. The authors are members of the students research group of the Silesian University of Technology. Group takes part in the "Aventics Pneumobil competition", where main sponsor is the company Aventics – a leading supplier of pneumatic components. Every year, since 2008, the competition takes place in Hungarian city of Eger. The main goal of competition is to build the vehicle that uses pneumatic components and drives on compressed air. The main objective of the competition is the use of a pneumatic cylinder as the main drive element. This complicates the drive system, because you have to convert linear motion of the actuator to the rotary motion of the wheel.

1.1 Introduction to optimization

Optimization is a process in which we are looking for best solution of problem based on the imposed criteria. Very often, the seemingly best solution does not fulfils all of criteria. The optimization process sought to find solution that would meet the following criteria:

- high efficiency,
- maximum drive torque,
- occupied space,
- air consumption,
- efficiency of performance.

Basic vehicle technical data used in this process:

- length = 2490 mm (< 2500 mm);
- width = 1400 mm (< 1700 mm) ;
- height = 1260 mm (< 1314mm = 90% of the width) ;
- wheel base = 1750 mm;
- track gauge = 1210 mm;
- driver's shoulder level = 750 mm;
- clearance = 60-100 mm on the back (adjustable suspension);
- total mass with driver: 250kg;
- max speed (approximately) = 50km/h;

Fig. 1. Vehicle of team PIKIOT. Rendered picture for Autodesk Inventor.

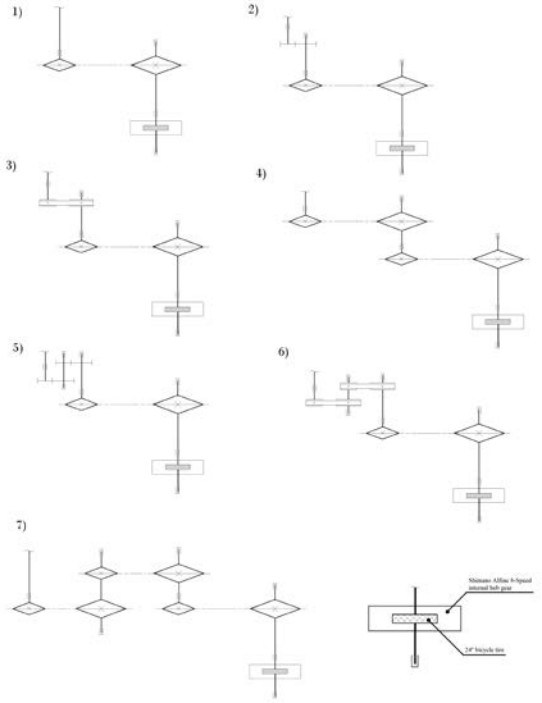

Fig. 2. Subsystem 1 of transmission structure.

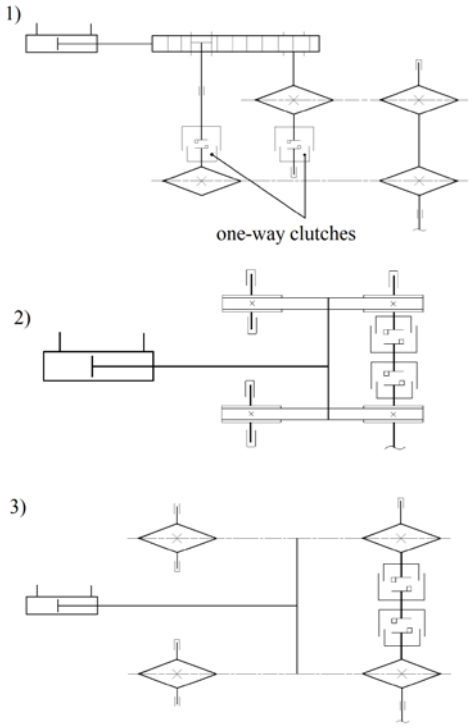

Fig. 3. Subsystem 2 of transmission structure.

2. OPTIMIZATION PROCESS

2.1 Drive system concepts

The first part of the process was to present a field of possible solutions, The main goal was to find a transmission structure with an appropriate transmission ratio. Each of the drive solution had fixed elements. It was the PRA80 cylinder and the 8 gear Shimano Alfine 8 planetary hub [Shimano]. The presented solutions analysed gear, belt and chain transmissions. The presented systems were combinations of subsystems from Fig.2 and Fig.3. Due to the number of systems, a special naming system has been created:

"Engine X.Y"

where:

X – number of subsystem 1, which transform linear motion to rotary motion,

Y – number of subsystem 2, which transfer motion to rear wheel.

2.2 Efficiency analysis

To check the efficiency of the systems, theoretical efficiency for each element was assumed [Shimano][StieberClutch] [MechanicsGuide][SkoćŚwitoński]. The efficiency of the system is the product of the efficiency of individual subsystems. The assumed efficiency of subsystems is presented in Table 1.

Table 1. The efficiency of individual links in the kinematic chain

Name of subsystem of kinematic chain	Efficiency η
Gear transmission	0,94
Chain transmission	0,9
Belt transmission	0,85
One-way clutch	0,99
Planetary hub	0,98

2.3 Maximum drive torque analysis

In order to compare the torque of the systems, the dimensions of the elements of kinematic systems were assumed [Kurmaz][Osiński]. This allowed the comparison of general transmission properties under the same conditions. The values of driving torque have been calculated based on the formula:

$$M_{x-y} = F_{x^*} \frac{d_p}{2} * \eta * i_y \quad (1)$$

where:

M_{x-y} – drive torque at "x" bar pressure in "y" gear [Nm],

F_x – force from piston [N],

d_p – pitch diameter [m],

η – efficiency,

i_y – gear ratio.

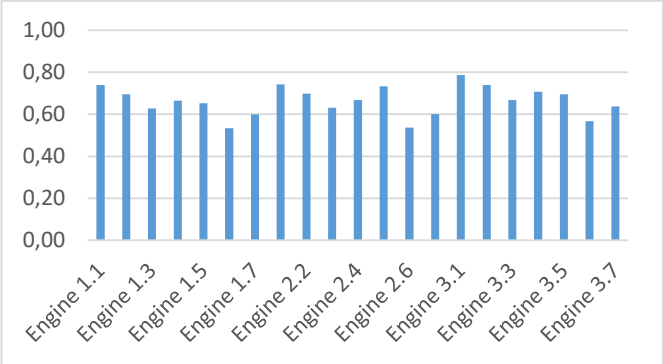

Fig. 4. Graph of efficiency systems.

The calculations were performed for 2, 6, 3 and 10 bar pressure on each of the 8 gears. Calculations do not include the efficiency of the pneumatic cylinder. Its efficiency changes with the speed of extension, which would require experimental verification.

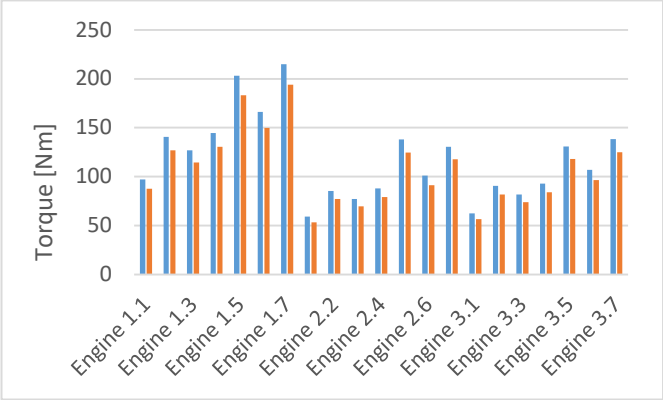

Fig. 5. Torque for 1-st gear at pressure 2 bar.

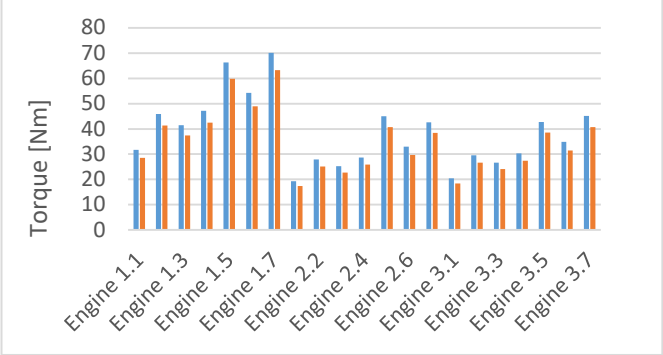

Fig. 6. Torque for 8-th gear at pressure 2 bar.

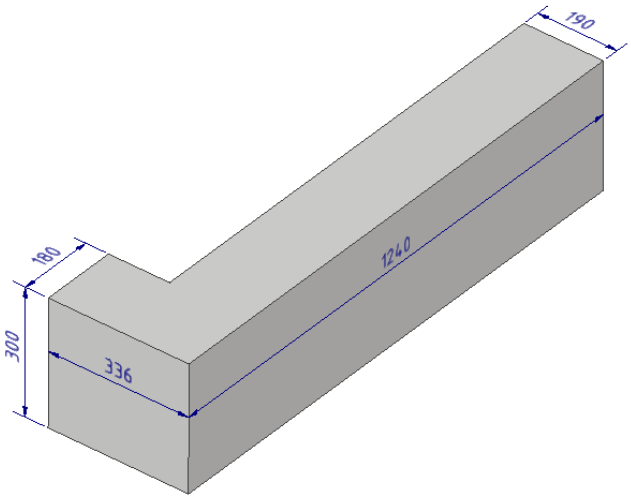

Fig. 7. Dimension of free space for drive system.

2.4 Geometrical analysis

The drive system has been designed for the existing vehicle frame. A very important criterion for optimization was the limited space in the frame.

The entire analysis was one of the most important criteria. It turned out that after the above analysis, out of 21 variants only 3 passed the above assumption. variants 1.1, 1.2 and 1.3 were analysed for performance.

3. PERFORMANCE ANALYSE

Only 3 out of 21 variants have been approved for further analysis. The performance analysis compares the maximum theoretical speeds achieved by the propulsion systems and the simulation of qualifying for the arcade race. This analysis allowed to predict the influence of the gear ratio on the actual characteristic of the drive while driving.

2.5 Maximum theoretical speed analysis

The maximum speed was calculated based on the analysis of the kinematic chain of each system [SkoćŚwitoński][Siłka] [MechanicsGuide]. The vehicle speed achieved depends on:

- Actuator piston stroke speed;
- System ratio;
- Resistance of movement;

Traffic resistances were included in the vehicle transit simulation during the qualifying race. The speed was calculated from the following formula:

$$v = \frac{\omega * r_d}{i_n} * 3{,}6 \qquad (2)$$

where:

v – vehicle speed [km / h]

- ω – angular velocity of the first shaft depending on the actuator's extension speed [rad / s]
- r_d – rolling circle radius 0,3 [m]
- i_n – transmission of the drive system on the "n" gear.

Table 2. The efficiency of individual links in the kinematic chain

	Gear ratio		
Gear	Engine 1.1	Engine 1.2	Engine 1.3
1	2,726	4,194	4,194
2	2,231	3,432	3,432
3	1,921	2,955	2,955
4	1,688	2,597	2,597
5	1,437	2,21	2,21
6	1,175	1,807	1,807
7	1,012	1,558	1,558
8	0,89	1,369	1,369

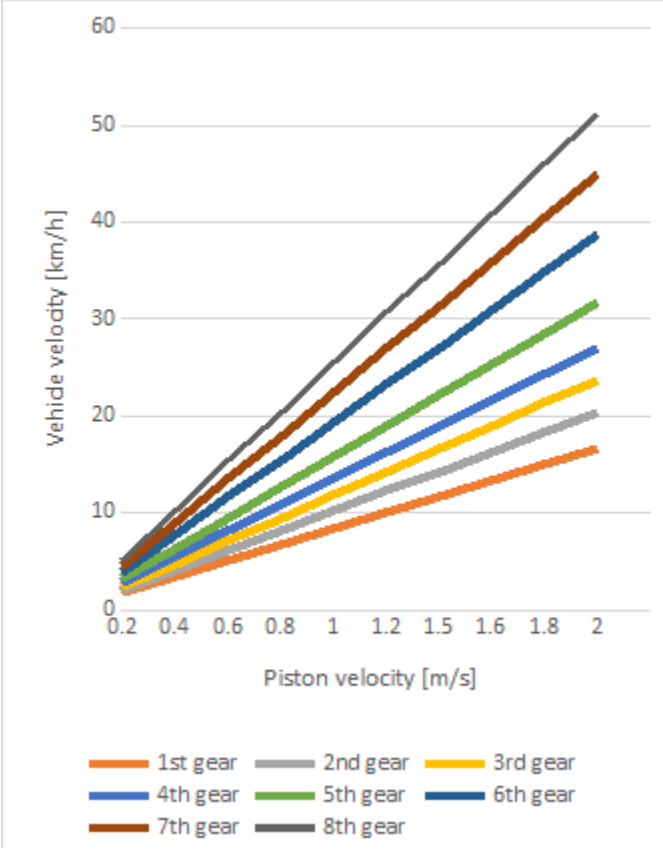

Fig. 8. Dependence of vehicle speed on piston stroke speed for individual gears [Engine 1.1]

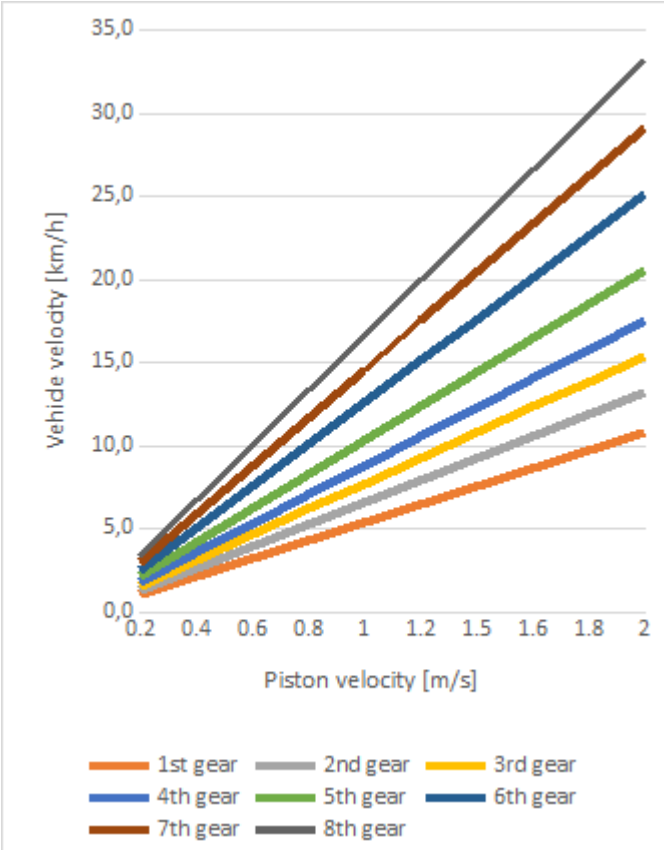

Fig. 9. Dependence of vehicle speed on piston stroke speed for individual gears [Engine 1.2 and 1.3]

3.2 Simulation of qualifying race

The track for the qualifying race is 580 meters long. The main requirements for the passage verification are [Aventics]:

- A minimum average speed of 15 km / h;
- Maximum pressure drop in the cylinder equal to 70 bar.

If any of the above requirements are not met, the vehicle is not allowed to race. In order to simulate and compare the vehicle's journey, the following assumptions were made:

- The vehicle moves from start to finish in 4th gear;
- The working pressure of the system is 6.3 bar;
- Braking before reversing takes place over a distance of 10 meters;
- The engine does not work during braking;
- Constant resistance to movement.

The adoption of these assumptions significantly simplified the analysis of the route and allowed for comparison of results under identical conditions. The total resistances consist of the following components [Siłka]:

- Vehicle inertia resistance

- Rolling resistance
- Air resistance
- The resistance to the rise

During the calculations, air resistance was not taken into account, because the value of this force was small in relation to the whole sum of resistance and it did not affect the calculation. The remaining forces were calculated from the formulas [Siłka]:

- Rolling resistance

$$F_t = G * f_t * \cos\alpha \quad (3)$$

$$G = m * g \quad (4)$$

where:

G – vehicle weight [N]

m – vehicle weight [kg]

g – Earth acceleration [m / s2]

f_t – coefficient of rolling friction [m]

α – tilting angle of the surface [˚]

- Inertia resistance

$$F_b = m * a * \delta \quad (5)$$

$$\delta = \frac{m_z}{m} \quad (6)$$

where:

m – vehicle weight [kg]

a – acceleration of the vehicle [m / s2]

δ – coefficient of rotating masses

m_z – vehicle replacement mass

- The resistance to the rise

$$F_w = m * g * \sin\alpha \quad (7)$$

where:

m – vehicle weight [kg]

g – Earth acceleration [m / s2]

α – tilting angle of the surface [˚]

- The vehicle movement resistance is the sum of the resistances listed above

$$F_o = F_t + F_b + F_w \quad (8)$$

- Driving force

$$F_n = \frac{M_{x-y}}{r_d} \quad (9)$$

where:

M_{x-y} –drive torque at pressure "x" bar, in gear "y" [Nm] Formula 2.1

r_d – rolling circle radius 24 "[m]

After determining the driving force and the resistance force, the formula (2.10) calculates the theoretical acceleration of the vehicle for each of the propulsion systems.

$$a = \frac{F_n - F_o}{m} \quad (10)$$

where:

F_n – driving force [N]

F_o – resistance [N]

m – vehicle weight [kg]

Table 3. Summary of data and results from the race simulation

	Engine 1.1	Engine 1.2	Engine 1.3	Unit
Diameter of the piston	80	80	80	mm
Diameter of the piston rod	25	25	25	mm
Stroke of the piston	250	250	250	mm
Gear ratio	1,688	2,597	2,597	
Efficiency of the drive system	0,74	0,69	0,63	
Driving force	625,3	904,3	817,7	N
Total resistance	359,73	512,67	465,61	N
Computation acceleration of the vehicle	1,3	1,95	1,75	m/s^2
Maximum vehicle speed in 4th gear	25,6	12,	10,5	km/h
The volume of the actuator's duty cycle	2,39	2,39	2,39	dm^3
Number of cycles	41,6	48,5	59,7	
Volume of air used for "cycles	99,5	115,98	142,72	dm^3
The volume of air after expansion from 6.3 bar.	626,83	730,66	899,14	dm^3
The volume of air in the tank after expansion from 200 bar	10	10	10	dm^3
The volume of air in the tank after expansion from 200 bar.	2000	2000	2000	dm^3
Volume difference	1373,17	1369,34	1100,89	dm^3
The pressure in the cylinder after the race	137,32	126,93	110,09	bar
Time of the qualification race	93,4	169,4	203,1	s
Average speed	22,4	12,3	10,3	km/h

The course of the race is shown in the following charts:

- for Engine 1.3

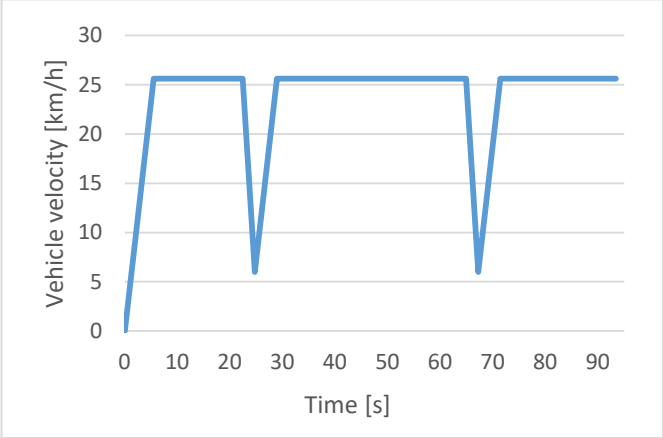

Fig. 10. Speed dependence on the time of the qualifying race for Engine 1.1

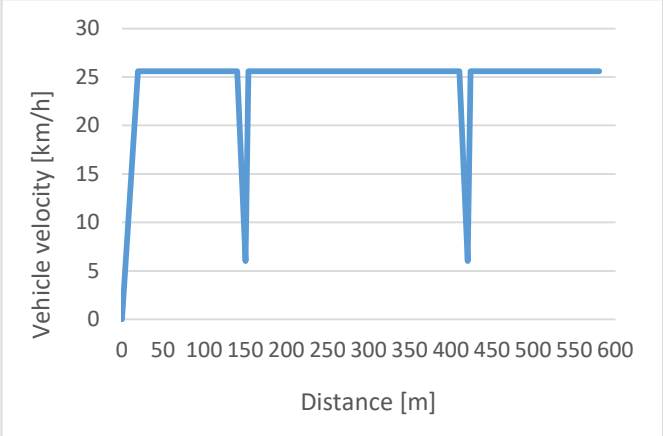

Fig. 11. Speed dependence on the distance for the qualifying race for Engine 1.1

- for Engine 1.2

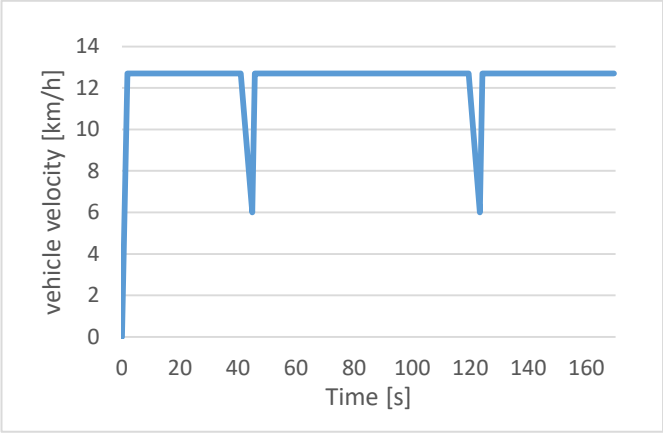

Fig. 12. Speed dependence on the time of the qualifying race for Engine 1.2

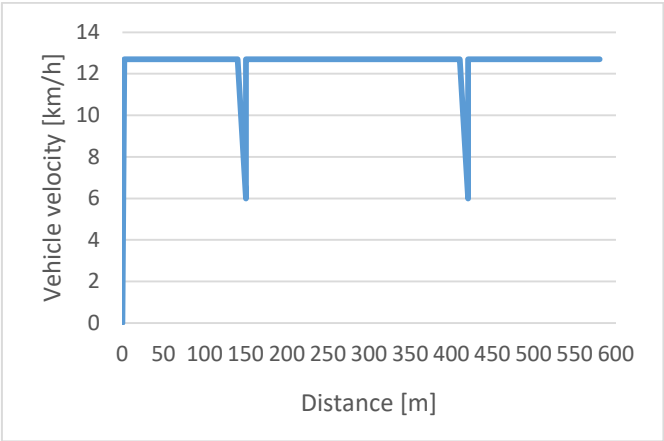

Fig. 13. Speed dependence on the distance for the qualifying race for Engine 1.2

- for Engine 1.3

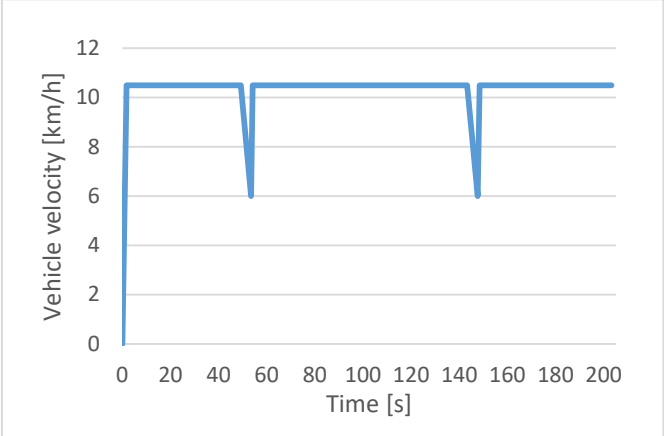

Fig. 14. Speed dependence on the time of the qualifying race for Engine 1.3

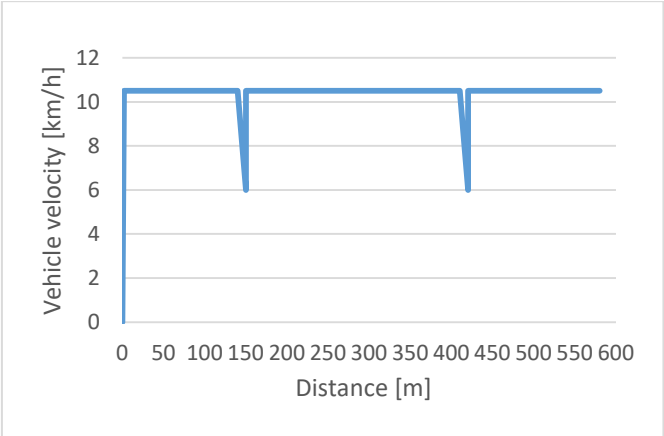

Fig. 15. Speed dependence on the distance for the qualifying race for Engine 1.3

4. CAD MODEL

After the analysis, a 3D model of the optimal system was created. In the development of MES modules, a virtual model of the drive system was verified and created. The system was then built and drives our vehicle.

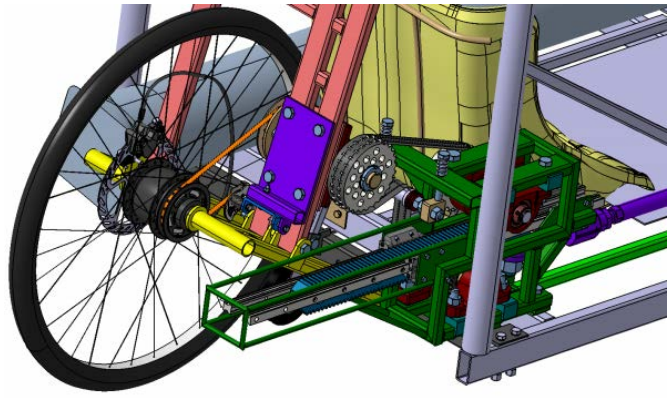

Fig. 16. View from outside on drive system

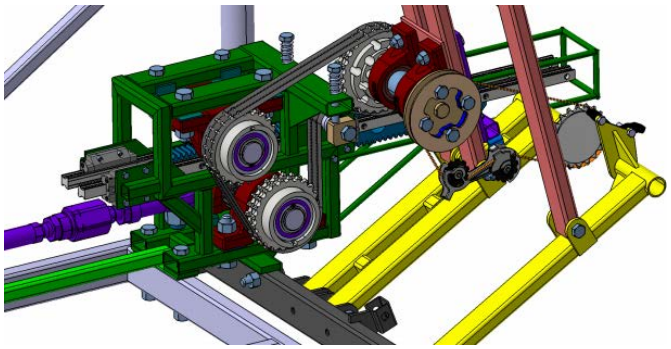

Fig. 17. View form inside vehicle on drive system

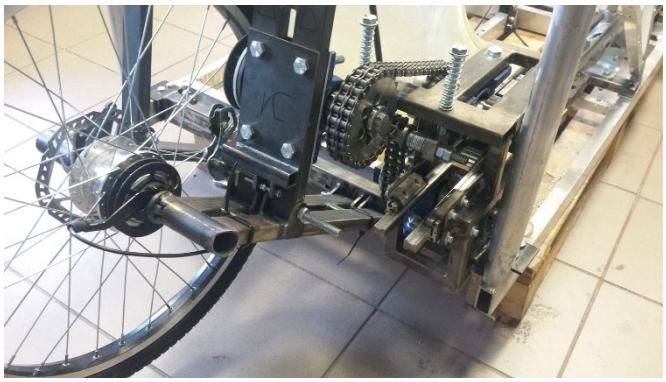

Fig. 18. The drive system in preparation for the Pneumobil 2019 competition.

5. CONCLUSIONS

Thanks to the conducted analysis of efficiency, drive torques, compactness of the structure, speeds achieved in individual gears, it can be stated that Engine 1.1 is the optimal design. Only the simulation of the crossing showed that this system is the only one that meets all the imposed requirements. The remaining concept did not meet the criterion of average travel speed and air consumption. The main factor that influenced the results of the analysis is the transmission of the system. Despite the fact that Engine 1.2 and Engine 1.3 have much higher drive torques, which allows achieving high accelerations compared to Engine 1.1. This results in the fact that the maximum speed of the vehicle in specific gears is more than half the speed. The Engine 1.1 design has a similar ratio to normal vehicles. In the lowest gear we have the highest gear ratio to facilitate starting off and in the highest gear the gear ratio is smaller than one, which makes it possible to achieve high speeds. From the graphs of the speed vs. road and speed vs. time graphs, it can be seen that acceleration takes up a small part of the entire journey, and the maximum speed allows achieving the assumed results. In addition, the analysis carried out does not take into account the lower and higher gear ratios, which would allow a much more efficient defeat of the track. Further analysis should check the properties of the pneumatic system that powers the drive system. It is also necessary to conduct tests and check the results obtained from the analysis. Only after analysis on the actual system can the analysis be considered complete.

REFERENCES

Kurmaz O. Kurmaz L.: Designing nodes and machine parts. Wydawnictwo Politechniki Świętokrzyskiej, Kielce 2011. (in polish)

Osiński Z.: Fundamentals of machine design. Wydawnictwo naukowe PWN, Warszawa 2002. (in polish)

Mechanics guide, REA-SJ, Warszawa 2008. (in polish)

Aventics Pneumobil competition regulations. http://en.pneumobil.hu/ (access 26.12.2018).

Shimano - http://www.shimano.com/en/ (access 26.12.2018)

Siłka W.: The theory of car movement, Wydawnictwo Naukowo-Techniczne, Warszawa 2002. (in polish)

Skoć A., Świtoński E.: Gearboxes, Wydawnictwo Naukowo-Techniczne, Warszawa 2017(in polish)

Stiebier Clutch http://www.stieberclutch.com/ (access 26.12.2018).

ADAPTIVE PNEUMATIC SUSPENSION USING LINEAR QUADRATIC CONTROL

DEMETER László, FORGÓ Zoltán

Sapientia EMTE Erdélyi Magyar Tudományegyetem
Műszaki és Humántudományok Kar, Marosvásárhely

As we live in a world, where the automotive industry has merged with the IT in almost all aspects, the question must be asked: how could the car be made even better? The suspension of vehicles has remained basically the same for the past 50 years, where we get a spring and a damper. But what if the suspension could be made smarter. Effort had been made for the car to read the road ahead, but even with this information, the reaction time and the smoothness is far from perfect. The best know suspension type is the air suspension, as it can smooth out bumps like nothing else. The fastest responding is the magnetic suspension. What if there would be a method to combine the two, floaty feeling of air suspension and the ability to quickly adapt as magnetic suspensions.

The main idea was, that if a pneumatic cylinder's chamber pressure can be kept steady during a bump, we could get the perfect ride. The solution would be simple, just measure the pressure and control it with electronic valves, so that the wheel moves up and down freely, without effecting the chassis. As turned out, this method was flawed, as the pressure was kept at a steady, the ride height kept changing, because no matter what the position, the force output by the cylinder is the same. So the other obvious thing to do would be the position control. Set a ride height position, and using the cloud control method, the chassis would not move. The problem caused here was by the nature of air. It expanded, causing a wobbling, un-damped effect, it never settled.

The solution for the perfect ride: we have to control the pressure as well as the position. With this idea, a Linear Quadratic control system was developed, and with the weighting of the elements, the ideal ride was achieved.

1. INTRODUCTION

This paper aims to propose a new solution to a part of automotive industry that is slowly evolving. The main consideration is a suspension that is able to cope with damaged road surfaces or speed bumps better than any currently know suspension type.

Taking into consideration the technology we have today, the most adjustable type of suspension has been selected as a base of study and development: the pneumatic suspension.

Pneumatic Suspension

A pneumatic suspension as seen in Fig. 1. Is built of a pneumatic cylinder (suspension cylinder), control valve, sensors, fittings and a pressure accumulator. High pressure air is being produced, typically above 10 bar, depending on the vehicle, which is than distributed in the appropriate chamber of the cylinder to increase its output force, or it is released to decrease it. This basic build is what gives the fundament to this study.

Pneumatic cylinders use the compressed energy of the gas to produce reciprocating linear motion and to achieve force transmission. These cylinders have lower weight and higher power density than electro- mechanical actuators. Taking this into consideration together with the fact that by the nature of gas, these cylinders can not only transmit force but also damps the movement of mass and dissipate some unwanted energy derived from the road as heat.

Manufactures have had other solutions, and today there are many types, ranging from floating piston, rubber chamber and even oil-pneumatic systems. As this paper focuses on the principles and the control system of such a build, a simplistic solution is used.

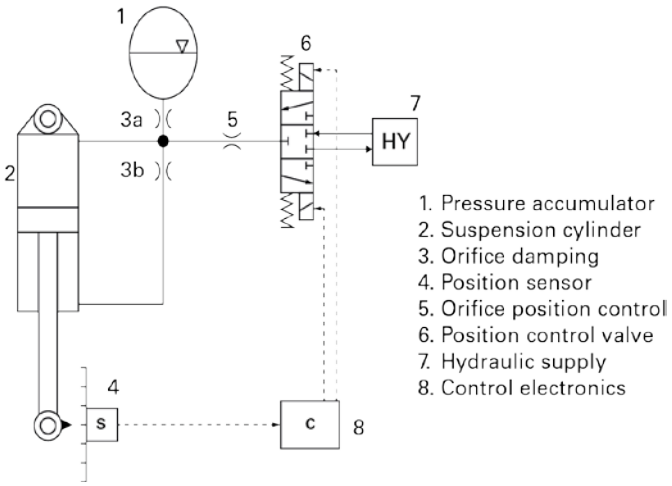

Fig. 1. Simple build of a pneumatic suspension. Source: https://goo.gl/images/QFyn7t

The paper is organised as follows: Section II describes the suspension model, Section III presents the mathematical basics used to build up the simulation environment. Section IV compares the different types of control systems with their

respective simulation results and Section V shows some conclusion remarks.

2. SYSTEM DESCRIPTION

As mentioned previously, the construction is simple. It consists of a pneumatic double actuating cylinder shown in Fig. 2.

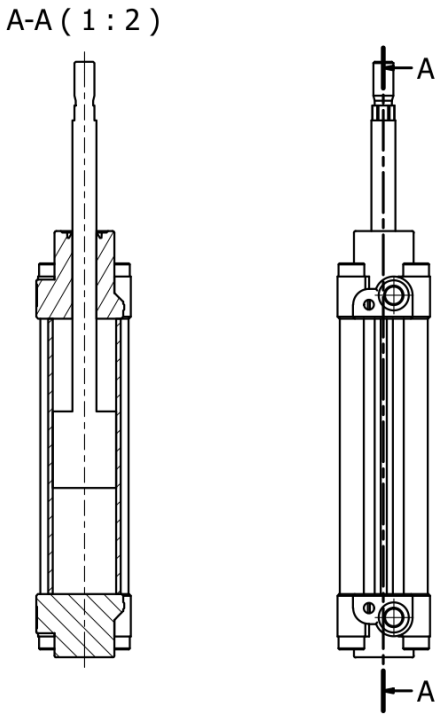

Fig. 2. Pneumatic Cylinder

The pneumatic cylinder is driven by a 5 way 3 position solenoid electro pneumatic valve, with closed centre position.

The two energised cases consist of connecting one chamber with the supply pressure and the other chamber with ambient pressure when one solenoid is on, the opposite happening with the other solenoid turned on. As mentioned, when in not energised position, the pressure in the two chambers remains the same as they will not be connected to the outside. The schematic of this pneumatic setup can be seen in Fig. 3.

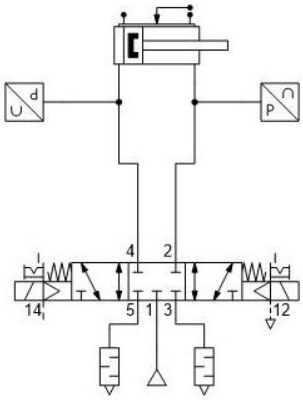

Fig. 3. Schematics representation of the pneumatic system

Other pneumatic components include an analogue position sensor for accurate measurement of the actual rod position and two pressure sensors for each chamber.

To validate the different test results from the simulation environment, a test bench was designed as shown in Figure 4.

This consists of the components of the suspension mentioned above, connected with its rod end another pneumatic cylinder, this with a bigger diameter pushing out more force. This provides the simulated road surface for the suspension. The suspension slides on a rail through ball rail runners, and on top of it sits a mass, simulating the mass of quarter car model. As this bench concept was imagined as a test base for Pneumobil suspension, the cylinders and the mass are small, considered as a miniaturised vehicle suspension.

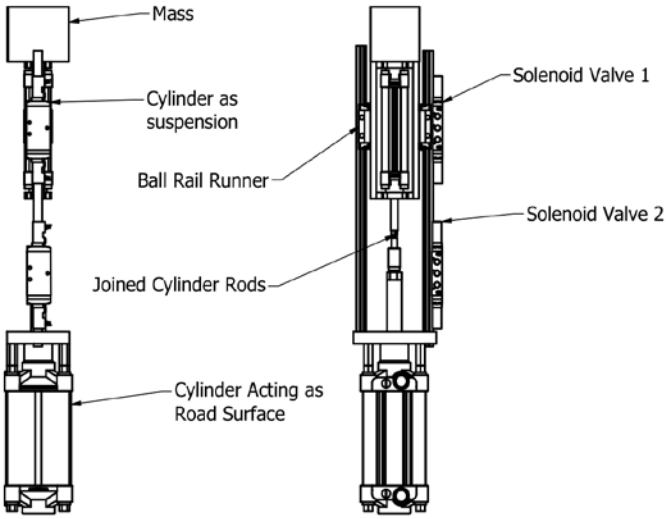

Fig. 4. Test Bench

As of now, the test bench is in form of model designed in Inventor 2019 and imported in Simscape for accurate representation of all physical aspects.

Furthermore, other details such as frictions or the the gas physical properties as specific heats, gas constant and adiabatic components are dealt with in the Simulink model, detailed later.

Due to the above mentioned, we consider the simulation models behaviour to be similar to a physically built test bench.

3. NONLINEAR MODEL OF ELECTRO- PNEUMATIC ACTUATOR

The mathematical basis for the modelling are given by several authors, but mainly by Adam Szabo, Tamas Becsi, Peter Gaspar and Szilard Aradi as writers of the scientific paper: Modeling of an electro-pneumatic gearbox actuator.

The model has been furthermore validated in Knorr Bremse Budapest Research and Development Centre, although these measurements are not available to the public.

Considering all these, some further details are to be given in terms of mathematical descriptions. For the model to be considered as correct, the dynamic behaviour of the system should be described with 90% accuracy.

The dynamic model consists of three parts: solenoid valve model, the chamber model and the mechanism including forces of friction and forces of pressure acting on the components.

The inputs are the valve commands, which are given by the Control Unit (CU), outputs are chamber pressures, rod position and forces. The very detailed mathematical model can be found in the related literature such as [1] and [2].

To reduce model complexity, some assumptions have been made:

1. The gas is perfectly mixed, no spatial variation is considered
2. Kinetic and potential energy of the gas is not taken into consideration
3. The magnetic elements in the valve are modeled assuming linear magneto- dynamically homogenous material.
4. All pressure forces are neglected on the solenoid valve armature
5. The masses of the pistons are assumed to be constant in time.

Since the two chambers are pressurized and depressurized by the same 5/3 solenoid valve, the mass change of these is equal to the mass flow rate of the solenoid valves, as such this and the air temperature are connected between these two components. The mass flow rate can be written as:

$$\dot{m} = A_{f1} p_1 \sqrt{\frac{2\kappa}{\kappa - 1} \frac{1}{R_{air} T_1} \left[(\pi)^{\frac{2}{\kappa}} - (\pi)^{\frac{\kappa+1}{\kappa}} \right]}$$

where A_{f1} is the area at vena contracta, κ is the heat capacity ratio, R_{air} is the gas constant for air, T_1 is the temperature inside the chamber, and π is the pressure ratio:

$\pi = \frac{p_2}{p_1}$, if $\frac{p_2}{p_1} \geq \pi_{crit}$ or π_{crit}, if $\frac{p_2}{p_1} < \pi_{crit}$,

where p_1 is the source side pressure and p_2 is the counter side pressure.

The chamber pressure gradient can be expressed as:

$$\dot{p} = \frac{\kappa_{air} R_{air} T_{inw} \dot{m} - k_{ht} A_{ht} (T_{ch} - T_{amb})}{V_{ch}} - \frac{\kappa_{air} P_{ch} \dot{V_{ch}}}{V_{ch}}$$

where T_{inw} is the temperature of the flowing air, $k_{ht}$and A_{ht} are the heat transfer coefficient and heat transfer area. V_{ch} is the volume of the chamber.

The mechanical model of the actuator is based on the conservation equation of momentum. The applied momentum balance of the pistons can be written as:

$$\dot{v_p} = \frac{\sum F_p - G - F_f}{m_p}$$

where F_p is the pressure force calculated from pressure and area od piston, G is the force of gravity on the mass of suspension and quarter car mass and F_f is the friction force.

The applied friction model contains the Coulomb friction and the viscous friction. The switching characteristic of the Coulumb friction is approximated by a sigmoid- function.

$$F_f = F_\mu \left(\frac{2}{1 + e^{-f(v1-v2)}} - 1 \right)$$

where F_μ is the friction force between the elements – cylinder and piston- , v1 and v2 are the speed of the friction elements and f is the gradient of the sigmoid function. [3]

4. CONTROL SYSTEMS

The last big part of the model is the CU, seen in Figure 5.

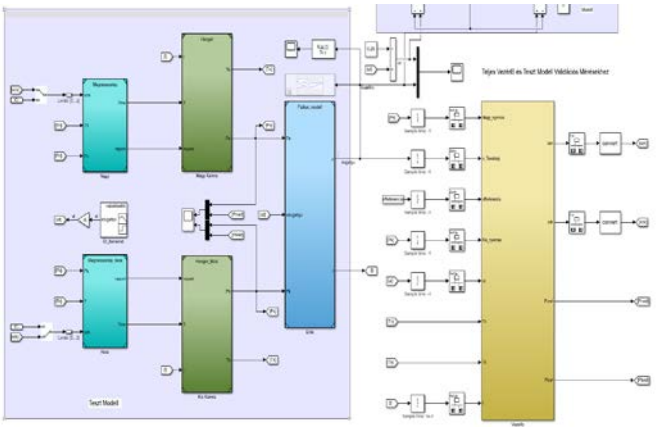

Fig. 5. From left to right: Valves, Chambers, Forces, CU

The original idea consisted of a simple pressure based control system, following the simple principle of the force that a cylinder can output depends on the area and the pressure. As the area does not change, if the pressure is kept as a constant, the forces on the two chamber, and as such the actuated force would remain constant. If we consider the bumps on the roads a disturbance, then we could say, that if the disturbances reacting on the rod increase the pressure on one of the chamber, by releasing the surplus or charging up to the needed pressure would stabilize the system. The stable system, provided the mass on it, in our case the chassis is constant means the rod position remains at a given height. The faster the response to the pressure change, the more stable it gets.

The test bench has valves that are able to be closed. This means, that when there is no disturbance, we close the gas in the chambers and the given forces are applied without constantly having to open or close the valves.

4.1. Pressure Control

The simple approach is given. If a certain pressure is reached the valve should open and let the gas out. At the same time, to complement the other chambers drop in pressure, the valve provides it with high pressure gas. When the threshold is reached, the valve goes into its middle setting, where it is closed (Figure 3.). To see the results, the disturbing motion, which in our case would be the road surface, and the rod

position is plotted on a graph. The absolute ideal situation would mean there is no movement at all in the rod.

Figure 6. shows the case when the valves are always closed. This is basically how some cheaper bicycle suspensions work. *Video: https://youtu.be/bD4xOe7fo_I*

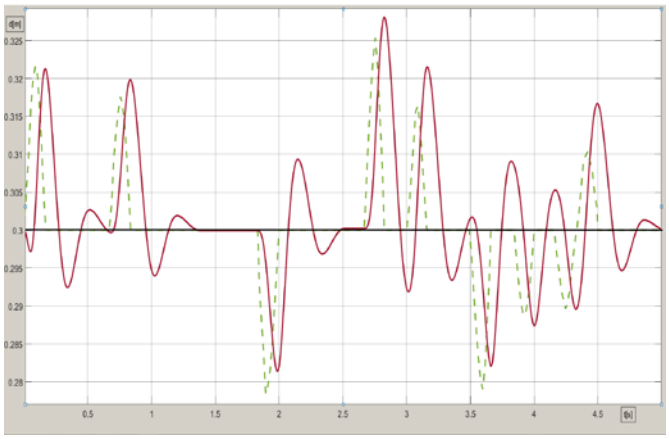

Fig. 6. Movement with closed valves- green dashed is the road surface, red continuous is the movement of the chassis or in our case the cylinder-

It is to observed that the acceleration of the disturbance is somewhat minimized, but the oscillations are far too great.

In Figure 7. the Pressure Controlled simulation results are shown.

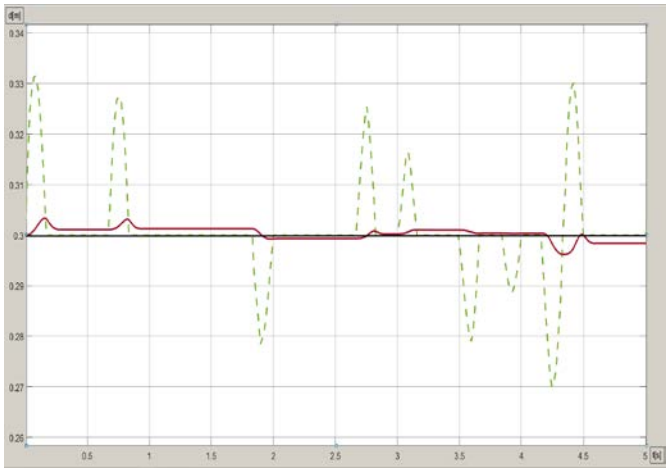

Fig. 7. Pressure Control

First, the most easily recognizable thing is that now the movement of the cylinder is much smaller, the red line stays much closer to the null point. On the other hand, a fault is observed here: the ride height is being shifted, or in the case of the test bench, the cylinder does not remain on the same height.

This problem can be explained very simply. The force a cylinder can output does not depend on the volume of air, as such it does not depend on the length of the chamber either. It only depends on the pressure and the constant diameter of the cylinder. And as the pressure is equalized, the length shifts as the two chambers do not equalize at the same time due to the pressure differences of ambient and the pressure found in the accumulator.

4.2. Pressure Control with PID

To see if improvements can be brought with a control system, I have designed a simple PID for this, as shown in Figure 8.

A PID control system is a Proportional Integral Derivative controller, or three term controller. It is a control loop feedback mechanism. An error value is continuously calculated *e(t)* as the difference between the desired setpoint and a measured process point. In our case it is the set pressure and the measured pressure. To this applies a correction based on proportional, integral and derivative terms.

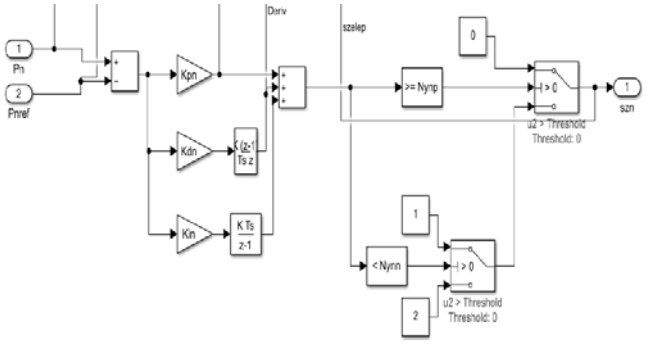

Fig. 8. Pressure Control with PID

$$u(t) = K_p e(t) + K_i \int_0^t e\,(t')dt' + K_d \frac{de(t)}{dt}$$

Where *u(t)* is the output signal, *K* coefficients for proportional, integral and derivative terms. The output of this function is the control signal on which it is decided whether to supply pressure, to release pressure or maintain the measured pressure as it is in reach of the error.

The simulation results of the PID controlled system seen in Figure 9. are very similar to those we had with simple pressure control. The movements are barely noticeably smaller in this case and the shifts in the position are maybe not as pronounced.

The PID parameters have been optimized with the Ziegler/ Nichols method. This is a heuristic method of tuning a PID controller. It is performed by setting the integral and derivative gains to zero. The proportional gain is then increased until it reaches the ultimate gain Ku, at which the output of the control loop has stable and consistent oscillations.

Video: https://youtu.be/UFzS9RzoAGc

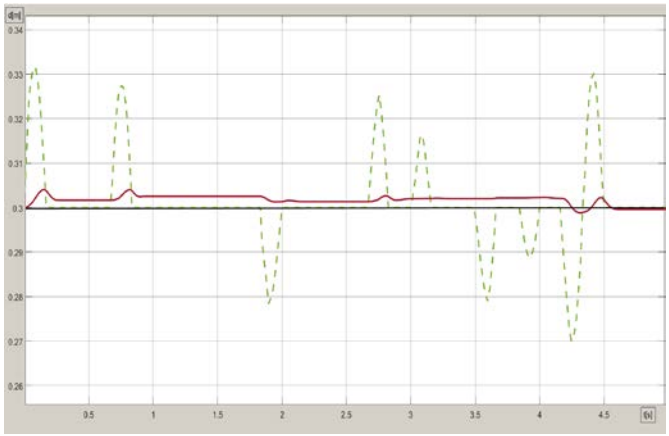

Fig. 9. Pressure control with PID

The gain and the oscillation periods are used to set the P, I and D gains depending on the type of controller used [4]:

Control Type	Kp	Ti	Td	Ki	Kd
P	0.5 Ku	-	-	-	-
PI	0.45 Ku	Tu/1.2	-	0.54Ku/Tu	-
PD	0.8 Ku	-	Tu/8	-	KuTu/10

Table 1. Ziegler- Nichols method

After tuning the PID, using MATLABs built in Control Systems Designer, the simulation has been run close to one hundred times to fine tune the parameters. As a result, this is the closest to the best PID that can be used on this system.

As the offset meant that in a real world, over time the ride height would increase or decrease so much as the end of the cylinder would be reached in certain situations, resulting in choppy ride. So I have decided to try out another form of control, sticking with PID but now trying to correct on the position alone.

4.3. Position control with PID

As seen in Figure 10. the control system is very similar to the previous, pressure based control, but in this case, the error would be calculated based on the reference height and the actual, measured height.

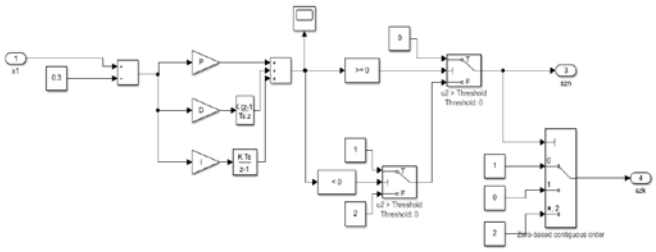

Fig. 10. Position Control with PID

It is said, that a pneumatic cylinder cannot be controlled precisely due to the nature of the expanding gas. This, with the fact, that due to the mass of everything starting from the valve to the delays caused by the solenoid meant that the results were not as expected.

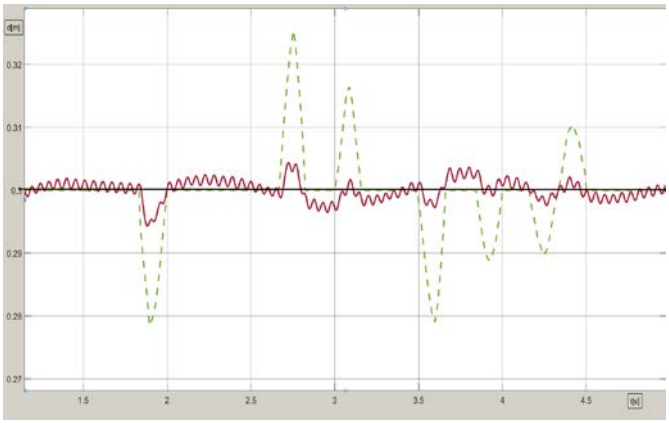

Fig.11. Position Control simulation results

Figure 11. shows the problem of this sort of control system. Because of the delays any output signal has to the system, around the reference point an oscillation starts to occur. Tried several PID configurations and valve opening configurations, no change made it have less oscillation than this. Although it is to be observed, how this method though oscillates, it does this around the reference point. This gave the idea for the next sort of control system, which can do what a PID cannot: calculate control signals based on two (or more) errors. This way, the control system would take into consideration both pressure- no oscillation- and position – no shifting in height.

4.4. Linear Quadratic Control System

The theory of optimal control is concerned with operating a dynamic system at minimum cost. The case where the system dynamics are described by a set of linear differential equations and the cost is described by a quadratic function is called the LQ [5] problem. One of the main results in the theory is that the solution is provided by the linear–quadratic regulator (LQR), a feedback controller whose equations are given below. The LQR is an important part of the solution to the LQG (linear–quadratic–Gaussian) problem. Like the LQR problem itself, the LQG problem is one of the most fundamental problems in control theory. [6]

The algorithm basically finds those optimal controller settings that minimized all the undesired deviations. In the suspension control unit case, this would be the offset position and the pressure difference. Although the LQR has several difficulties, the main one is the fact that is very hard to find the right weighting factors. I used the before mentioned automatic function built in MATLAB to rerun several times the simulation and adjust the parameters to the best value.

Considering the m input and n state system with $x \in R^n, u \in R^m$[7]:

$$\dot{x} = A(t)x + B(t)u(t); \quad x(0) = x_0$$

With a quadratic cost function defined as:

$$J = \int_0^\infty (x^t Q x + u^T R u + 2x^T N u)dt$$

The feedback control law for minimizing the value of the cost:

$$u = -Kx$$

Where K is:

$$K = R^{-1}(B^T P(t) + N^T)$$

P is given by the solved Riccati differential equation:

$$A^T P(t) + P(t)A - (P(t)B + N)R^{-1}(B^T P(t) + N^T) + Q = -P(\dot{t})$$

For the calculations MATLABs built in LQR algorithm has been used. The syntax is *lqr(A, B, Q, R)*. The output of this is the optimal gain matrix.

Problems to be satisfied [8]:

- The pair (A, B) is stabilizable
- R > 0 and $Q - NR^{-1}N^T >= 0$
- $Q - NR^{-1}N^T$, $A-BR^{-1}N^T$ has no unobservable mode on the imaginary axis

A and *B* matrixes had to be calculated. For this purpose, a MATLAB code was written, that created the 4x4 *A* matrix and the 4x2 *B* matrix.

With the two matrixes created, the *lqr* equation calculated the optimal *K* matrix. This than had to be split into two parts, one for each of the chambers.

Figure 12. and 13. Shows how this has been achieved with Simulink.

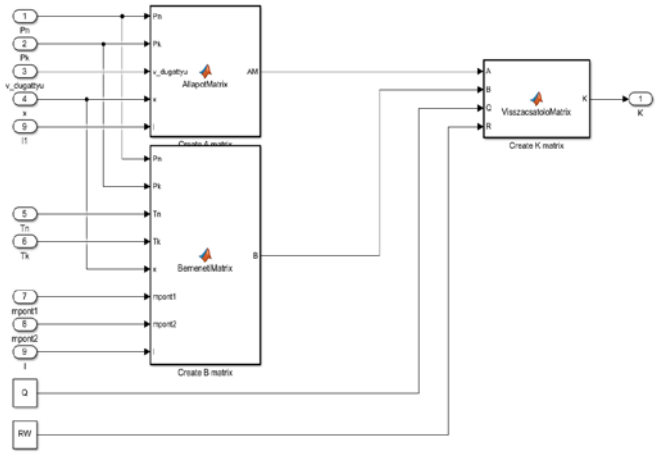

Fig. 12. Creating A and B matrixes, calculating optimal K matrix.

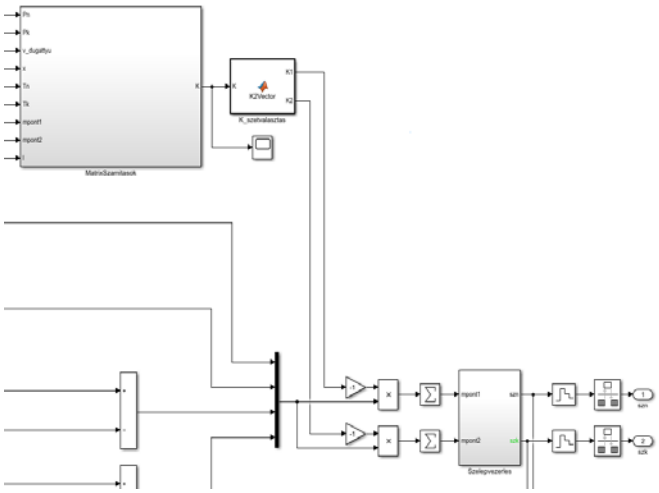

Fig.13. Splitting K matrix in two chambers and converting them to valve commands.

Results:

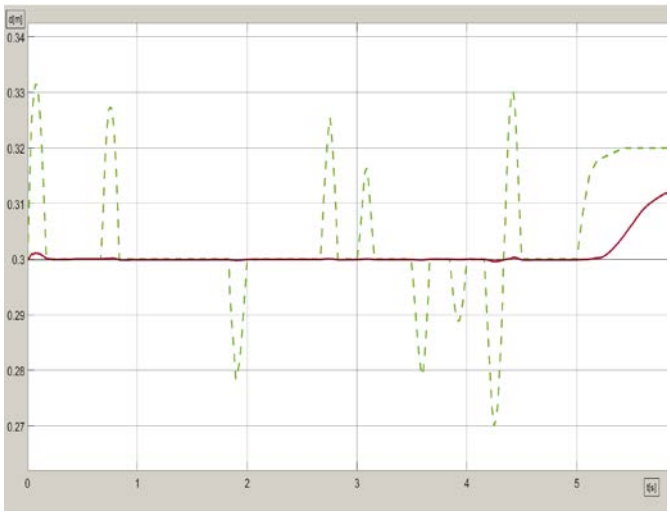

Fig. 14. LQR regulator simulation results

Video: https://youtu.be/scbLkPA2cs4

The results (Figure 14.) are as expected very close to the absolute perfect. Both Pressure and Position Control Systems traits are visible in this result, as there is a very slight shift and a very slight oscillation, but in this case these are so minor, that they are negligible. Only the biggest bumps give it somewhat of a challenge and even those were designed as a maximum height allowed by law and average length, approached by the vehicle at 40 km/h.

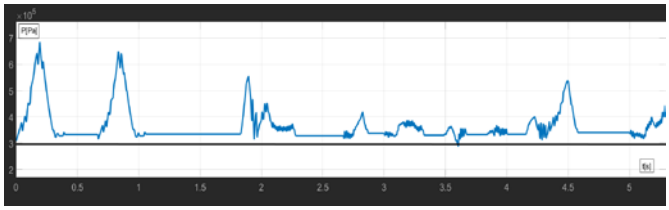

Fig.15. Pressure changes

Figure 14 shows that less than 2 bar increase is in the chamber even in the case of the biggest bump. This is why it manages to maintain such a minimal movement.

This smooth movement is achieved with multiple valve opening though. As seen in Figure 15. many openings and closings are needed to maintain this control.

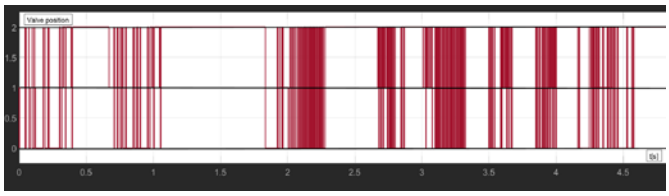

Fig. 16. Valve openings

In position 2 the valve is closed, in 1 is set to the supply and 0 is ambient.

Valve opening has also been put in the cost function as well, which slightly reduced the opening but increased the movement.

5. CONCLUSIONS

Upon creating the mathematical model, the simulation environment was given to which 4 types of control systems were added: Pressure control, Pressure control with PID, Position control with PID and LQ regulator. The pressure control proves to be besides the simplest and most cost effective one of the best performing. Adding the PID to that did not improve its performance by a lot, barely noticeable. The Position control was designed to fix the biggest issue caused by the Pressure control, the shifting in height. It did so but at the expanse of instability.

The last control system was the LQ, which combined the two previous. As a result, this had very little movement and high stability, while maintaining the correct height.

The caveat with these systems is the valve opening, as this would not be feasible in a real world application, as this would hamper the reliability. To fix this, a pressure valve would be needed, as the LQ can calculate for the exact pressure needed as well. This would probably result in even less movement, faster response. Further research will focus on this aspect of the development.

REFERENCES

[1] H. N´emeth, L. Palkovics, and K. M. Hangos, “Unified model simplification procedure applied to a single protection valve,” *Control Engineering Practice*, vol. 13, no. 3, pp. 315 – 326, 2005, aerospace IFAC 2002.

[2] B. Szimandl and H. N´emeth, “Dynamic hybrid model of an electropneumatic clutch system,” *Mechatronics*, vol. 23, no. 1, pp. 21 – 36, 2013.

[3] F. Al-Bender, “Fundamentals of friction modeling,” in *Proceedings, ASPE Spring Topical Meeting on Control of Precision Systems, MIT, April 11-13*, 2010. ASPE-The American Society of precision Engineering, 2010, pp. 117–122.

[4]https://en.wikipedia.org/wiki/Ziegler%E2%80%93Nichols_method

[5] B. Szimandl and H. N´emeth, “Closed loop control of electro-pneumatic gearbox actuator,” in *2009 European Control Conference (ECC)*, Aug 2009, pp. 2554–2559

[6]https://en.wikipedia.org/wiki/Linear%E2%80%93quadratic_regulator

[7] Gáspár Péter, “Allapotvisszacsatolás tervezése”, *Közlekedés- és Járműirányítási Tanszék, Budapesti Műszaki Egyetem*, 2017 Január, Seminar

[8] https://www.mathworks.com/help/control/ref/lqr.html

Designing the Suspension of the Airrari Pneumobile

Gábor Horváth, István Péter Szabó

University of Szeged Faculty of Engineering,
Moszkvai körút 9. HU6729 Szeged, Hungary
e-mail: pszi@mk.u-szeged.hu
horvath.mail.gabor@gmail.com

Abstract: The subject of our article is the design a front suspension of the Airrari pneumobile. The main was to create a spring-loaded front suspension, which is needed to make the pneumobile better, more stable and faster. The design is based on our previous rigid suspension pneumobiles experiences, road vehicles and race car literatures. Firstly, we created geometry with with different kind of CAD softwares, then simulated and optimalized the working of suspension with Lotus Shark Suspension. Based on the model, we manufactured the parts of the suspension which had been running in the pneumobile for three years. We have evaluated the work on our experiences and make suggestions to next year's four-wheeled pneumobile.

1. INTRODUCTION

The University of Szeged Faculty of Engineering has taken part the International Pneumobile Competition since 2009.

Our race teams achieved a lot of great successes, meanwhile we gained a lot of experience. In every year 2-4 racing cars participated from Szeged at the competition in Eger as well as at the gala races organised in Kecskemét and Budapest. So far 10 cars have been made in Szeged and each car had a lot of modifications.

Last years one of the main fields of our development was the front suspension. Until 2015 we use rigid suspension but the increasing speed made necessary to design a sprung one, because on the inner side of a three wheeled vehicle the wheel could lift up from the ground in a corner and the car drift out. A well-optimized sprung suspension is one of the most important components of a successful racing car. It results higher stability and cornering speed.

2. FRONT SUSPENSION GEOMETRIC CHARACTERISTIC

2.1 Track width and track width changing during move

A The large track width gives good stability, but the greater distance between the wheels, the smaller the load between the sides in the bend, and vice versa. It is important to note that any change in the track width may cause unwanted loss of adhesion and force the tires to excessive sideways, so minimize this. According to car literature, during 60mm squat if do 25mm track width, does not force the tire to slip, as its elasticity absorbs. Race car literature (Adams, 1993, Staniforth, 2006) often prefers tyre slip to force the tyres to more grip (racing tyres are able to take more strain in side-slip)

Since the change in value 0 can only be achieved with adaptive suspension, the aim is to keep it close to 0, and even if it changes, the track gauge will be reduced, thus helping lateral overload in our pneumobile.

2.2 Wheelbase

The large wheelbase provides softer springs for a better comfort. The shorter wheelbase better, smaller turning radius and better maneuverability with the same turning wheel angle as larger wheelbase. During the design, attention should be paid to the value of the wheelbase. (Tilt axis, steering angle misalignment, position of control levers.)

2.3 Camber angle

We distinguish three states, the extent of which is determined by the desired geometry: negative, positive and neutral. It has a great influence on running geometry and should be carefully selected, as it is a parameter of suspension that changes during the suspension travel.

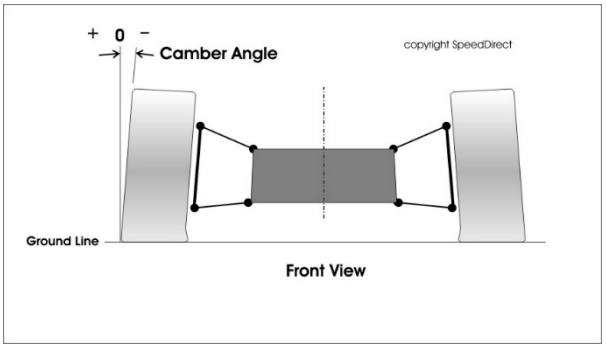

Fig. 1. Camber angle (speeddirect.com, 2018)

Variation of wheel inclination during suspension:

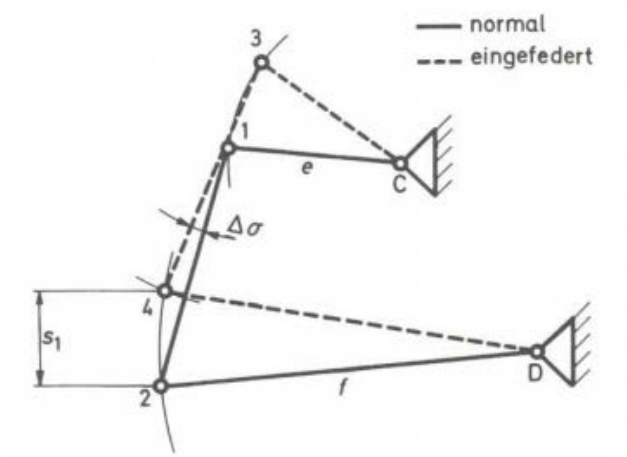

Fig. 2. Editing the change of the camber angle during the wheel inclination (Reimpell, 1983)

2.4 King pin inclination:

The king pin inclination defines the angle that is locked by the straight line defined by the center plane of the wheel and the hinges of the lower and upper swing arms. This angle plays a major role in the turning of the vehicle, as a result of which a lot of information comes back through the steering wheel to the driver on the side forces on the wheels. These forces are create the steering torque that straightens the wheels when the turn ends.

The outer wheel in the arc is able to pick up more force if it has negative camber, but the inner wheel is being positive camber without KPI. The effect of the king ping inclination both wheels will be positive for the direction of the power take-up,that is why the KPI is important.

The degree of the king pin inclination should also be taken into account when camber angle.

For modern cars, the value of the KPI is 11 ° to 15 ° (Reimpell et al., 2012).

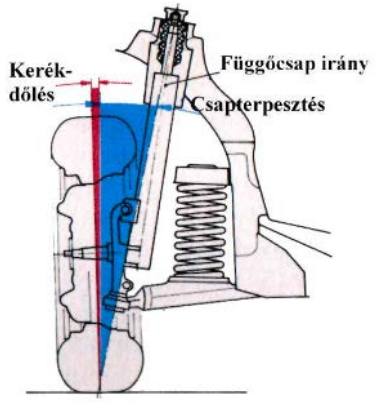

Fig. 3. King pin inclination (Varga Ferenc, 2014)

2.5 Caster angle

The caster angle is achieved by positioning the wheel's point of ground contact (F) and the point (V) of the pin on the ground relative to the direction of travel before or after the direction of travel. To do this, either the lower or upper hinge points must be moved forward or backward. We distinguish three kinds of types: negative, neutral, positive.

1: Negative
The point of pinching of the pins on the ground runs after the point of contact of the wheels. It is used very rarely and only for front-wheel drive cars, where its instability is offset by the wheel-driving torque, but is characterized by little steering resistance.
2: Neutral:
The wheel base of the wheel is the point of pinching the pins on the ground perpendicular to the direction of travel. Compared to the negative, it is safer, but no feedback from the wheels can become unstable.
3: Positive
The puncture point of the pins on the ground runs before the point of contact (V). It is characterized by high stability and contributes to the restoration of the wheels to the straight-ahead position. Greater power is required for steering, with the arc inside wheel protruding during riding, which is not advantageous, but in this condition more information is obtained from the wheels. As a result of the protrusion, the steering torque is greater. Excessive positive caster angle tends to instability in the same way as a negative caster as a result of road unevenness and side wind. Its value varies between 10mm and 40mm (Reimpell et al., 2012).

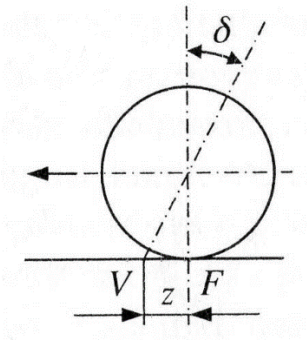

Fig. 4. Caster angle (Szaller, 2010)

2.6 Tilt point

We look at the car from front view. At rest, the center of gravity and the center of the tilting moment are aligned in a plane. As a result of the side forces acting on the racing car (centrifugal force during cornering, side slider, side wind), the body tilts around the tilt moment around the center and the center of gravity shifts to the side.

As the vertical load of the inner wheel decreases, the load on the outer wheel increases as much. However, the vertical load on the wheel and the lateral force it can take is not linear, but degressive. For example, if the vertical load of the outer wheel is doubled, the lateral force that it can take is doubled, but doubled. That is, overloading causes side force loss, which reduces the stability of the vehicle bending. So the sideways of the bodywork is an unfavorable phenomenon, it has to be mitigated." (Reimpell et al., 2012)

2.7 Steering angle misalignment

The wheels must roll without slipping during cornering. For good maneuverability and control, therefore, if the vehicle is at least two tracks, it is inevitable that the wheels roll on other circuits while steering, so they must be turned at different angles.

Perfect pro-Ackermann steering can only be done with adaptive steering geometry, which is unnecessary in our case. In order to approach the correct angular misalignment, the Causant editing mode can be used to determine the angle of the steerers that control the shaft stubs. This editing mode is sufficiently accurate, but the higher the steering, the greater the error, so slip occurs.

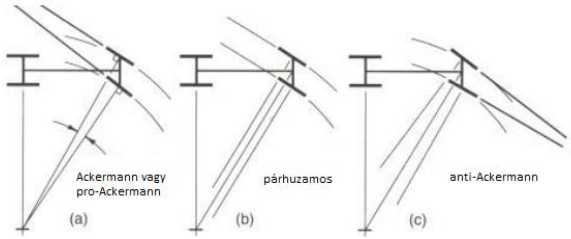

Fig. 5. Ackermann types (Milliken&Milliken, 1995)

Perfect pro-Ackermann steering can only be done with adaptive steering geometry, which is unnecessary in our case. In order to approach the correct angular misalignment, the Causant editing mode can be used to determine the angle of the steerers that control the shaft stubs. This editing mode is sufficiently accurate, but the higher the steering, the greater the error, so slip occurs.

2.8 Scrub radius

The positive scurb radius provides good straight run, but the steering is more difficult to move and causes uneven braking when steering, resulting in an automatically reverse steering rotation that can cause the racing car to break out.

In the case of a negative scurb radius, the braking force and the traction force affect the steering through this lever. During braking, it acts as a stabilizing torque in case of a different adhesion factor, prevents the car from breaking out. (Varga Ferenc, 2014).

The neutral scurb radius prevents the higher force requirements at steering in case of brakeing or flat tire.

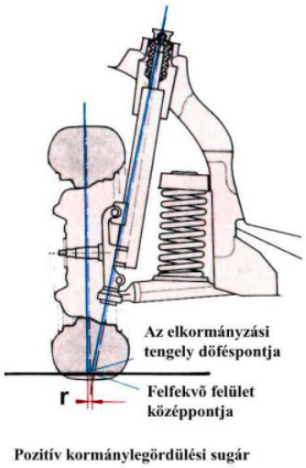

Fig. 6. Positive scurb radius (Varga Ferenc, 2014)

2.9 Steering knuckle design

Due to incorrectly placed control rod the movement of the suspension changes the angle of the toe. Which leads to an uncontrolable situation. This phenomenon called „bump-steer". This cen be avoided by a correct design. The following picture shows, that the control rod joints are at U ans T, the steering trapezoids U point connect to the wheel at EG line.

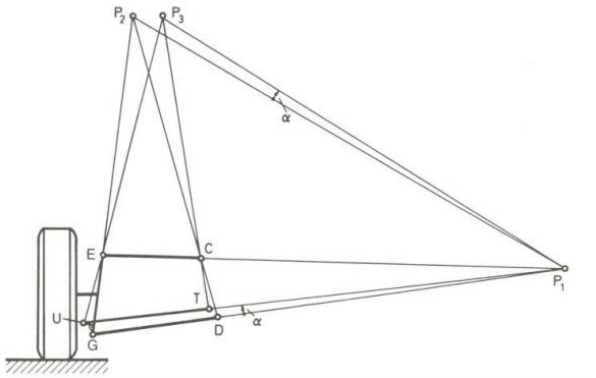

Fig. 7. Steering trapezoids stubs edition, when they placed front of the axle (Reimpell et al., 2012)

3. DESIGNING THE FRONT SUSPENSION OF THE AIRRARI PNEUMOBILE

The length of the swing arms is given by the track width and the wagon body, both of which are given parameters. The length of the lower and upper swing arms must be different so that no track widht changes occur during the buckling and the camber changes in negative direction and. The lower link arm had a maximum length of 220 mm. Leaving the adjustment option, the lower link arm is 210 mm long. The length of the upper swing arm was determined by the distance between the lower and upper swing arms by the desired height and buckling and the desired geometry. Its

length is 145mm.

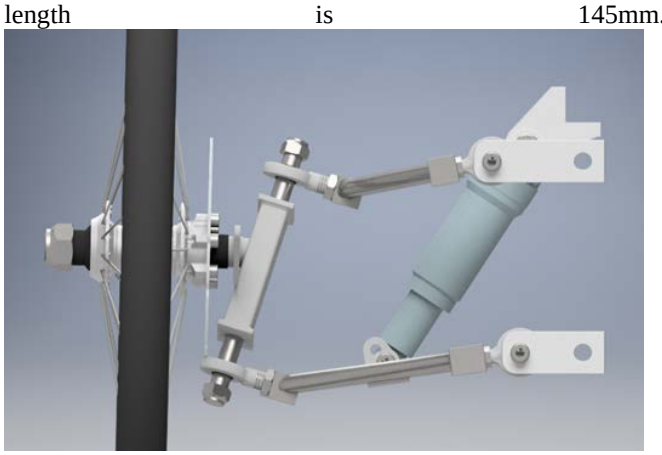

Fig. 8. Front suspension, Inventor 3D model

The distance between the pivot arms must be greater than the distance between the pivot points on the frame. This distance is what determines the geometry of the tilt point and wheel movement. I was looking for approximate values here, which is the most suitable for the culture of motion I am looking for because the final values were simulated in the Lotus Shark Suspension Analysis program.

I have defined the framing points for the frame so that the steering does not have one swing arm in its way.

Their combined position on the frame was determined by the height adjustment and the unobstructed movement of the steering rods.

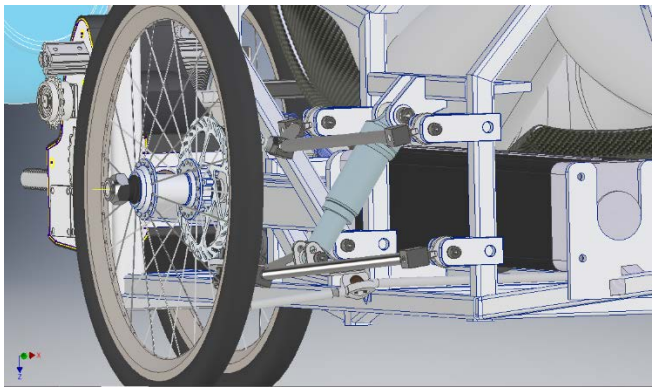

Fig. 9. The tie rods between the brackets and the cylinder and the frame

The change in the point of contact of the soil during the buckling is critical as it causes loss of adhesion. This should not be reduced to 0, but only with adaptive geometry, but it should strive to maintain the highest possible value. In our case, this was reduced to 2.32 mm with the Lotus Shark Suspension software.

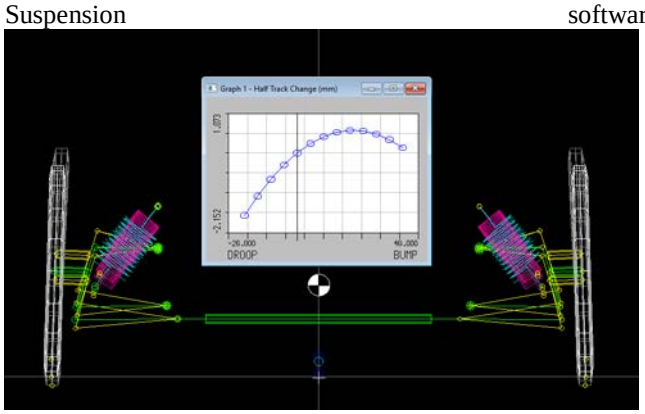

Fig. 9. Contact point (track widht) change during total motion range.

In the case of buckling, I had to take into account the fact that I would like to have a steering wheel scurb radius of +10 mm (Adams, 1993) so that the braking forces can attack as little as possible. For this purpose, an angle of more than 8-11 ° specifically recommended for racing cars had to be used in the literature, resulting in a 145 mm long swinging arm, which turned the stub axle in 15°.

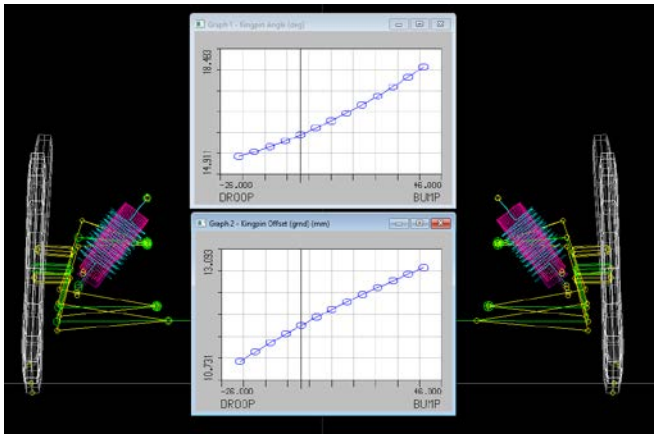

Fig. 11. King pin inclination (°) and scrurb radius (mm) during total motion range

Aspects of skidding considered in design:

It is important that we have a negative ti in the entire movement range of the chassis with a starting value between -0 ° 30 'and -2 ° (Adams, 1993). The reason for this is that we want to use the outer wheel to increase the load during cornering.

For the desired 2 ° tilt, the shaft is not perpendicular to the stub axle, but at an angle of 77 degrees to compensate the

king pin inclination.

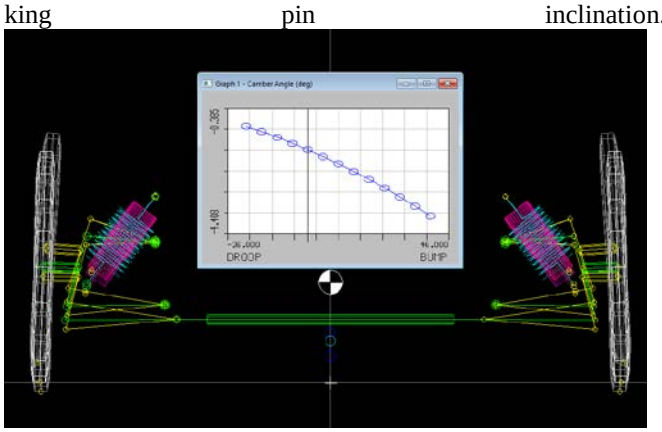

Fig. 12. Camber gain during total motion range

The tilt point is defined by the position of the swing arms. Since I did not want the car can tilt easily, I would have liked to keep in the range of 2.5-10cm from the ground. (Racing car literature advised (Adams, 1993)). As a result of well-defined swing-arm positions and lengths, this has been achieved.

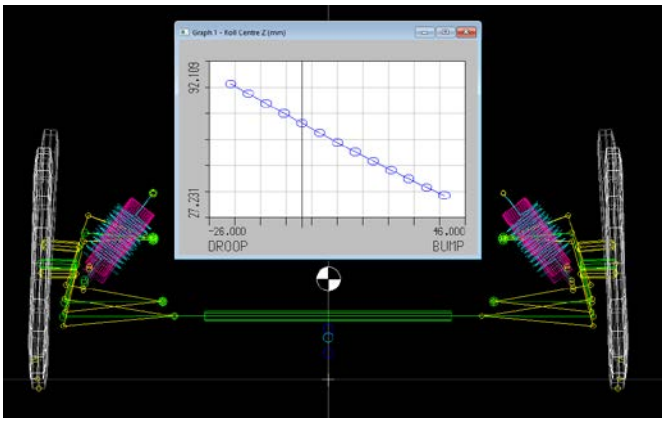

Fig. 13. Tilting point from the ground during total motion range

In case of force shifting during cornering, I would like to keep the momentary center at the longitudinal symmetry axis of the car body so that it does not accidentally get near the wheel base.

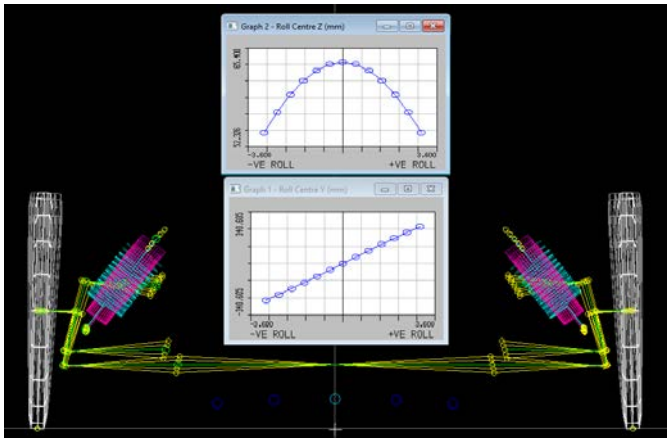

Fig. 14. Change in tilt point for lateral load (turning)

Due to the large caster angle chosen, the lower and upper king pivots of the spindle had to be pushed from each other, which required at least one swing arm to be asymmetrical.

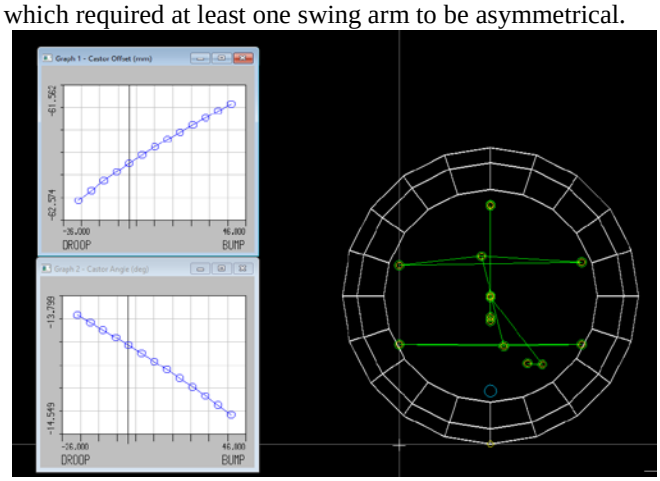

Fig. 15. Caster offset (mm) and caster angle (°) change during total motion range

After analyzing the tilt and the Ackermann angles, I analyzed the forces in the rolling height as well as in the fully enclosed state:

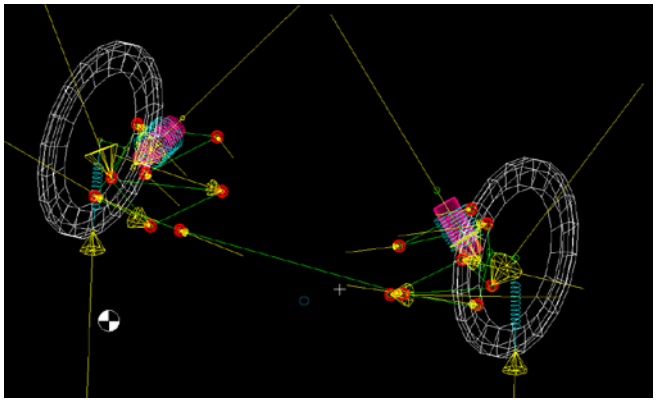

Fig. 16. Effect of forces in a fully locked state, examined in Lotus Shark

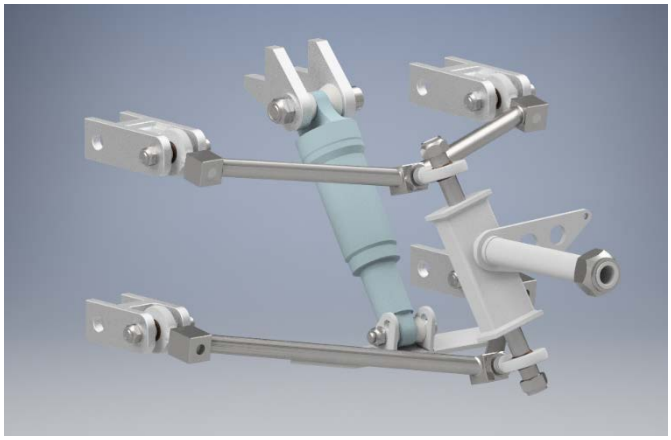

Fig. 17. Suspension model

Based on the results of the finite element analysis, I concluded that the elements of the chassis have proper

strength properties.

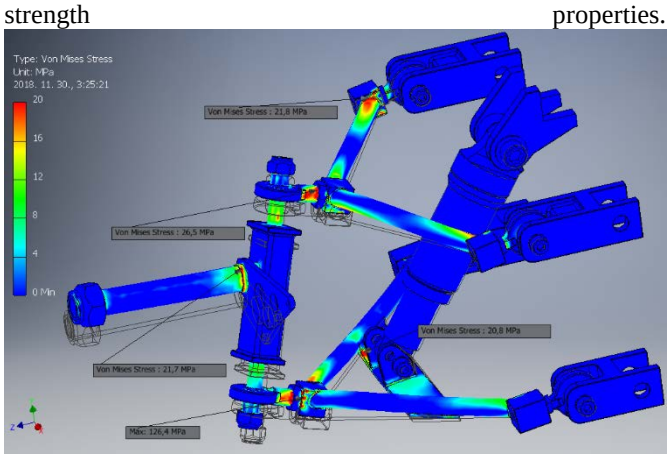

Fig. 18. Finite element analysis

Because of the narrow legroom and the low-placed steering rods, a unique steering gear was required, so I planned a rack-and-pinion steering gear. The simplest possible design and cost efficiency was expected. The target 6 meter turn circle and the planned handlebars had a gear that turns a 180 degree turn of the wheel into a 30 mm straight line displacement. I have used a toothed gear and toothed rack. To eliminate backlashes and adjustability, the distance between the rack support bearings is adjustable, and the steering shaft is supported by deep groove ball bearings at the bottom.

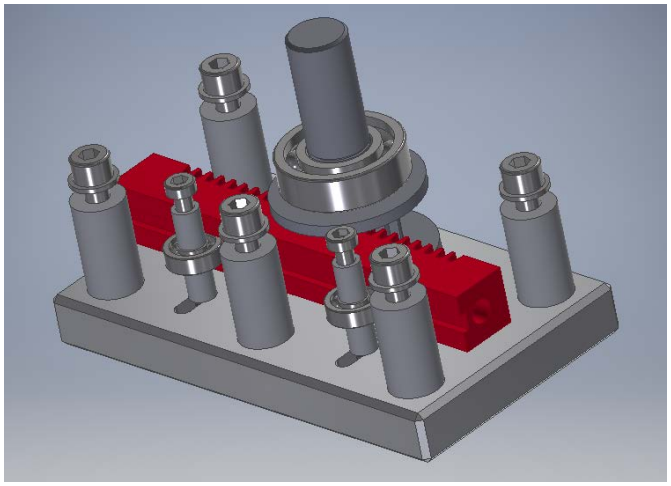

Fig. 19. The steering gear without top cover for better illustration

Fig. 20. Prefabricated elements of the front axle and steering gear before welding, drilling and assembly

Fig. 21. Airrari is at the 2018 Aventics International Pneumobile Competition

4. CONCLUSIONS

I went into a very complicated and deep science, and understanding of its basic function was a great challenge. I have learned how complex a system involves a chassis and how its parameters affect each other. During my planning, I expanded my knowledge with several programs and met many helpful people during my work. In addition to planning, I was able to contribute to the success of a team with the parts and other tasks I produced, I could see my

work during the operation, and I could even compete with it. During the race, I gathered a lot of experience and evaluated my work to design an even more optimized chassis in the future.

REFERENCES

Adams, H. (1993). *Chasis Engineering*. HPBooks, ISBN: 1-55788-055-7

Staniforth, A. (2006). *Competition Car Suspension*. J H Haynes & Co Ltd, Fourth Edition, ISBN: 1-844253287

Milliken, W. F. & Milliken, D. L., (1995). *Race Car Vehicle Dynamics*. Example Product Manufacturer. ISBN: 1-560915269

Reimpell, J. (1983). *Fahrwerktechnik: Federung, Fahrwermechanik*. Vogel Communications Group GmbH & Co. KG, ISBN: 3802305132

Szaller, L. (2010). *Gépjárművek dinamikája és szerkezettana*. 2. kiadás, Tankönyvmester Kiadó, ISBN: 9639668214

Reimpell, J., Betzler, J. W., Bári, G., Hankovszki, Z., Kádár, L., Lévai, Z., Nagyszokolyai, I. (2012). *Gépjármű-futóművek I.*, Typotex Kiadó, ISBN: 978-963-279-606-2

Building Telemetry System of Pneumobile Applying NI Devices

György Juhász*, Gusztáv Áron Szíki, Kornél Sarvajcz ***,
Péter Hunor Póta****, Bence Márk Szeszák*****

** University of Debrecen, Faculty of Engineering, Department of Mechanical Engineering,
2-4 Ótemető Street, Debrecen, H-4028, juhasz@eng.unideb.hu*

*** University of Debrecen, Faculty of Engineering, Department of Basic Technical Studies,
2-4 Ótemető Street, Debrecen, H-4028, szikig@eng.unideb.hu*

**** University of Debrecen, Faculty of Engineering, Department of Mechatronics Engineering,
2-4 Ótemető Street, Debrecen, H-4028, sarvajcz@eng.unideb.hu*

***** University of Debrecen, Faculty of Engineering, Department of Mechanical Engineering,
2-4 Ótemető Street, Debrecen, H-4028, pota.petya@gmail.com*

****** University of Debrecen, Faculty of Engineering, Department of Mechanical Engineering,
2-4 Ótemető Street, Debrecen, H-4028, szeszakbence@gmail.hu*

Abstract: Our teams have been developing pneumatic engines and studying them theoretically and experimentally for several years. In our present study we introduce a telemetry system built up of NI devices and give its limits. We describe the used materials and measurement devices together with the measurement process and results. Finally, based on our results, we give recommendations for further experimental studies and new ways of application.

1. INTRODUCTION

The Faculty of Engineering of the University of Debrecen has been designing and constructing alternative driven race cars for more than a decade. The applied technology has improved a lot since the simple technical solutions of the first races. We do not only build cars driven by a pneumatic engine but also applying developed telemetry system in them. Developing telemetry systems is now a basic task, in order to understand the operation of the pneumatic system and realize the developmental potentials in it. Our teams have been dealing with developing pneumatic engines and studying them theoretically and experimentally for several years. Our results so far are described in literature [1, 2, 3, 4, 12]. In our present study we introduce a telemetry system built up of NI devices and give its limits. We describe the used materials and devices and demonstrate the measurement and evaluation process. Finally, based on our results, we give recommendations for further experimental studies and new ways of application.

2. INSTRUMENTATION, MEASURED QUANTITIES

2.1 Applied devices

The main points of view for choosing the data acquisition system were mobility [5], possibility for data storage and wireless data transfer, and industrial design, because of varying strains and environmental conditions. It was also important that the DC supply of the vehicle could be used for supplying the applied instruments. To meet all the above requirements, we chose the CompactRIO system of National Instruments [6]. The applied sensors for the measurements were the ones sold by the main organiser of the competition. The above sensors are also parts of the vehicle during the competition.

Table 1. Applied devices

NI controller	NI-cRIO 9074 controller [6]
NI modules	NI-9201 analogue input module [7] NI-9269 analogue output module [8]
Distance measuring sensor	SM6-AL distance measuring sensor [9]
Pressure measuring sensor	PE5 pressure measuring sensor [10]

2.2. *Measured quantities*

- Pressure of air inside the power cylinders
- Pressure of air flowing out of the puffer cylinder
- The position of piston in the power cylinder

2.3. *Derived diagrams*

- Distance-time diagram of the piston
- Velocity-time diagram of the piston
- Acceleration-time diagram of the piston
- Distance-force diagram of the piston
- Velocity-time diagram of the vehicle
- Power-time diagram of the vehicle

3. MEASUREMENT METHOD

The applied software for the telemetry system was NI-LabVIEW 2014 [11]. The task of the telemetry system is to receive the signals of the sensors – that are built in the car – and transfer them to a computer. The sensors convert the physical signals into electronics ones like voltage or current, and then these signals are processed and digitalised by the data acquisition system [12]. The software controls the data acquisition system by collecting the measured data, analysing them and visualizing the results. We used two different measurement methods. In case of the first one controlling and data storing were performed by the cRIO, in case of the second one controlling by the PLC and data storing by the cRIO. In both cases reproducibility was important, thus the position of sensors (sampling) was the same in both cases. Figure 1. shows the saving and controlling block diagram of cRIO.

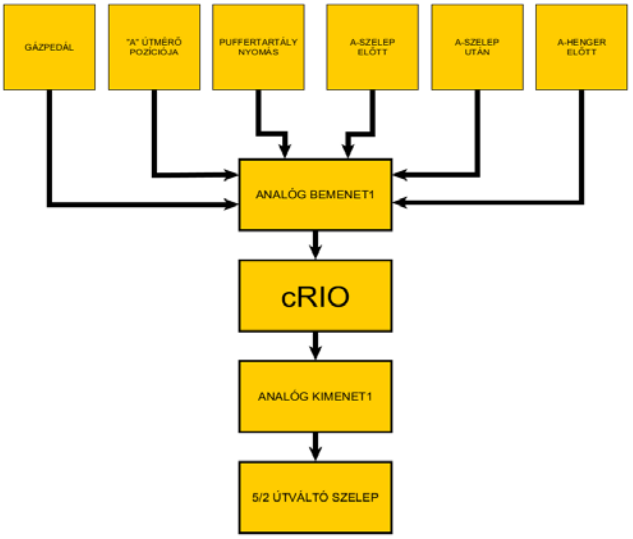

Fig. 1 Saving and controlling block diagram of cRIO

4. MEASUREMENT RESULTS

The diagrams that are presented in this section were obtained from that measurements when the cRIO was applied for controlling. Figure 2. shows the air pressure inside the puffer cylinder as a function of time during the operation of the pneumatic engine.

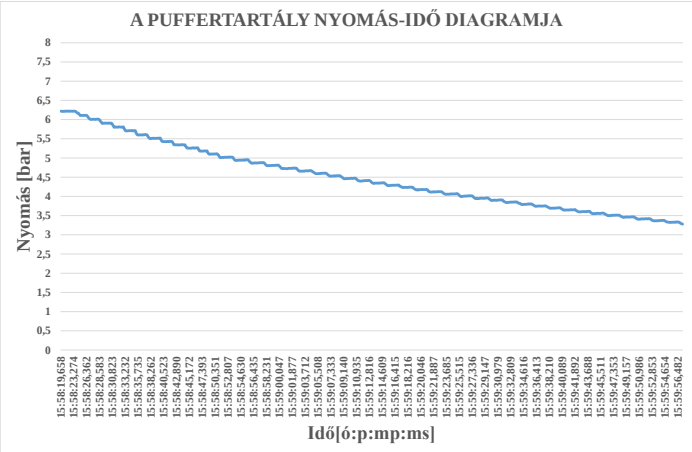

Fig.2. Air pressure as a function of time inside the puffer cylinder during the operation of the pneumatic engine.

Figure 3. shows the measured air pressure in front of and behind the valve (valve "A") which is used for operating the power cylinder in the pneumatic engine.

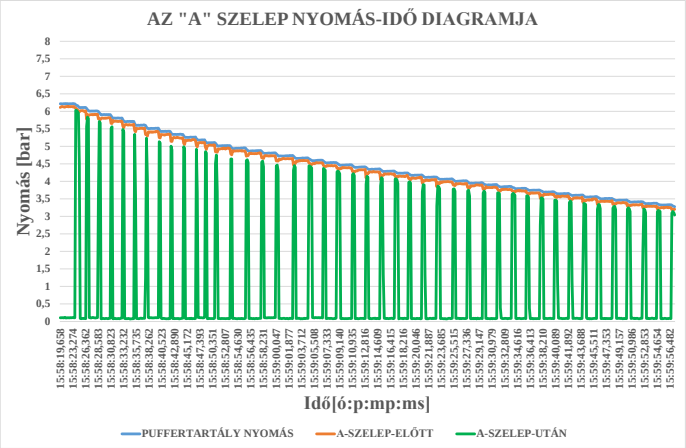

Fig.3. Air pressure in front of and behind valve "A"

Figure 4. shows the loading pressure of the power cylinder (cylinder "A") of the pneumatic engine

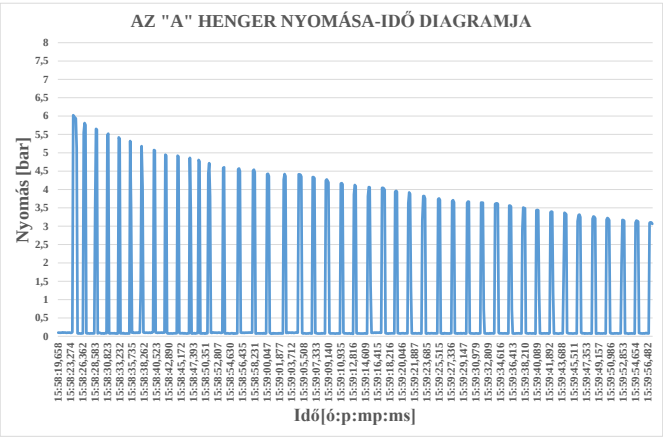

Fig. 4. Loading pressure inside the power cylinder of the pneumatic engine

Figure 5. shows the position of the piston in the power cylinder as a function of time. The position was derived from the electric signal of the distance measuring sensor.

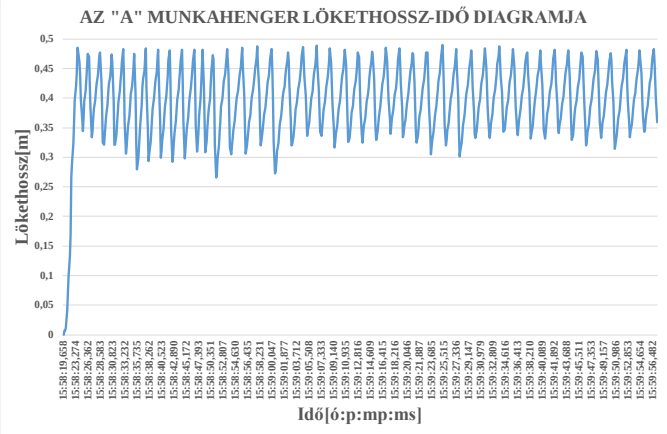

Fig. 5. The position of the piston in the power cylinder as a function of time

Figure 6 shows the velocity-time function of the piston which was derived from its position-time function (Figure 5).

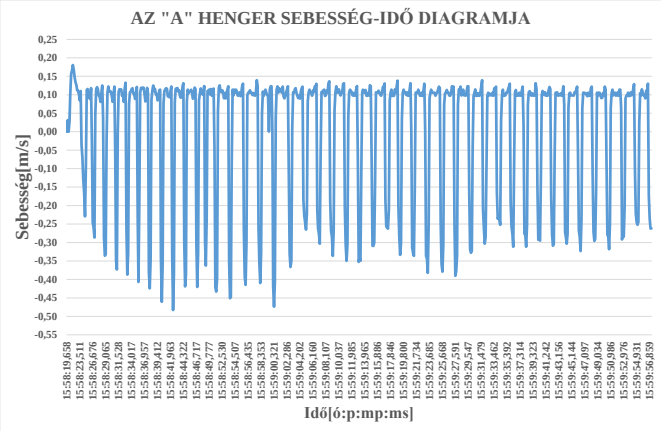

Fig. 6. The velocity-time function of the piston

Figure 7. shows the acceleration-time function of the piston which was derived from its velocity-time function (Figure 6).

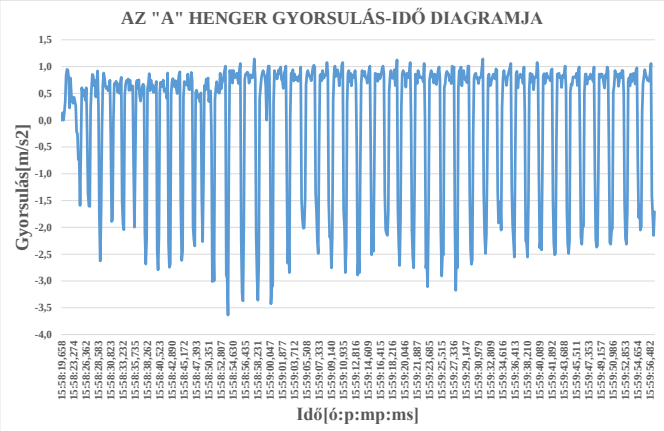

Fig. 7. Acceleration-time function of the piston

5. CONCLUSION

Evaluating the measured data, it became clear, that the losses in the pneumatic engine are significantly bigger than the previously accepted ones. The aim of our experimental work – beyond the testing of our telemetry system – was the realisation of the controlling of the power cylinder in the pneumatic engine. It turned out, that although we can realise controlling with the applied devices, our system must be developed to be effectively applicable for the above purpose. On the other hand, the measurements and evaluation of data was successful, data loss or damage were not realised. Two measurements were performed: The first one in “laboratory conditions”, the second one in “race situation”. In both cases pressure drop was observable through the valve, and through the distance between the puffer and power cylinders. Thus, pneumatic connections must be shortened as much as it is possible. In the near future we intend to realise the measurement of vehicle speed, and also the controlling of two or more power cylinders. We also intend to realise a wireless communication, which is applicable for the transmission of data – measured on the vehicle during the race – to the team members in the box.

REFERENCES

[1] Veszelszki Krisztián, Szeszák Bence Márk (2016): Pneumobil gördülési ellenállásának vizsgálata, TDK
[2] Juhász Botond (2014): Számítógépes program a pneumobil menetdinamikai paramétereinek számításához, TDK
[3] Szeszák Bence Márk (2017): Pneumobil gördülési ellenállásának mérése, Szakdolgozat
[4] Szeszák Bence Márk, Sütő Tamás Sándor (2017): Pneumobil gördülési ellenállásának vizsgálata terhelt állapotban, TDK
[5] K. Sarvajcz, A Váradiné Szarka (2016): Development of portable measuring system for testing of electrical vehicle’s heat energy recovery system, Journal of Physics: Conference Series 772 (2016) 012033
[6] NI cRIO 9074 Datasheet, http://www.ni.com/hu-hu/support/model.crio-9074.html letöltve: 2018-10-22
[7] NI cRIO 9201 Datasheet, http://www.ni.com/hu-hu/support/model.ni-9201.html letöltve: 2018-11-11
[8] NI cRIO 9269 Datasheet, http://www.ni.com/hu-hu/support/model.ni-9269.html letöltve: 2018-11-11
[9] SM6-AL Datasheet, https://www.aventics.com/de/de/pneumatics-shop/sensoren-serie-sm6-al-pro.692583 letöltve: 2018-11-02
[10] PE5 Datasheet, https://www.aventics.com/en/products/pneumatic-products/sensor-technology/pressure-sensors/series-pe5/ letöltve: 2018-11-02
[11] Robert H. Bishop (2014): Learning With LabVIEW, Marquette University, ISBN-13: 978-0-12-402212-3
[12] Juhász Botond (2013): A pneumobil jellemzőinek vizsgálata NI eszközrendszer segítségével, TDK

Modelling and Validation of a Pneumobil

Tamas Szakacs
University of Óbuda, BGK MEI
1034 Budapest Bécsi út 96/B
+3616665406 **szakacs.tamas@bgk.uni-obuda.hu**

Abstract: The paper introduces an earlier presented, reworked pneum atic model of the PowAir team's pneumobil vehicle developed at the University of Óbuda.

The Matlab/Simulink® model begins at the energy of the gas stored in the high-pressure tank, and goes through the thermodynamic, fluid mechanic, and mechanical description of the pressure reducing valve, the pressure, flow, and gas behavior in the system, the cooperation of the puffer tank, and the pneumatic piston.

The earlier modell has been extended with a two-chamber piston, and a vehicle body modell.

The goal of the modelling is to describe the pressure, force, flow, and speed behavior of the piston, in order to optimize power, and gas consumption. Further goal of the modelling is to develop, and optimize control strategies, in special attention on maximizing vehicle power, and traveling range.

After the modell development, modell validation, and simulation results are also presented.

1. INTRODUCTION

In the previous conference ACIOV 2018 a pneumatic modell was presented in other to investigate thermodynamic, fluidmechanic, and mechanic behaviour of a pneumatic system of a pneumobil. During application of that modell it turned out that a more detailed description is required to develop and validate pneumobil engine control system. In this paper the future developed modell will be presented.

Modelling the gas behaviour in a pneumo-mechanical complex system is not an easy task. The temperature, pressure, the gas flow is continuously changing in time, and space, virtually the gas constant can only be considered constant. There is one quantity that can be used as base of the description that is the mass flow.

As the first step I have described the thermodynamic behaviour of the gas bottle. The bottle is a constant volume, changing mass system. The enclosed gas amount builds up a pressure, which is changing as the consumption reduces the mass.

The next component is the pressure regulator valve, which is a lot more complex system as the bottle. First, the mass flow is bidirectional, while the bottle supplies, the consumers consuming the air.

The pneumatic piston is even more complex task, while there is not only pressure building up at a given volume, but the volume is changing as the piston starts moving, and there is also energy transformation from pneumatic to mechanic.

The model was built in Matlab/Simulink® environment. The name of the blocks, functions are their mathematical equations, which helps to understand the logic of the submodells *(See Fig.1).*

1.1

2. DESCRIPTIONS

The following chapters the modified, and extended components of the model will be introduced, in the next chapter the complete model will be shown, and finally measurement validations will be presented.

The main differences between the 2018, and the 2019 modells are the followings:

- The piston is a dual chamber one, in order to simulate exhaust pressure drop, and pre-charging of the reverse-side chamber.
- A controller block is added to simulate engine control, including ECO mode
- Directional valves are added to control gas flow
- The number of connecting lines are reduced in order to simplify the model.
- Blocks are colored for aesthetic reasons, and better understandability.

During the modell creation it was always kept in the focus that the model should remain simple and easy to understand.

Physical quantities are given in practical units (liters, Celsius, bars…) which within the model are converted to SI units: (m^3, Kelvin, Pa). Such converters can be found in all models. Like the one shown in Fig.4-8 (l2m^3, C2K Pa2bar)

Fig 1 shows the pneumatic schematics of the pneumobile.

Fig 2, and 3 show the difference of the top layers of the original, and the advanced model.

The most significant changes on the top layer are the controller block, and the dual chamber piston

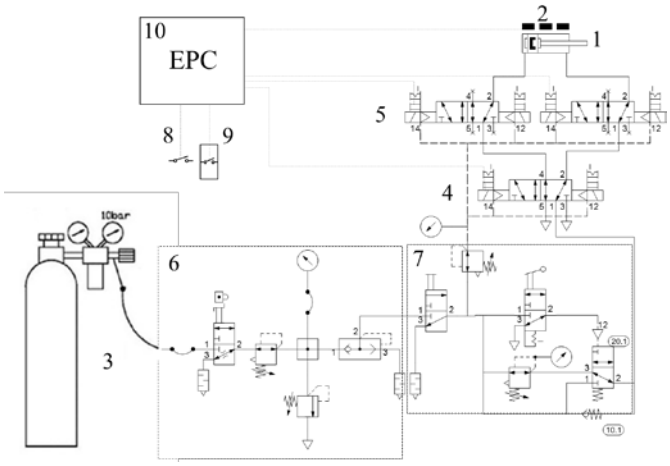

Fig 1.Schematics of the pneumatics

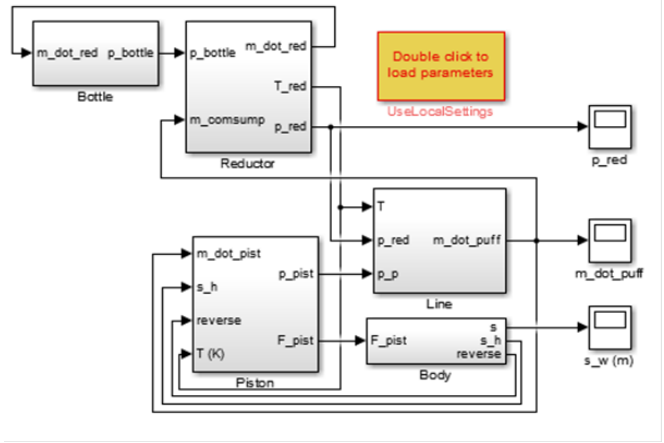

Fig 2.The 2018 modell

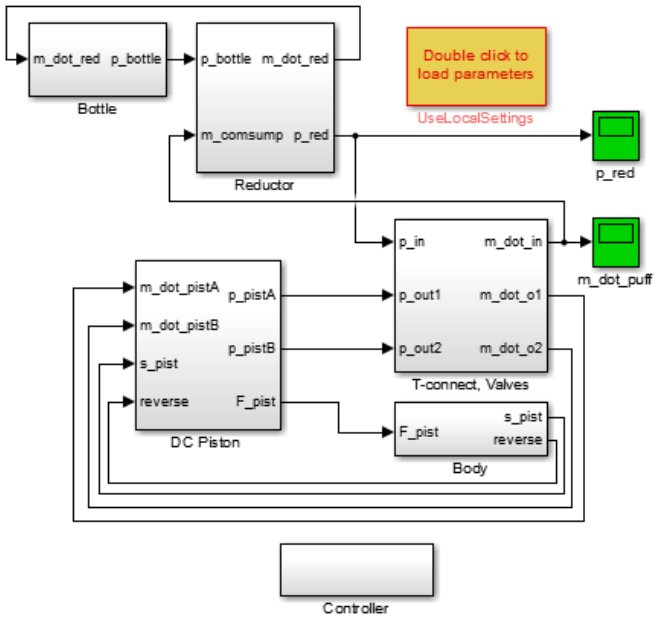

Fig 3.The new, 2019 modell

The bottle modell has not changes significantly. the Fig 3 presents the colour codes of inputs, outputs, constants and scopes.

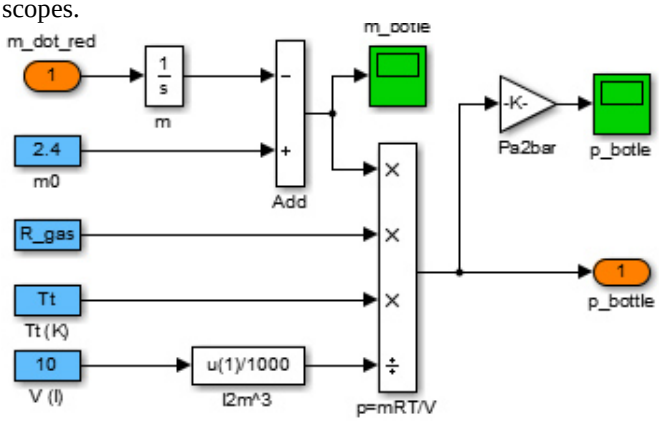

Fig 4.The bottle modell

In the new model the body mass, and the reductor submodels are principally also the same, only the number of output ports are reduced by making the different variables global variables.

The bottle, body and reductor models are described in the ACIPV 2018 Conference paper. (Szakács, 2018)

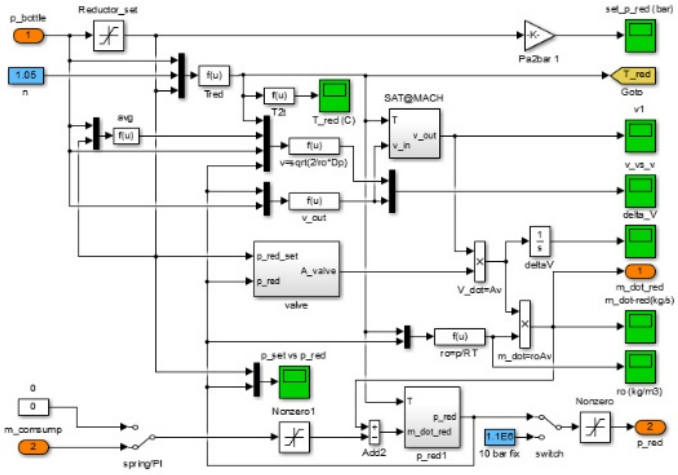

Fig 5.The new reductor modell

Significant changes has been made in the piston model. The 2018 model included a piston model with one chamber modelled both chambers of the piston. Simulating the piston reversing was solved by resetting the piston chamber mass integrator, like if the chamber pressure was released without transient.

This method is a great simplification of reality, which did not allow exhaust transient, and reverse chamber pre-charging modelling for power model.

During test measuring result analysis it became obvious that there is a need of developing a two-chamber piston model in order to gain accurate measuring results

The 2018, one chamber piston model is shown on fig 5, the new, two-chamber modell is on Fig 6.

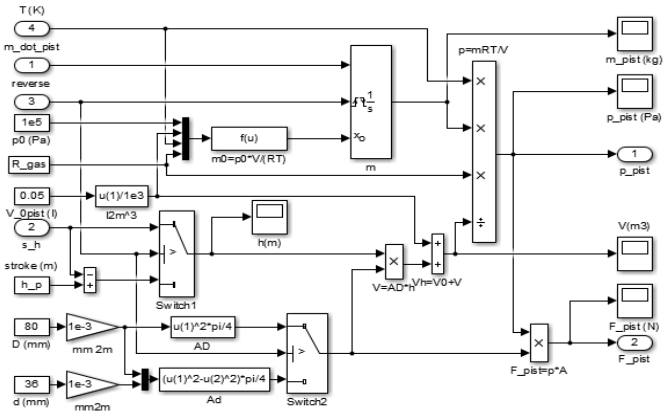

Fig 6.The 2018, one chamber piston modell

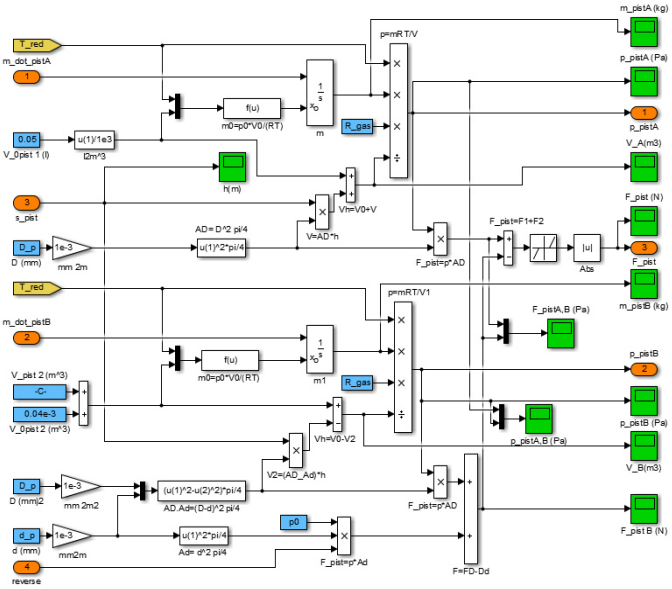

Fig 7.The new, dual chamber piston modell

The two-chamber piston required to develop a T-junction model, because the air had to divide in between the chambers.

The model is virtually duplication of the one chamber model, with common force calculation on the piston rod.

The chambers are alternatively connected to the supply air, or the environment. One chamber is filled, the other is exhausting. To control which one is filled and which is exhausting the pressure there was need to develop directional control valves.

The controller modell in this phase is controlling the ECO expansion during long distance run. The piston direction control signal is calculated in the body submodell. At this state there is no pre-chare control on the engine.

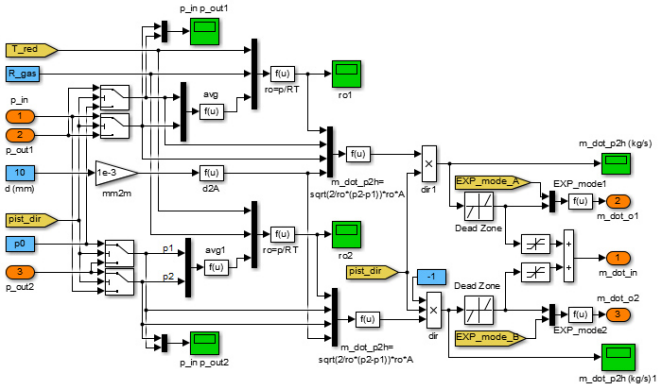

Fig 8.Valves, and T-junction modell

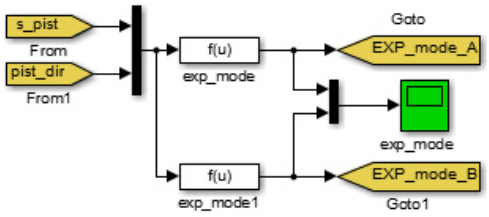

Fig 9.The controller modell

The controller is not connected to the other blocks of the model by data line, which represent that the electric steering does not mix pneumatic, or mechanic lines.

In the long term the controller will be replaced by the controller algorithm to be programmed in the vehicle, and even further goal is to use hardware in the loop modelling using the embedded controller.

3. VALIDATION

Validation measurements carried out in order to gain information about piston chamber pressures. And piston speed during a straight run, on a measuring track.

A car setting of 8 bars system pressure, and 30% expansion mode has been selected (Heisz,2017). The chamber pressures and piston position were recorded.

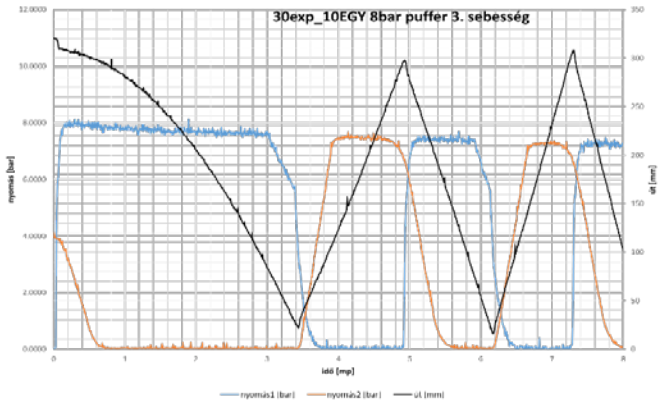

Fig 10.Measuring results

The results are shown on Fig 9.

Having the same parameters set on the model, there was a simulation run. the simulation results of the two channel pressures are shown in Fig. 11.

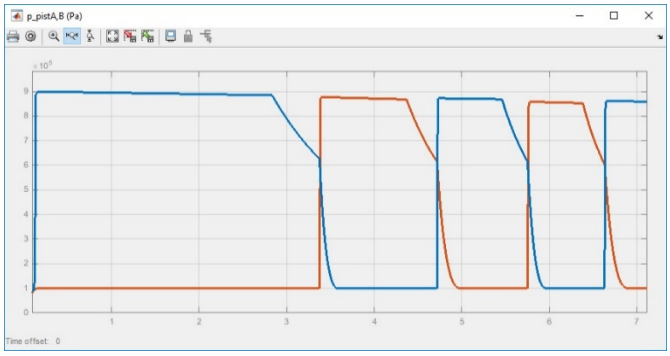

Fig 11.Simulated piston chamber pressures

The test measuring results include piston rod displacement too, which simulation counterpart is shown in Fig. 12

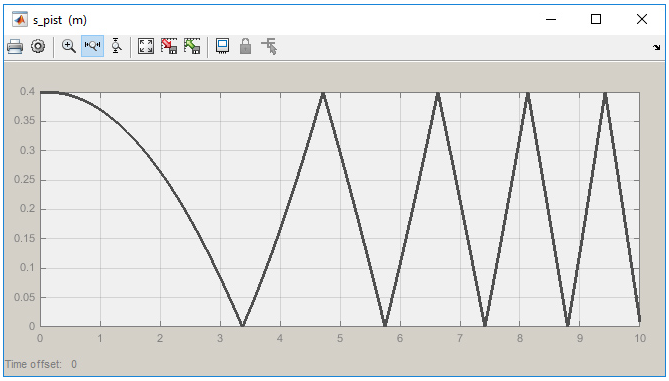

Fig 12.Piston stroke during simulation

The simulation results show a very good match with the measuring results. Comparing Fig 10, and 9, it can be seen that the pressure drop during motion of the cylinder, the near adiabatic expansion of the enclosed gas during ECO mode, the exhaust transient of the released gas all show the same tendency as measured.

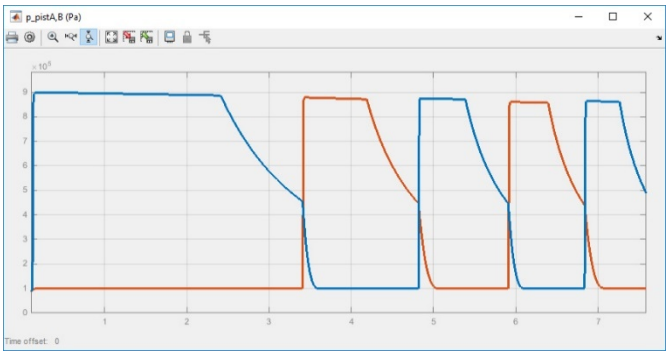

Fig 13.Simulated piston chamber pressures at 50% expansion

The main differences between simulated, and measured is the chamber A (orange line on Fig 10) has a time offset, compared to chamber B (blue line.) It seems like there is a delay in the system either because of the valve timing, or theoretical failure in the controller.

Further simulations:

After the validation further simulations has been run in order to investigate expansion modes. Different expansion percentages were set. The 80% expansion mode expanded till one bar relative pressure, which appeared the maximum expansion. The 90% expansion resulted stall in piston stroke.

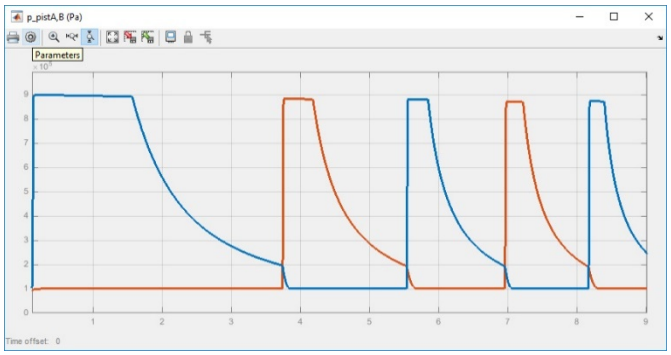

Fig 14.Simulated piston chamber pressures at 80% expansion

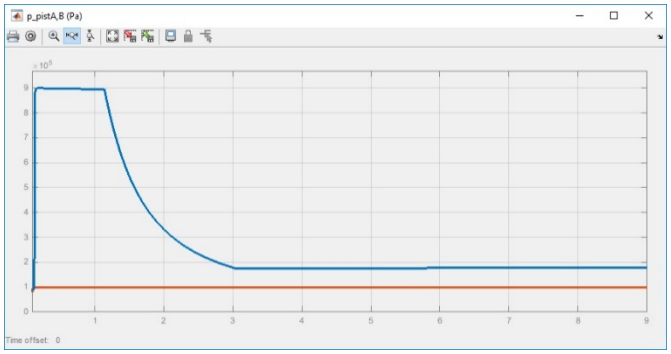

Fig 15.Simulated piston chamber pressures at 90% expansion

4. CONCLUSION

The pneumatic model after the modifications made from 2018 version to 2019 is capable to help working out engine control unit, furthermore test, and compare different power, and ECO theories. By comparing expected behavior, and measuring results system level anomalies can be detected, and corrected, like the pressure shift anomaly in the forward channel of the piston.

Further development can be the integration of the control software, and hardware in the loop simulation of the embedded control system of the physical car.

REFERENCES

Szakács, T: Pneumatic modelling of a pneumobil In: Pokorádi, László (editor.) Proceedings of the 2nd Agria Conference on Innovative Pneumatic Vehicles ACIPV 2018 Eger, Hungary : Óbudai Egyetem, (2018) pp.25-30. , 6 p.

Heisz P. Thesis work Óbudai Egyetem, (2017)

Drive Alternatives. Is the Future Surely in the Electric Drive?

István Tibor TÓTH

University of Szeged, Faculty of Engineering, Technisal Department
Szeged, Hungary (Tel: +36209585580; e-mail: istvan.tibor.toth@gmail.com)

Abstract: My view is that, unfortunately, there are a lot of biased, somewhat preconceptual “analyzes” exist and are born on the subject electric vehicle. The calculations of these theories also carrying the burden of show significant shortcomings, and whilst has some with their partial truths they are capable of misleading, confusing, or guiding those who are receptive to it. It is more convenient and unfortunately, in many cases seems to be sufficient, to use a well-known, or popular used, trendy reference instead of meaningful critical evaluation and thought. My goal is not to persuade and to direct the direction, rather to the extent of the uncertainty needed, to encourage reflection, to try to examine those of the subject matter, which is becoming more and more fashionable in our age. This is also served by a series of questions and conclusions which expressed in the questions. More eyes see more when they open them, perhaps from the dangers and opportunities as well. That is why my interpretation deviate from the largely accepted ones, I willingly interpret the directions of development differently and make a somewhat different principle comparison than usual.

1. INTRODUCTION

Pretty trite statement, but the feeling is that history will repeat itself again today. The ongoing sales force more and newer products in the field of drive systems for vehicles as in any other field. Referring to the environment, not only looking for a more efficient system, but a so-called renewable energy sources, or green-energy drives can be developed as alternative to the classic internal combustion engine.

As I see, factors that primarily affect the development of drive systems are mostly non-technical. As a drive system I understood a full range of conventional internal combustion engines and all the alternative-powered drives alike. This variety, backgrounds of interests, policies etc. and guidelines, guarantees the complexity of definition, but classifying can help at least discover new perspectives.

2. THE LACONIC, IRONIC, OR ICONIC RESPONSE TO INFLUENCING FACTORS IS BLUNT AND SIMPLY: **MONEY, MONEY, MONEY AND MONEY**.

1. - **Money from the side of the required expenditures**, i.e. which solution would be the cheapest, the fastest to develop, which can be realized with the lowest investment and expected production costs, which has the minimum market entry cost.

2. - **Money from the side of financing**, that is, to which other sources, subsidies, financial investors, etc. can be obtained.

3. - **Money from the revenue and profit side**, which is the most profitable in the shortest possible time, or which one can be utilized for the longest time, with the lowest cost, which has the expected maximum profit.

4. - Money from the side of the cost and expected results of creating other lucrative related, linkable product lines, real and virtual transactions. (Renewable Energy Industry, Political Benefits, Mining (Li, Co), Battery Industry, etc.)

These aspects are covered by technical, social, environmental, etc. questions only concern "converted to HUF", „strictly in monetary level" and, in fact, it is not really a condition that the created product is technically and/or otherwise useful, predictable, and indeed can be sustained over the long term.

Since neither of these factors is significantly related to the other, they may even require contradictory conditions (for example, a higher-intensity financial support may have been obtained earlier than a demonstrably non-profit-making investment than a profit-oriented one), so the output is uncertain for external viewer. In addition, they would require an economics approach to their answers, which we know produces only partially clear results if they give us a useful result, which is acknowledged, confirmed by time.

Let's look at the "surely" part of the title question from an engineering point of view.

3. OPTIMIZING THE USE OF MOTION ENERGY.

What are the loss elements that can be reduced, avoided, utilized or reversed?
In the case of Internal Combustion Engines (ICE), to reduce efficiency, reduce friction, heat, hydraulic, pneumatic and mechanical inertia losses, improve fuel and air mixture trimming, improve combustion, and secondary heat recovery still bring significant progress. This is confirmed by the fact that several street gasoline constructions have exceeded the thermal efficiency of 40%, while the Formula 1 witch kitchen has higher than 50% thermal efficiency, and there are still

some ideas about the efficiency of the adiabatic motor above them. At the same time, even with the best thermal efficiency, the ICE will not be able to recover, to recycling the produced, but for some reason it became unnecessary motion energy. To do this, the energy stream must be equipped with a step that enables the system to absorb, store and re-use energy.

Hybrid technologies have appeared in mechanical, electrical and hydro-pneumatic versions. A new horizon of development opportunities has been opened.

It is worth thinking, calculating a little, how much we can win with the improvements. Of course, here you have to separate the benefits of the emission environment, which are not necessarily clear at system level, which could also be discussed, interpreted in detail, but in another article.

Losses from friction, rolling, air resistance, deformation can only be reduced, but cannot be recovered according to the current technical and scientific interpretation.

Heat loss, in addition to being reduced, can be partially utilized, recovered under certain conditions. For example at lower outdoor temperatures it can be used for heating, saving the energy of a separate heater, and is also suitable for pre-heating the fuel and for reaching the operating temperature faster. However, the heat recovery process has not yet developed in the heat, vehicles have not yet been used for cooling their different heat-losses, such as in trigeneration systems, which have the cause. Due to limited conditions (temperature differences and location of heat sources), in spite of the great heat loss only a small part can be utilized.

The true recuperative energy source is the kinetic and potential energy of the vehicle. Optimally 0% can be recovered, because even if it seems contradictory, the optimum is if there is no need to brake, we can roll out and there are no geological differences. At the other end, in a hurrying driving style, but still in a flat plane, braking energy as a source of recuperation can approach the level of energy used for acceleration, depending on the length of the section and average speed, even 80-90% of the total energy could be spent.

Because of such promising cases, attention was paid to recuperation systems. The first recuperative vehicles were in operation already in the 1880s. There were also electric (1886 the Sprague Electric Railway & Motor Company [1]) and pneumatic drives (between 1892 and 1900 the improved Hardie Compressed Air Locomotive [2]).

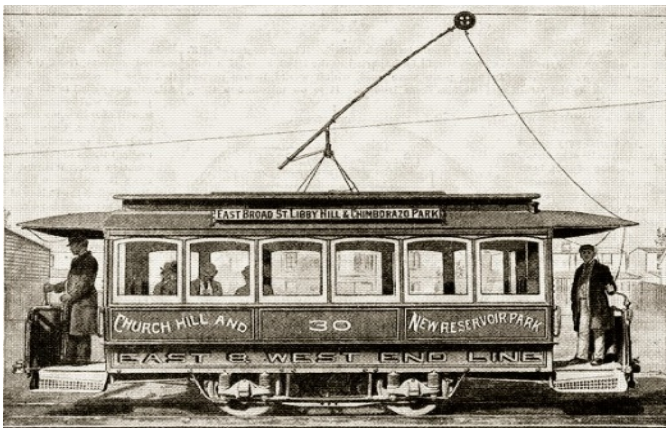

Fig. 1. One of Sprague's original electric street cars on the Richmond Union Passenger Railway, 1888. [https://spellerweb.net]

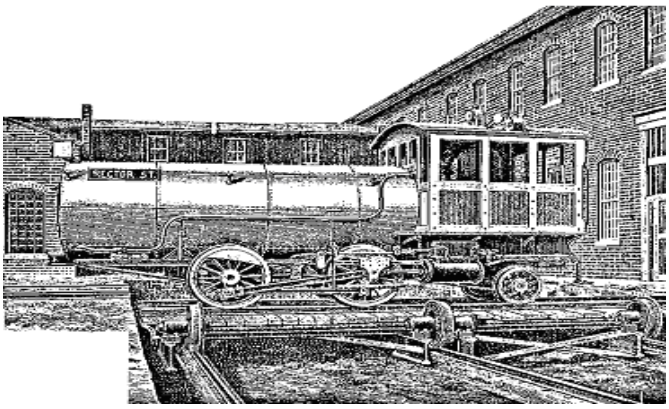

Fig. 2. Side view of a Hardie locomotive, 1897. [www.douglas-self.com]

Metropolitan public transport is the most typical scene of this type of operation. Scheduling times, stops, and intersections are driving down slowdowns and accelerations, moreover, within a full working time, up to 200 km per day per vehicle.

That's why it seems like a legitimate one wondering question: - How can Toyota have been producing hybrid passenger cars for more than 20 years now, and in public transport that is much more interested in this theory, have attempts been made again in the last decade, and active developments are just 7-8 years old?

With the emergence of power electronics in the trams, technology and tools were available since the 1990s, such as Tatra T6A2 in Szeged, but due to network conditions and other factors, the resulting savings and related results did not reach the stimulus threshold of the influencers and the general public.

Fig. 3. Tatra T6A2 capable of recuperation.
http://szkt.hu/jarmuveink#villamosok 2016.10.

In the case of a fleet operated from a given power supply network, the automatic or self-conducting mode, which is also gaining strength today, could be extremely effective. If vehicles on the network are slowed down and accelerated in line with each other, then recuperated energy can be utilized to the maximum, almost only with recuperation and transit losses. However, this requires a "very smart" system and drive control, which is the first to appear with large capital manufacturers, such as the Volvo, Mercedes, BMW fleet control concepts, which take into account the location, speed, expected destination of the other participants in the traffic, the horizontal and vertical path of the roads, quality, congestion and most of the factors affecting movement. This is also a topic worth to examine.

4. THE MECHANICAL HYBRID.

The idea of the KERS (Kinetic Energy Recovery System) is based on the principle of motion energy stored in the flywheel $E = 1/2mv^2$. The available energy density can be up to 120 Wh / kg, which is competitive with modern lithium ion batteries, in addition, it is very fast to pick up and release energy. It was also used in the Formula 1 with an electric storage, but there was also an example of purely mechanical KERS in cars.

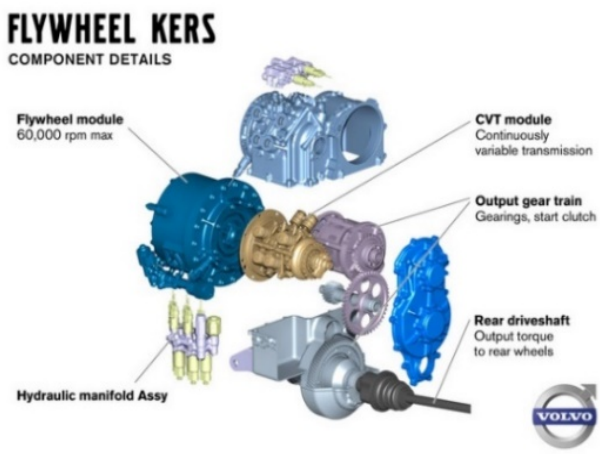

Fig. 4. Flywheel KERS.
http://totalcar.hu/magazin/hirek/2013/04/27/lendkerekes_hajtason_dolgozik_a_volvo/

5. THE HYDRO-PNEUMATIC AND PNEUMATIC HYBRID.

The compressed air hybrid system is, in principle, simpler, cheaper and lighter than an electric hybrid, but because of the calculated losses under 500,000 pieces per year, the manufacturer PSA put it on ice. [3]

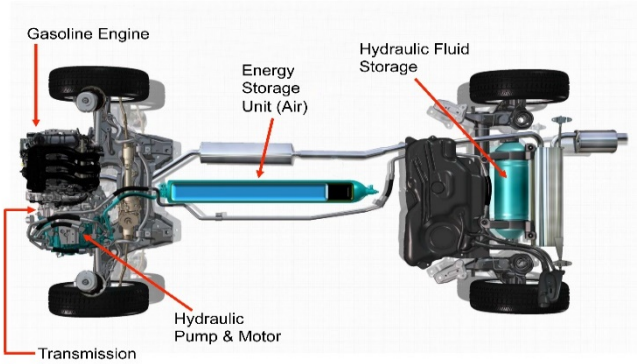

Fig. 5. The PSA Hybrid Air. 2013. [carknack.net/wordpress]

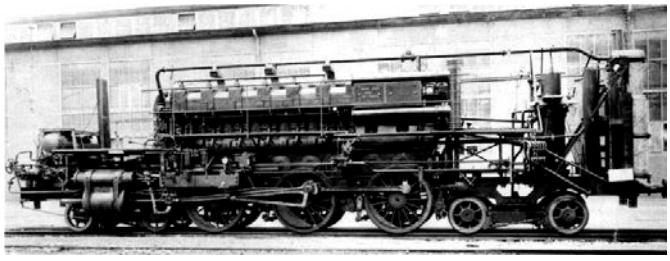

Fig. 6. The internals of the V3201
[http://www.aqpl43.dsl.pipex.com/MUSEUM/LOCOLOCO/diesair/diesair.htm]

But already in 1930, the last developments in the German Diesel-Pneumatic Hybrid Locomotive said about a 1,200 horsepower diesel and compressed-air powered hybrid

locomotive V3201 (Fig. 6.). The diesel engine driven compressor supplied the necessary air to the pneumatic drive system and the heat loss of the diesel engine was used to reach 26% efficiency emprovement.

In addition to the primary direction were more interesting ideas. Like the compressed-air energy storage bicycle from 1902 (Fig. 5.), a kind of hybrid. The primer drive by pedal got help from a compressed-air motor. The ten-cylinder compressor built into the rear wheel pumped up the reservoir under the top tube.

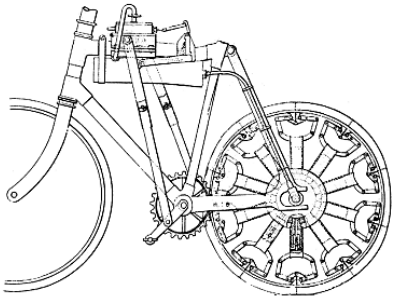

Fig. 7. Compressed-air energy-storage bicycle [http://www.aqpl43.dsl.pipex.com/MUSEUM/TRANSPORT/oddbike/oddbike.htm]

In 1926 Lee Barton Williams from Pittsburg claimed a car started on gasoline and after 10 mph it switched to compressed air only.

If we believe in the contemporary newspaper article, it was really competitive in the air motor: “A side view of the compressed air car, showing the four fuel tanks which will drive the car 500 miles at a speed of 35 miles an hour. The engine requires no cooling system, no ignition system, no carburator, nor the hundreds of moving parts included in a standard gasoline motor.” (Fig. 8.)

In 1980s invented by Oskar H.W. Coester, and developed by Aeromovel Global Corp. the continuously supplied air driving technology. The reinterpretation of the engine gave a new particular solution. (Fig. 9)

Fig. 8. Compressed air car from Los Angeles [www.automostory.com]

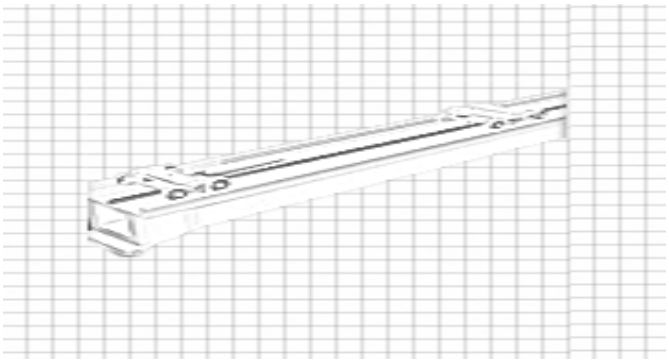

Fig. 9. The principle of “Aeromovel drive”

The Jakarta case has a 3135 m long simple loop line served by 3 vehicles, 288 passengers each. The maximum speed is 70 km/h and the average energy consumption is the today’s most fuel efficient electric vehicles of a similar level, 2,93 kWh/vehicle-km according to the company’s website. [www.aeromovel.com.br]

6. THE ELECTRIC HYBRID.

The pioneers of modern hybrid history is Toyota and Honda, but in fact, only Toyota has produced serious amount (>4 million Prius and 6 million of others in 20 years). We can also say that, as a precursor to modern electric drive, due to shortcomings in energy storage, it is the most viable tool for improving efficiency. These vehicles can take longer distances, these are less or not tied to the electrical service infrastructure and can now meet the expected expectations with a proven long life. In addition, it can be sold with profit.

7. PURELY ELECTRICALLY POWERED VEHICLES.

It is a construction that has been proclaimed, has a long history, but has suffered a great loss in history. In 1828, Hungarian Ányos Jedlik built the first electric motor and in

1830 the first electric powered carriage was in operation. In 1899, the first 100 km / h car was driven by an electric drive. In 1900, 1575 of the 4192 cars produced in the US were electric by 1681 steam cars and 936 petrol engines. [4] In 1912, the number of electric cars operated reached a peak of 30,000 and invented the starter, which drew so much into the spread of internal combustion engines that "by the mid-1930s, cars powered by electricity actually disappeared from the ground". [5] Until the 1970s, only minor attempts were made, when the recent oil crisis shook the development of electric road vehicles, but the real revival only in the XXI. century.

Partly parallel is the life of the electric train, the tramway and the trolleybus, but due to its network nature and as public transport, it is perhaps less, though sometimes even more volatile. The main thing is that they could have enjoyed their renaissance in our time.

As history has shown, it must be separated the operated from the network and self-propelled, autonomous vehicles, although in recent years more people are working to find the two structures to interact with each other to share the benefits of both systems. The question arises as to whether the advantages can only be shared without disadvantages? Separation occurs basically in operating voltage and range, but can be considered the device and energy supply, as well as other infrastructure investment, sustainment, maintenance and replacement costs, requirements, usable volume and load capacity, traffic flexibility, touch protection, availability capability, efficiency, recovery utilization, and other operating restrictions.

The initial advancement of the autonomous electric drive was hampered by the expansion of other alternatives to it and by the constraints of energy storage almost a hundred years ago.Then the batteries were heavy, the range was short and it took too long to recharge. What about now?
Now, batteries are heavy, the range is short, and recharging takes a lot of time. In addition, too complex control (BMS) and temperature control are needed, the price of the battery is a significant item in the price of the vehicle and its life expectancy is uncertain.

The development of battery technology is unquestionable, but the fundamental problems seem to have not changed in the past century. The energy density achieved and available in the foreseeable future for commonly used lithium-based batteries is also several lever lower than fossil fuels have.

8. COMPARISON AND EVALUATION.

Calculating the total weight of the accupack, taking into account the cooling-heating and other auxiliary components required for operation, it is now good to have an energy density of 120 Wh/kg, while diesel fuel/petrol with the same conditions has 8-9000 Wh/kg. Of course, the efficiency of use should also be taken into account so that the comparison is adequate.

Because real, measured consumption values are available, instead of theory, the real Wh/km values should be compared in the comparison. I could also say that based on my own measurements - but I could quote here countless published metrics on the consumption of electric and diesel cars. According to publicly available data, electric cars with lower power consumption are 100-150 Wh/km, and similar-scale diesel engines show consumption of 4-5 l/100km (388-486 Wh/km). For higher performance vehicles, this value is 180-230 Wh/km and 7-10 l/100km (680-972 Wh/km). This means that the specific energy consumption of an electric car is roughly four times lower than that of diesel, while the difference in the energy density of 'fuel' is eighty-fold. 4 versus 80, i.e. twenty times the weight for the same range energy carrier in an electric car like a diesel. However, this still does not cover the reality, because the full discharge of the lithium battery can significantly reduce its lifetime, so usually depending on the manufacturer automatically in advance with software delineates 20-50% of the capacity, which means an additional 25-100% by weight. Diesel does not need this gold reserve, but if we leave 1 liter in the 60-liter tank, there is no serious consequence.

INTERESTING FACTS AND DATA.

¤	Energy density Wh/kg	Renewable	Price¤	Infra-structure
Lead·battery	100¤	Partly¤	Irrelevant¤	Partly¤
Lithium·battery¤	140¤	Partly¤	Significant	NO¤
Metal·Hybride·battery¤	100¤	Partly¤	Irrelevant¤	Partly¤
Hydro-pneumatic	600-···1200	YES¤	Unknown¤	Partly¤
Mechanical KERS¤	120¤	YES¤	Unknown/Irrelevant¤	YES¤
Fossil¤	8-9000	Partly¤	Habitual¤	YES¤

¤	Specific·energy·consumption [Wh/km·(l/100km)]¤	Required reserve·[%]¤	„fuel”·mass·to·1000·km [kg](140/·8-9000)	Recharging time·[h]¶ (e·3kW-170kW)¤
Small·e-car¤	100-150¤	20-50¤	893-2143	0,58-50¤
Small·diesel	388-486¶ (4-5)¤	1-5¤	43,5-64¤	0,03-0,05¤
Bigger e-car¤	180-230¤	20-50¤	1607-·····3286¤	1,06-76,7¤
Bigger diesel	680-972¶ (7-10)¤	1-5¤	76,1-128	0,05-0,1¤

9. CONCLUSIONS

Now it seems to be winning electric drive with batteries, but I do not want to understand, why spend companies billions on admittedly unprofitable production of e-cars, when PSA did not started the seemingly competitive and ready to manufacture Hybride Air cars.

I think the changes will be even more serious, just a matter of time. It is pity that while many solutions should be taken away, not necessarily because of technical or general economic reasons.

Go for it, continue the Pneumobil development!

REFERENCES

https://en.wikipedia.org/wiki/Frank_J._Sprague (24.04.2019.)
http://www.douglas-self.com/MUSEUM/LOCOLOCO/airloco/airloco.htm#h (24.04.2019.)
http://mno.hu/autopult/egyelore-befellegzett-a-levegos-hibrideknek-1269553 (24.04.2019.)
http://factually.gizmodo.com/about-40-of-american-made-cars-in-1900-were-steam-powe-1597522738 (24.04.2019.)
http://www.alternativenergia.hu/az-elektromos-autozas-rovid-tortenete/68280 (24.04.2019.)
http://www.eliptic-project.eu/thematic-pillars (24.04.2019.)
http://www.autoblog.hu/hirek/a-fiat-14-ezer-dollart-veszit-minden-elektromos-500-ason/ (24.04.2019.)
https://sg.hu/cikkek/83328/egy-elektromos-f1-lokest-adna-az-elektromos-autoknak (24.04.2019.)
Railway Locomotives and Cars, 20. volume. Simmons-Boardman Publishing Corporation, 1846. https://books.google.hu/books?id=CFAjAQAAMAAJ&pg=PA552&lpg=PA552&dq=baron+von+rathen+system&source=bl&ots=QxIlYsLuGz&sig=R15olUZCZsw-bxLg2pNGmiZYRrk&hl=hu&sa=X&ved=0ahUKEwjosabOmdPSAhXCkSwKHWXlAzIQ6AEIGDAA#v=onepage&q=baron%20von%20rathen%20system&f=false (10.03.2017.)
http://www.aqpl43.dsl.pipex.com/MUSEUM/TRANSPORT/comprair/comprair.htm#fs (10.03.2017.)
http://www.automostory.com/first-air-car.htm (10.03.2017.)
RailroadPix.Com Railroad Photos - Homstk27.jpg http://www.railroadpix.com/rrphotos/detail/538.html (10.03.2017.)
http://www.aqpl43.dsl.pipex.com/MUSEUM/LOCOLOCO/diesair/diesair.htm (10.03.2017.)
http://www.aqpl43.dsl.pipex.com/MUSEUM/TRANSPORT/oddbike/oddbike.htm (10.03.2017.)
http://www.aeromovel.com.br/en/projeto/jakarta/ (10.03.2017.)

Graph Modelling of Pneumatic Vehicle Control System

Pokorádi, László*. Szakács, Tamás**

* Óbuda University, Institute of Mechatronics and Vehicle Engineering
H-1081 Budapest, Népszinház u. 8 (e-mail: pokoradi.laszlo@bgk.uni-obuda.hu)
** Óbuda University, Institute of Mechatronics and Vehicle Engineering
H-1081 Budapest, Népszinház u. 8 (e-mail: szakacs.tamas@bgk.uni-obuda.hu)

Abstract: Pneumatic drive is an alternative to alternative car protrusion. However pneumatic engine control requires an adequate control system to fulfill all the requirements of being powerful, and economic in the same time. Like in conventional cars, the engine control requires microcontroller control, which is handling sensors data, and controlling actuators, like pressure-, and directional control valves in many driving modes. Thanks to Aventics/Emerson pneumobile competition many ways of vehicle control systems have been developed since 2008, including mechanical, electro-pneumatic, PLC, relays, and so on. Adequate control systems are already available, for all these methods, but flexibility, and reliability issues are forcing us to use different approach of design in order to recognize component impacts, and exposion to other components. Using this method help us to identify the components, which require special attention to make robust, or developing fault tolerant control method to keep up vehicle functionality in case of component failure.

1. INTRODUCTION

The Aventics/Emerson Company is organizing the Pneumobil competition since 2008. The race cars developed to this competition has to fulfill different requirements. There are three main races which are the long-distance, the slalom, and the acceleration races. During the years the competition became tight, cars became faster, and more efficient. In order to be competitive the engine and powertrain control of the cars must be well developed, and optimized.

Different control strategies are required for the different races. The long-distance race requires a very efficient drive to utilize all the energy stored in the nitrogen bottle. The slalom track requires good handling, and driver skills, the acceleration race requires powerful engine.

The aim of this paper is to show application of an algorithm developed by Pokorádi (2018) for the investigation of control system of “Ignite” pneumobil of PowAir Óbuda University team

The remainder of this article is structured as follows: Section 2 shows the investigated control system. Section 3 presents the method to determine the connection matrices in cases of its different modes. Section 4 shows the conclusions can be deduced from the results of graph modelling and analysis of control system. Finally, the Authors summarize their work in Section 5.

2. THE CONTROL SYSTEM

For the protrusion of the engine a Ø100 mm, 400 mm stroke Aventics pneumatic piston is used (1.1) (See Fig. 8 in the Appendix)

The piston is controlled by two, electro-pneumatically controlled CD12 5/3 directional control valves (9.2) the steering of the valves is done by a Texas Instruments TM4C123G controller, and the attached power switching electronics.

The system is extended by two CD12 monostable 3/2 electric controlled directional control valves (9.1) which are responsible for the filling, and draining of the P1-es puffer tanks (4x13,38l)

The system pressure control is done, by Aventics „stepless adjustable system pressure unit” set. (15.1), which main components: one NL4-RGS, and a ED02 E/P pressure control valves.

Besides that, there is a CD04 monostable 3/2 NO/NC pneumatically controlled valve (8.1) which is responsible for the low-pressure circuit pressure and a P2 puffer tank (2l), a check valve (12.1). There are different sensors in the circuit, like 4db PE5-ös pressure (6.3), and one SM6-AL analogue linear position sensor, and reed relay position sensors (6.1).

In case of ECO driving mode, the supply air is closed in the working chamber of the piston by one set of 5/3 direction control valves, while the open other set of 5/3 valves are draining the counter-chamber. the system is equipped with

the mandatory emergency stop system, which drains the pressure from the pneumatics, and releases the piston locked position. (14.1),

There are further two electrically controlled TC08 2x3/2 NC/NC valves (9.3) to control the switching Ø16/25 pistons in the gearbox (3.1).

The steering has three basic modes for the three races. They are:

- Long-distance race (ECO mode)
- Slalom track (Normal mode)
- Acceleration race (Power mode)

Besides the three basic modes there are two additional ones: Long-distance race

- Malfunction mode and
- Emergency mode

The block diagram of the complete control system is shown on Fig 1.

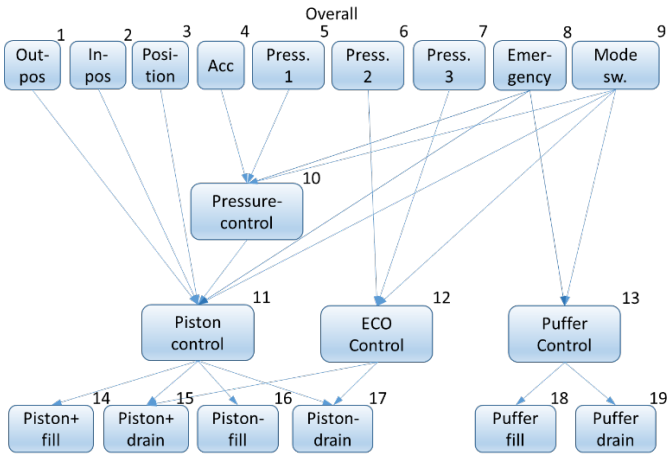

Fig 1. The overall control system

Besides the Emergency mode, the accelerator pedal potentiometer (block 4 in Fig 2-Fig 7) plays an important role in all modes. The piston position linear sensor (3) plays role in all the functions besides malfunction-, and emergency modes. The function of the rest of the blocks are described in the following chapters.

2.1 The ECO mode

The goal of the long-distance race is to achieve the maximum distance using one 10l bottle of 200bar nitrogen. In this race mode the energy content of the compressed gas must be utilized at the most efficient way, ant turned to motion energy, by maintaining at least 15km/h round speeds according to the regulations.

The mode selector switch is in ECO mode in this race. All the three pressure sensors are used. pressure 1 (5) together with the acceleration pedal (4) are determining the system pressure (10), pressure 2, and 3 (6, and 7) are controlling end-expansion pressures at stroke end positions maintained by ECO control (12).

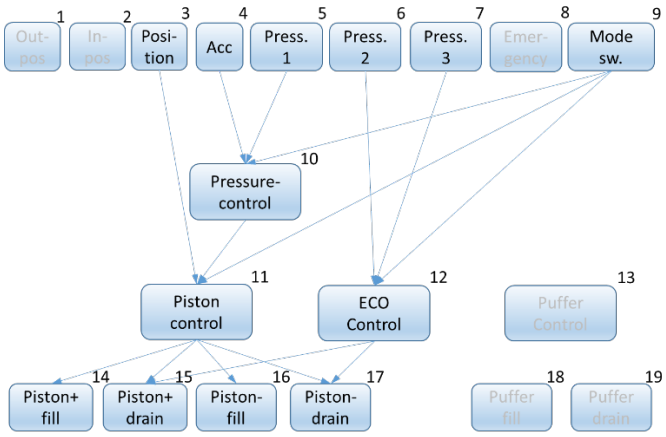

Fig 2. The ECO mode

2.2 The Normal mode

The normal model of the controller is used during the slalom race. This mode differs from the ECO mode by not using the ECO function, and the pressure 2, and 3 sensors.

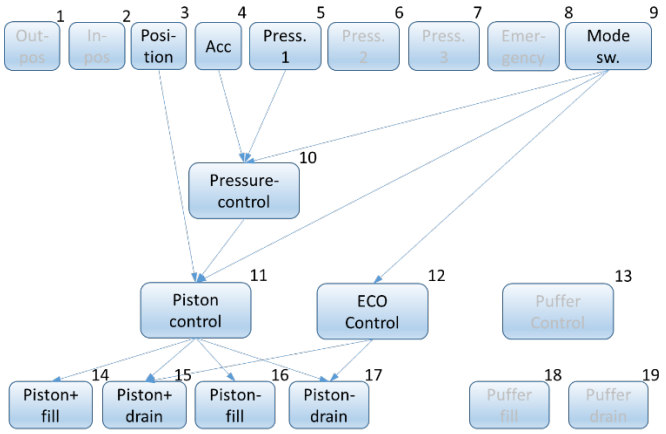

Fig 3. The Normal mode

2.3 The Power mode

In the acceleration race, the engine control is in power mode. The puffer tanks are pre-charged, and at launch till the emptying of the tanks the regulator, and the puffers are parallel supplying air to the engine, increasing the air amount and reducing pressure drop caused by the redactor choke. There is no ECO mode, and the controlling of the pistons is done by a modified algorithm. The piston opposite chambers are pre-filled, before the road reaches end-stoke position, which results faster piston reversing.

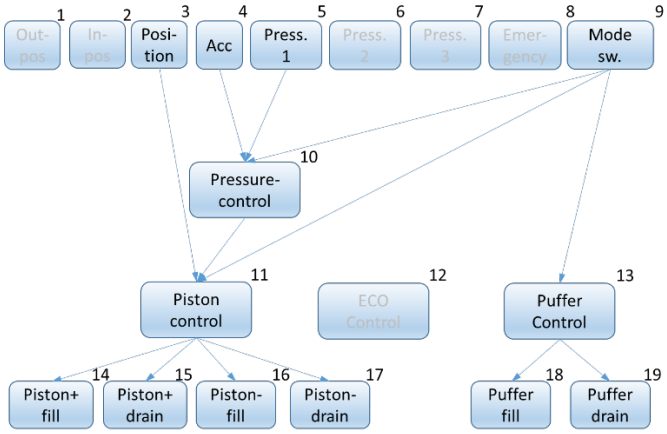

Fig 4. The Power mode

2.4 The Malfunction mode

In the malfunction mode the basic functions of the steering are maintained. The linear sensor (3) is replaced by reed piston position sensors (1, and 2). There is no pre-charge, ECO, and puffer functions. The control algorithm is on basic mode.

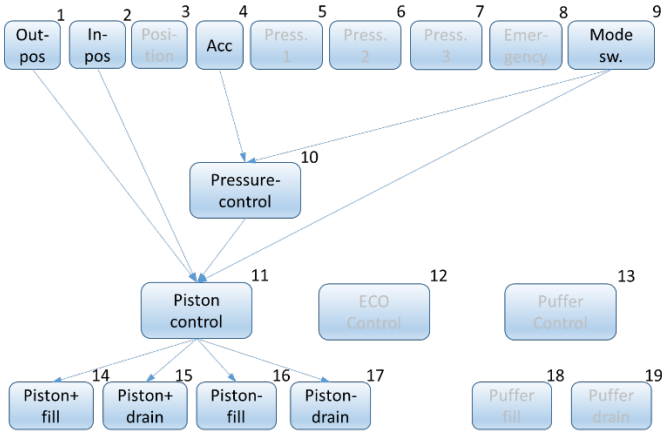

Fig 5. The Malfunction mode

2.5 The Emergency mode

When releasing the emergency button, the controller must free the piston locking, releasing the pressure in the puffers, and drain the system pressure.

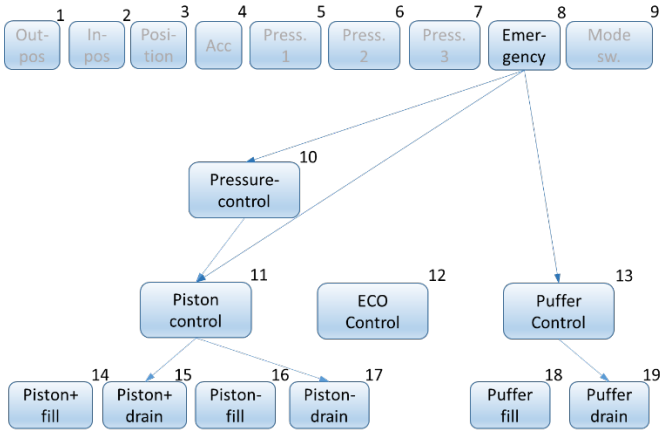

Fig 6. The Emergency mode

3. GRAHP MODELLING OF CONTROL SYSTEM

A graph $G = (N,L,f)$ is a 3-tuple consisting of a set of nodes N, a set of links L, and a mapping function $f : L \rightarrow N \times N$, which maps links into pairs of nodes. Nodes directly connected by a link are called adjacency nodes (Korn & Korn, 1974).

When the node-pair order does not matter in linking the node pair, G is an undirected graph. In an undirected graph pi ~ pj is equivalent to $p_j \sim p_i$.

A graph is a directed one, if $_{pi} \sim p_j$ is not $p_j \sim p_i$. Commuting a node pair does make a difference in the graph's topology. Links are directed, by definition, in a directed graph. A link defined by the node pair (p_j; p_i.) is not the same as a link defined by node pair (p_i; p_j). In fact, both links may exist in a directed graph.

The direct links are ignored in the graph's adjacency matrix A – which shows the number of links directly connecting node i to node j. This number is stored at row i, column j of the adjacency matrix.

The connection matrix **Z** contains a 1 in row i column j if one or more links connect node i to node j. In other words, connection matrix shows that can we get at node j from node i. For example, the connection matrix can be used for troubleshooting or to determine “sink states” of technical processes in engineering practice.

3.1. Determination of Connection Matrix

Firstly, the adjacency matrix should be determined. This task is an easy one, because considering the system the neighboring aggregates and their direct interconnection can be seen easily.

It is obvious that element of the k-th power matrix A^k of matrix **A** shows the number of independent k-long paths from node i to node j. Precise and exact mathematical proof of the proposition mentioned above can be seen in book of Pokorádi (2008).

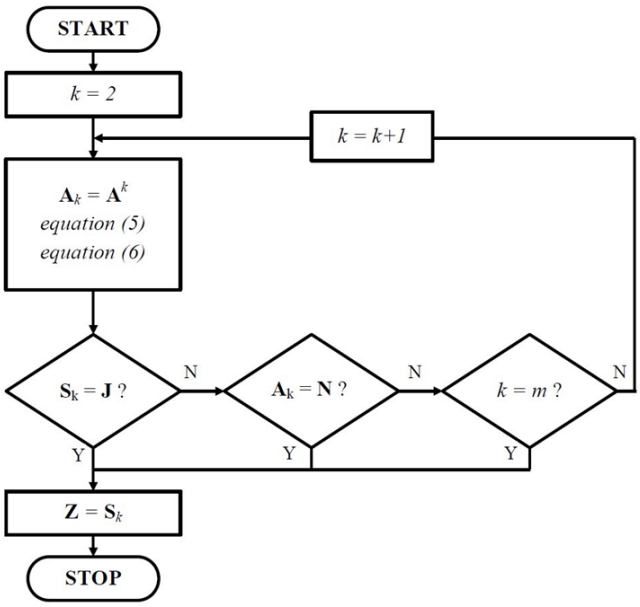

Fig 7. Block Diagram of Connection Matrix Determination

The element **H** of

$$\mathbf{H}_k = \sum_{n=1}^{k} \mathbf{A}^n \tag{1}$$

summarized the matrix of power matrices shows the number of independent, maximum *k*-long paths from node *i* to node *j*.

Let us generate signum matrix $\mathbf{S}_k$ of $\mathbf{H}_k$ using following function:

$$\mathbf{S}_k = sign\ \mathbf{H}_k \quad s_{ij}^{[k]} = sign\ h_{ij}^{[k]}\ , \tag{2}$$

where:

$$\operatorname{sign}\eta = \begin{cases} 1, & \text{if } \eta > 0 \\ 0, & \text{if } \eta = 0 \\ -1, & \text{if } \eta < 0 \end{cases}, \tag{3}$$

If

$$\mathbf{A}^k = \mathbf{N}, \tag{4}$$

where **N** is zero (null) matrix, then the length of the longest path of graph is *k - 1*.

The equality

$$\mathbf{S}_k = \mathbf{J}\ , \tag{5}$$

where **J** is matrix of ones, means that all nodes have connection with all other ones.

It is obvious too, that the longest path (circuit which connects all nodes) of graph has equal number of its nodes of graph denoted *m*.

Using the above mentioned statement and equations (6) and (7), the method of connection matrix determination can be depicted by block diagram of Fig 7

The connection matrix shows the interconnection between nodes.

The exposure vector

$$\mathbf{e} = [e_k] \quad e_k = \sum_{j=1}^{m} z_{jk} \tag{6}$$

represents the exposedness of nodes, in other words which node depend on the other ones mostly.

The impact vector

$$\mathbf{i} = [i_k] \quad i_k = \sum_{j=1}^{m} z_{kj} \tag{7}$$

shows which node(s) ha(s)ve affect to other ones in the highest degree.

Using depicted method all above mentioned pneumobil modes have been investigated. The following part of this Section the adjacency and connection matrices and exposure and impact vectors will be shown.

3.2 The ECO mode

$$\mathbf{A}_{ECO}=\begin{bmatrix}
0&0&0&0&0&0&0&0&0&0&0&0&0&0&0&0&0&0&0\\
0&0&0&0&0&0&0&0&0&0&0&0&0&0&0&0&0&0&0\\
0&0&0&0&0&0&0&0&0&0&1&0&0&0&0&0&0&0&0\\
0&0&0&0&0&0&0&0&0&1&0&0&0&0&0&0&0&0&0\\
0&0&0&0&0&0&0&0&0&1&0&0&0&0&0&0&0&0&0\\
0&0&0&0&0&0&0&0&0&0&0&1&0&0&0&0&0&0&0\\
0&0&0&0&0&0&0&0&0&0&0&1&0&0&0&0&0&0&0\\
0&0&0&0&0&0&0&0&0&0&0&0&0&0&0&0&0&0&0\\
0&0&0&0&0&0&0&0&0&1&1&1&0&0&0&0&0&0&0\\
0&0&0&0&0&0&0&0&0&0&1&0&0&0&0&0&0&0&0\\
0&0&0&0&0&0&0&0&0&0&0&0&0&0&1&1&1&1&0&0\\
0&0&0&0&0&0&0&0&0&0&0&0&0&0&0&1&0&1&0&0\\
0&0&0&0&0&0&0&0&0&0&0&0&0&0&0&0&0&0&0&0\\
0&0&0&0&0&0&0&0&0&0&0&0&0&0&0&0&0&0&0&0\\
0&0&0&0&0&0&0&0&0&0&0&0&0&0&0&0&0&0&0&0\\
0&0&0&0&0&0&0&0&0&0&0&0&0&0&0&0&0&0&0&0\\
0&0&0&0&0&0&0&0&0&0&0&0&0&0&0&0&0&0&0&0\\
0&0&0&0&0&0&0&0&0&0&0&0&0&0&0&0&0&0&0&0
\end{bmatrix}\quad(8)$$

$$\mathbf{Z}_{ECO}=\begin{bmatrix}
0&0&0&0&0&0&0&0&0&0&0&0&0&0&0&0&0&0&0\\
0&0&0&0&0&0&0&0&0&0&0&0&0&0&0&0&0&0&0\\
0&0&0&0&0&0&0&0&0&0&1&0&0&1&1&1&1&0&0\\
0&0&0&0&0&0&0&0&0&1&1&0&0&1&1&1&1&0&0\\
0&0&0&0&0&0&0&0&0&1&1&0&0&1&1&1&1&0&0\\
0&0&0&0&0&0&0&0&0&0&0&1&0&0&1&0&1&0&0\\
0&0&0&0&0&0&0&0&0&0&0&1&0&0&1&0&1&0&0\\
0&0&0&0&0&0&0&0&0&0&0&0&0&0&0&0&0&0&0\\
0&0&0&0&0&0&0&0&0&1&1&1&0&1&1&1&1&0&0\\
0&0&0&0&0&0&0&0&0&0&1&0&0&1&1&1&1&0&0\\
0&0&0&0&0&0&0&0&0&0&0&0&0&0&1&1&1&1&0&0\\
0&0&0&0&0&0&0&0&0&0&0&0&0&0&1&0&1&0&0\\
0&0&0&0&0&0&0&0&0&0&0&0&0&0&0&0&0&0&0&0\\
0&0&0&0&0&0&0&0&0&0&0&0&0&0&0&0&0&0&0&0\\
0&0&0&0&0&0&0&0&0&0&0&0&0&0&0&0&0&0&0&0\\
0&0&0&0&0&0&0&0&0&0&0&0&0&0&0&0&0&0&0&0\\
0&0&0&0&0&0&0&0&0&0&0&0&0&0&0&0&0&0&0&0\\
0&0&0&0&0&0&0&0&0&0&0&0&0&0&0&0&0&0&0&0
\end{bmatrix}\quad(9)$$

$$\mathbf{e}_{ECO}=\begin{bmatrix}0\\0\\0\\0\\0\\0\\0\\0\\0\\3\\5\\3\\0\\6\\9\\6\\9\\0\\0\end{bmatrix}\qquad \mathbf{i}_{ECO}=\begin{bmatrix}0\\0\\5\\6\\6\\3\\3\\0\\7\\5\\4\\2\\0\\0\\0\\0\\0\\0\\0\end{bmatrix}\quad(10)$$

3.3 The Normal mode

$$\mathbf{A}_{N}=\begin{bmatrix}
0&0&0&0&0&0&0&0&0&0&0&0&0&0&0&0&0&0&0\\
0&0&0&0&0&0&0&0&0&0&0&0&0&0&0&0&0&0&0\\
0&0&0&0&0&0&0&0&0&0&1&0&0&0&0&0&0&0&0\\
0&0&0&0&0&0&0&0&0&1&0&0&0&0&0&0&0&0&0\\
0&0&0&0&0&0&0&0&0&1&0&0&0&0&0&0&0&0&0\\
0&0&0&0&0&0&0&0&0&0&0&0&0&0&0&0&0&0&0\\
0&0&0&0&0&0&0&0&0&0&0&0&0&0&0&0&0&0&0\\
0&0&0&0&0&0&0&0&0&0&0&0&0&0&0&0&0&0&0\\
0&0&0&0&0&0&0&0&0&1&1&1&0&0&0&0&0&0&0\\
0&0&0&0&0&0&0&0&0&0&1&0&0&0&0&0&0&0&0\\
0&0&0&0&0&0&0&0&0&0&0&0&0&0&1&1&1&1&0&0\\
0&0&0&0&0&0&0&0&0&0&0&0&0&0&0&1&0&1&0&0\\
0&0&0&0&0&0&0&0&0&0&0&0&0&0&0&0&0&0&0&0\\
0&0&0&0&0&0&0&0&0&0&0&0&0&0&0&0&0&0&0&0\\
0&0&0&0&0&0&0&0&0&0&0&0&0&0&0&0&0&0&0&0\\
0&0&0&0&0&0&0&0&0&0&0&0&0&0&0&0&0&0&0&0\\
0&0&0&0&0&0&0&0&0&0&0&0&0&0&0&0&0&0&0&0\\
0&0&0&0&0&0&0&0&0&0&0&0&0&0&0&0&0&0&0&0
\end{bmatrix}\quad(11)$$

$$\mathbf{Z}_{N}=\begin{bmatrix}
0&0&0&0&0&0&0&0&0&0&0&0&0&0&0&0&0&0&0\\
0&0&0&0&0&0&0&0&0&0&0&0&0&0&0&0&0&0&0\\
0&0&0&0&0&0&0&0&0&0&1&0&0&1&1&1&1&0&0\\
0&0&0&0&0&0&0&0&0&1&1&0&0&1&1&1&1&0&0\\
0&0&0&0&0&0&0&0&0&1&1&0&0&1&1&1&1&0&0\\
0&0&0&0&0&0&0&0&0&0&0&0&0&0&0&0&0&0&0&0\\
0&0&0&0&0&0&0&0&0&0&0&0&0&0&0&0&0&0&0&0\\
0&0&0&0&0&0&0&0&0&0&0&0&0&0&0&0&0&0&0&0\\
0&0&0&0&0&0&0&0&0&1&1&1&0&1&1&1&1&0&0\\
0&0&0&0&0&0&0&0&0&0&1&0&0&1&1&1&1&0&0\\
0&0&0&0&0&0&0&0&0&0&0&0&0&0&1&1&1&1&0&0\\
0&0&0&0&0&0&0&0&0&0&0&0&0&0&1&0&1&0&0\\
0&0&0&0&0&0&0&0&0&0&0&0&0&0&0&0&0&0&0&0\\
0&0&0&0&0&0&0&0&0&0&0&0&0&0&0&0&0&0&0&0\\
0&0&0&0&0&0&0&0&0&0&0&0&0&0&0&0&0&0&0&0\\
0&0&0&0&0&0&0&0&0&0&0&0&0&0&0&0&0&0&0&0\\
0&0&0&0&0&0&0&0&0&0&0&0&0&0&0&0&0&0&0&0\\
0&0&0&0&0&0&0&0&0&0&0&0&0&0&0&0&0&0&0&0
\end{bmatrix}\quad(12)$$

$$\mathbf{e}_{N}=\begin{bmatrix}0\\0\\0\\0\\0\\0\\0\\0\\0\\3\\5\\1\\0\\6\\6\\6\\6\\0\\0\end{bmatrix}\qquad \mathbf{i}_{N}=\begin{bmatrix}0\\0\\5\\6\\6\\0\\0\\0\\7\\5\\4\\0\\0\\0\\0\\0\\0\\0\\0\end{bmatrix}\quad(13)$$

3.4 The Power mode

$$\mathbf{A}_P = \begin{bmatrix}
0&0&0&0&0&0&0&0&0&0&0&0&0&0&0&0&0&0&0&0\\
0&0&0&0&0&0&0&0&0&0&0&0&0&0&0&0&0&0&0&0\\
0&0&0&0&0&0&0&0&0&0&1&0&0&0&0&0&0&0&0&0\\
0&0&0&0&0&0&0&0&0&1&0&0&0&0&0&0&0&0&0&0\\
0&0&0&0&0&0&0&0&0&1&0&0&0&0&0&0&0&0&0&0\\
0&0&0&0&0&0&0&0&0&0&0&0&0&0&0&0&0&0&0&0\\
0&0&0&0&0&0&0&0&0&0&0&0&0&0&0&0&0&0&0&0\\
0&0&0&0&0&0&0&0&0&0&0&0&0&0&0&0&0&0&0&0\\
0&0&0&0&0&0&0&0&0&1&1&0&0&0&0&0&0&0&0&0\\
0&0&0&0&0&0&0&0&0&0&1&0&0&0&0&0&0&0&0&0\\
0&0&0&0&0&0&0&0&0&0&0&0&0&1&1&1&1&0&0&0\\
0&0&0&0&0&0&0&0&0&0&0&0&0&0&0&0&0&0&0&0\\
0&0&0&0&0&0&0&0&0&0&0&0&0&0&0&0&0&1&1&0\\
0&0&0&0&0&0&0&0&0&0&0&0&0&0&0&0&0&0&0&0\\
0&0&0&0&0&0&0&0&0&0&0&0&0&0&0&0&0&0&0&0\\
0&0&0&0&0&0&0&0&0&0&0&0&0&0&0&0&0&0&0&0\\
0&0&0&0&0&0&0&0&0&0&0&0&0&0&0&0&0&0&0&0\\
0&0&0&0&0&0&0&0&0&0&0&0&0&0&0&0&0&0&0&0
\end{bmatrix} \quad (14)$$

$$\mathbf{Z}_P = \begin{bmatrix}
0&0&0&0&0&0&0&0&0&0&0&0&0&0&0&0&0&0&0&0\\
0&0&0&0&0&0&0&0&0&0&0&0&0&0&0&0&0&0&0&0\\
0&0&0&0&0&0&0&0&0&0&1&0&0&1&1&1&1&0&0&0\\
0&0&0&0&0&0&0&0&0&1&1&0&0&1&1&1&1&0&0&0\\
0&0&0&0&0&0&0&0&0&1&1&0&0&1&1&1&1&0&0&0\\
0&0&0&0&0&0&0&0&0&0&0&0&0&0&0&0&0&0&0&0\\
0&0&0&0&0&0&0&0&0&0&0&0&0&0&0&0&0&0&0&0\\
0&0&0&0&0&0&0&0&0&0&0&0&0&0&0&0&0&0&0&0\\
0&0&0&0&0&0&0&0&0&1&1&0&1&1&1&1&1&0&0&0\\
0&0&0&0&0&0&0&0&0&0&1&0&0&1&1&1&1&0&0&0\\
0&0&0&0&0&0&0&0&0&0&0&0&0&1&1&1&1&0&0&0\\
0&0&0&0&0&0&0&0&0&0&0&0&0&0&0&0&0&0&0&0\\
0&0&0&0&0&0&0&0&0&0&0&0&0&0&0&0&0&1&1&0\\
0&0&0&0&0&0&0&0&0&0&0&0&0&0&0&0&0&0&0&0\\
0&0&0&0&0&0&0&0&0&0&0&0&0&0&0&0&0&0&0&0\\
0&0&0&0&0&0&0&0&0&0&0&0&0&0&0&0&0&0&0&0\\
0&0&0&0&0&0&0&0&0&0&0&0&0&0&0&0&0&0&0&0\\
0&0&0&0&0&0&0&0&0&0&0&0&0&0&0&0&0&0&0&0
\end{bmatrix} \quad (15)$$

$$\mathbf{e}_P = \begin{bmatrix}0\\0\\0\\0\\0\\0\\0\\0\\0\\3\\5\\0\\1\\6\\6\\6\\6\\2\\2\end{bmatrix} \qquad \mathbf{i}_P = \begin{bmatrix}0\\0\\5\\6\\6\\0\\0\\0\\9\\5\\4\\0\\2\\0\\0\\0\\0\\0\\0\\0\end{bmatrix} \quad (16)$$

3.5 The Malfunction mode

$$\mathbf{A}_m = \begin{bmatrix}
0&0&0&0&0&0&0&0&0&0&1&0&0&0&0&0&0&0&0&0\\
0&0&0&0&0&0&0&0&0&0&1&0&0&0&0&0&0&0&0&0\\
0&0&0&0&0&0&0&0&0&0&0&0&0&0&0&0&0&0&0&0\\
0&0&0&0&0&0&0&0&0&1&0&0&0&0&0&0&0&0&0&0\\
0&0&0&0&0&0&0&0&0&0&0&0&0&0&0&0&0&0&0&0\\
0&0&0&0&0&0&0&0&0&0&0&0&0&0&0&0&0&0&0&0\\
0&0&0&0&0&0&0&0&0&0&0&0&0&0&0&0&0&0&0&0\\
0&0&0&0&0&0&0&0&0&0&0&0&0&0&0&0&0&0&0&0\\
0&0&0&0&0&0&0&0&0&1&1&1&0&0&0&0&0&0&0&0\\
0&0&0&0&0&0&0&0&0&0&1&0&0&0&0&0&0&0&0&0\\
0&0&0&0&0&0&0&0&0&0&0&0&0&1&1&1&1&0&0&0\\
0&0&0&0&0&0&0&0&0&0&0&0&0&0&0&0&0&0&0&0\\
0&0&0&0&0&0&0&0&0&0&0&0&0&0&0&0&0&0&0&0\\
0&0&0&0&0&0&0&0&0&0&0&0&0&0&0&0&0&0&0&0\\
0&0&0&0&0&0&0&0&0&0&0&0&0&0&0&0&0&0&0&0\\
0&0&0&0&0&0&0&0&0&0&0&0&0&0&0&0&0&0&0&0\\
0&0&0&0&0&0&0&0&0&0&0&0&0&0&0&0&0&0&0&0\\
0&0&0&0&0&0&0&0&0&0&0&0&0&0&0&0&0&0&0&0
\end{bmatrix} \quad (17)$$

$$\mathbf{Z}_m = \begin{bmatrix}
0&0&0&0&0&0&0&0&0&0&1&0&0&1&1&1&1&0&0&0\\
0&0&0&0&0&0&0&0&0&0&1&0&0&1&1&1&1&0&0&0\\
0&0&0&0&0&0&0&0&0&0&0&0&0&0&0&0&0&0&0&0\\
0&0&0&0&0&0&0&0&0&1&1&0&0&1&1&1&1&0&0&0\\
0&0&0&0&0&0&0&0&0&0&0&0&0&0&0&0&0&0&0&0\\
0&0&0&0&0&0&0&0&0&0&0&0&0&0&0&0&0&0&0&0\\
0&0&0&0&0&0&0&0&0&0&0&0&0&0&0&0&0&0&0&0\\
0&0&0&0&0&0&0&0&0&0&0&0&0&0&0&0&0&0&0&0\\
0&0&0&0&0&0&0&0&0&1&1&1&0&1&1&1&1&0&0&0\\
0&0&0&0&0&0&0&0&0&1&0&0&1&1&1&1&1&0&0&0\\
0&0&0&0&0&0&0&0&0&0&0&0&0&1&1&1&1&0&0&0\\
0&0&0&0&0&0&0&0&0&0&0&0&0&0&0&0&0&0&0&0\\
0&0&0&0&0&0&0&0&0&0&0&0&0&0&0&0&0&0&0&0\\
0&0&0&0&0&0&0&0&0&0&0&0&0&0&0&0&0&0&0&0\\
0&0&0&0&0&0&0&0&0&0&0&0&0&0&0&0&0&0&0&0\\
0&0&0&0&0&0&0&0&0&0&0&0&0&0&0&0&0&0&0&0\\
0&0&0&0&0&0&0&0&0&0&0&0&0&0&0&0&0&0&0&0\\
0&0&0&0&0&0&0&0&0&0&0&0&0&0&0&0&0&0&0&0
\end{bmatrix} \quad (18)$$

$$\mathbf{e}_m = \begin{bmatrix}0\\0\\0\\0\\0\\0\\0\\0\\0\\2\\5\\1\\0\\6\\6\\6\\6\\0\\0\end{bmatrix} \qquad \mathbf{i}_m = \begin{bmatrix}5\\5\\0\\6\\0\\0\\0\\0\\7\\5\\4\\0\\0\\0\\0\\0\\0\\0\\0\\0\end{bmatrix} \quad (19)$$

3.6 The Emergency mode

$$\mathbf{A}_{em}=\begin{bmatrix}
0&0&0&0&0&0&0&0&0&0&0&0&0&0&0&0&0&0&0&0\\
0&0&0&0&0&0&0&0&0&0&0&0&0&0&0&0&0&0&0&0\\
0&0&0&0&0&0&0&0&0&0&0&0&0&0&0&0&0&0&0&0\\
0&0&0&0&0&0&0&0&0&0&0&0&0&0&0&0&0&0&0&0\\
0&0&0&0&0&0&0&0&0&0&0&0&0&0&0&0&0&0&0&0\\
0&0&0&0&0&0&0&0&0&0&0&0&0&0&0&0&0&0&0&0\\
0&0&0&0&0&0&0&0&0&0&0&0&0&0&0&0&0&0&0&0\\
0&0&0&0&0&0&0&0&0&1&1&0&1&0&0&0&0&0&0&0\\
0&0&0&0&0&0&0&0&0&0&0&0&0&0&0&0&0&0&0&0\\
0&0&0&0&0&0&0&0&0&0&1&0&0&0&0&0&0&0&0&0\\
0&0&0&0&0&0&0&0&0&0&0&0&0&0&1&0&1&0&0&0\\
0&0&0&0&0&0&0&0&0&0&0&0&0&0&0&0&0&0&0&0\\
0&0&0&0&0&0&0&0&0&0&0&0&0&0&0&0&0&0&0&1\\
0&0&0&0&0&0&0&0&0&0&0&0&0&0&0&0&0&0&0&0\\
0&0&0&0&0&0&0&0&0&0&0&0&0&0&0&0&0&0&0&0\\
0&0&0&0&0&0&0&0&0&0&0&0&0&0&0&0&0&0&0&0\\
0&0&0&0&0&0&0&0&0&0&0&0&0&0&0&0&0&0&0&0\\
0&0&0&0&0&0&0&0&0&0&0&0&0&0&0&0&0&0&0&0
\end{bmatrix} \quad (20)$$

$$\mathbf{Z}_{em}=\begin{bmatrix}
0&0&0&0&0&0&0&0&0&0&0&0&0&0&0&0&0&0&0&0\\
0&0&0&0&0&0&0&0&0&0&0&0&0&0&0&0&0&0&0&0\\
0&0&0&0&0&0&0&0&0&0&0&0&0&0&0&0&0&0&0&0\\
0&0&0&0&0&0&0&0&0&0&0&0&0&0&0&0&0&0&0&0\\
0&0&0&0&0&0&0&0&0&0&0&0&0&0&0&0&0&0&0&0\\
0&0&0&0&0&0&0&0&0&0&0&0&0&0&0&0&0&0&0&0\\
0&0&0&0&0&0&0&0&0&0&0&0&0&0&0&0&0&0&0&0\\
0&0&0&0&0&0&0&0&0&1&1&0&1&0&1&0&1&0&1&0\\
0&0&0&0&0&0&0&0&0&0&0&0&0&0&0&0&0&0&0&0\\
0&0&0&0&0&0&0&0&0&0&1&0&0&0&1&0&1&0&0&0\\
0&0&0&0&0&0&0&0&0&0&0&0&0&0&1&0&1&0&0&0\\
0&0&0&0&0&0&0&0&0&0&0&0&0&0&0&0&0&0&0&0\\
0&0&0&0&0&0&0&0&0&0&0&0&0&0&0&0&0&0&0&0\\
0&0&0&0&0&0&0&0&0&0&0&0&0&0&0&0&0&0&0&0\\
0&0&0&0&0&0&0&0&0&0&0&0&0&0&0&0&0&0&0&0\\
0&0&0&0&0&0&0&0&0&0&0&0&0&0&0&0&0&0&0&0\\
0&0&0&0&0&0&0&0&0&0&0&0&0&0&0&0&0&0&0&0\\
0&0&0&0&0&0&0&0&0&0&0&0&0&0&0&0&0&0&0&0
\end{bmatrix} \quad (21)$$

$$\mathbf{e}_{em}=\begin{bmatrix}0\\0\\0\\0\\0\\0\\0\\0\\0\\1\\2\\0\\1\\0\\3\\0\\3\\0\\2\end{bmatrix} \qquad \mathbf{i}_{em}=\begin{bmatrix}0\\0\\0\\0\\0\\0\\0\\0\\6\\0\\3\\2\\0\\1\\0\\0\\0\\0\\0\\0\end{bmatrix} \quad (22)$$

4. DISCUSSIONS

The following conclusions can be deduced from the results of graph model-based analysis:

The exposure vectors:

The explosion vectors are column vectors, which elements are showing the number of other elements acting on the block. The blocks numbered 1-9 shown in the overall system structure scheme (Fig 2) are having zero values, because those blocks are not depending on any of the other system elements. The explosion of the rest of the blocks are examined from function to function.

The ECO mode (ECO)

In ECO mode the greatest exposure values are 9 (blocks 15 and 17), and 6 (blocks 14, 16) these four blocks are the piston motion controlling directional valves.

In Normal (N), Power (P), and Malfunction (m) modes the greatest exposure values are 6 (blocks 14- 17). These four blocks are the piston motion controlling directional valves. Value 5 can be seen on block Nr. 11, which is the controlling of the piston directional valves. Any failure of these block resulting critical function fall-out.

The Emergency mode (em)

In Emergency mode the greatest exposure values are 3 for blocks 15, and 17 and 2 for blocks 19 and 11

The Impact vectors

The combined system function schematic block (Fig.2) it can be seen that the blocks 14-19- are not having effect on any other blocks, therefore their value are zeros.

The ECO mode (ECO)

In ECO mode the greatest impact values are 5 for block 3 (linear position sensor) and 6 for 4, and 5 blocks (acceleration pedal, and pressure sensor 1)

The Normal mode (N)

In Normal, and Power modes the greatest impact values are 6 for blocks 4 and 5 (acceleration pedal, and pressure sensor 1) and 7 for block 9, which is the control mode selector switch.

The Malfunction mode (m)

In Malfunction mode the greatest impact values are 6 for block 4 (acceleration pedal sensor) and 7 for block 9 (Program selector switch)

The Emergency mode (em)

In Emergency mode the greatest impact values are 6 for block 8, and 3 for block 10.

To deduce comprehensive conclusions the summarized exposure and impact vectors have been introduced, by

$$\begin{aligned}\mathbf{e}_{\Sigma}&=\mathbf{e}_{ECO}+\mathbf{e}_{N}+\mathbf{e}_{P}+\mathbf{e}_{m}+\mathbf{e}_{em}\\ \mathbf{i}_{\Sigma}&=\mathbf{i}_{ECO}+\mathbf{i}_{N}+\mathbf{i}_{P}+\mathbf{i}_{m}+\mathbf{i}_{em}\end{aligned}, \quad (23)$$

equations.

The summarized exposure vector, and impact vectors of investigated control system:

$$\mathbf{e}_{\Sigma} = \begin{bmatrix} 0 \\ 0 \\ 0 \\ 0 \\ 0 \\ 0 \\ 0 \\ 0 \\ 0 \\ 12 \\ 22 \\ 5 \\ 2 \\ 24 \\ 30 \\ 24 \\ 30 \\ 2 \\ 4 \end{bmatrix} \quad \mathbf{i}_{\Sigma} = \begin{bmatrix} 5 \\ 5 \\ 15 \\ 24 \\ 18 \\ 3 \\ 3 \\ 6 \\ 30 \\ 23 \\ 18 \\ 2 \\ 3 \\ 0 \\ 0 \\ 0 \\ 0 \\ 0 \\ 0 \end{bmatrix} \tag{24}$$

Out of the five modes the block 15, and 17, which are controlling the drain of the piston chambers in ECO mode have explosion value of 9, and value 6 have blocks 14-16 in all other, but emergency functions. The conclusion can be drawn that the piston motion control valves 14-17 are the most exposed blocks.

The summarized explosion vector shows that blocs 15, and 17 have a value of 30, and blocks 14, and 16 have a value of 24.

The conclusion can be drawn that the piston directional control valves are the most exposed elements in the system, the malfunction of the rest of the system elements have the greatest impact on them. The fall-out of these elements results a complete break-down of the vehicle.

Examining the summarized impact vectors, the conclusion can be drawn that the greatest impact of all the element has the block Nr. 9, which is the mode selector switch. Therefore its construction has to be robust, and the signal processing must be laid out in the way, in case of signal loss a default basic control program mas to run. In contrary to elements 14-17 its function loss does not result a complete break-down of the vehicle.

The second greatest impact numbers are elements 10, and 4 which are the pressure steering, and acceleration pedal blocks. The acceleration pedal sensor can be doubled, the pressure control function is a program code, which can be tested and debugged

5. SUMMARY

The paper showed an easy-usable algorithm to investigate the network structure systems such as control system of pneumobil. Using the proposed method it is possible to determine the connection matrix of investigated systems if its adjacency matrix is known.

During prospective scientific research related to this field of the applied mathematics and the science of engineering management, the Authors would like to develop other mathematical models and methods to investigate engineering systems such as sensor networks in automotive engineering and to investigate their uncertainties and reliability.

REFERENCES

Korn, G.A., Korn, T.M. (1975). Mathematical Handbook for Scientists and Engineers, Courier Dover Publications.

Pokorádi, L. (2008). Rendszerek és folyamatok modellezése, Campus Kiadó, Debrecen.

Pokorádi, L. (2018). Methodology of Advanced Graph Model-based Vehicle Systems' Analysis, Proc. of the IEEE 12th International Symposium on Applied Computational Intelligence and Informatics (SACI 2018), 555-560.

ACKNOWLEDGMENTS

The research presented in this paper was carried out as part of the EFOP-3.6.2-16-2017-00016 project in the framework of the New Széchenyi Plan. The completion of this project is funded by the European Union and co-financed by the European Social Fund.

APPENDIX

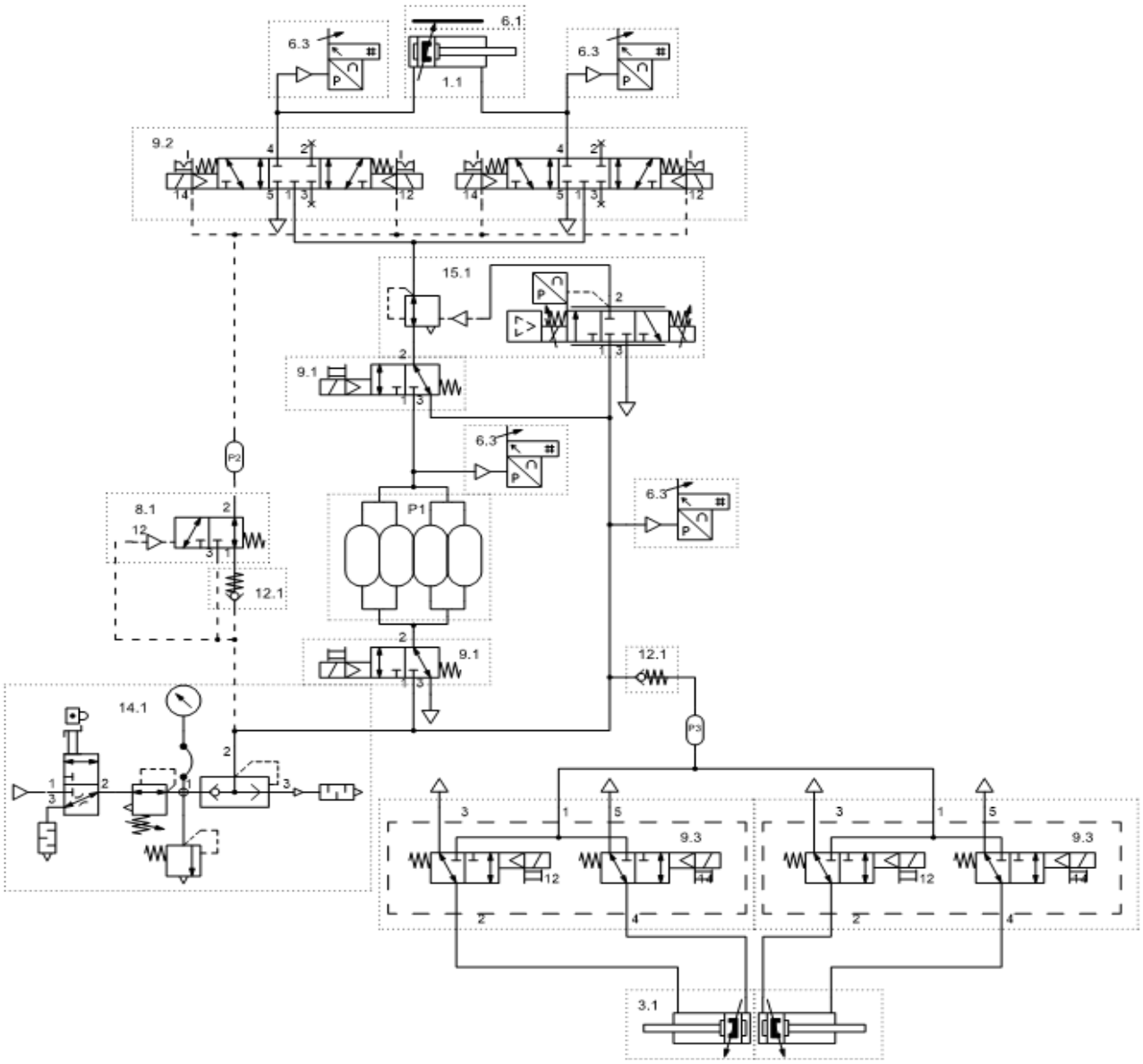

Fig. 8 Schematics of the pneumatic system.

Autonomous Possibilities of a Pneumatic Driven Vehicle

Pintér Péter*. Kurucz János**

**Óbudai Egyetem, Budapest, Népszínház utca 8, 1081 (pinter.peterm@bgk.uni-obuda.hu)*
***Óbudai Egyetem, Budapest, Népszínház utca 8, 1081(truckerhat93@gmail.com)*

This paper shows our plan to give some basic autonomous drive ability to our pneumobile which we will build for the race in the May of 2019.

1. INTRODUCTION

First of all we need to introduce some of our vehicle's parts in order to further understand the possibilities and boundaries of automation.

Or car's engine's hart is a standard ISO 15552 Aventics PRA double acting cylinder with 100mm inner diameter. The linear movement created by the cylinder we will convert into rotary with two rectifier bearings so it can drive our driven wheel.

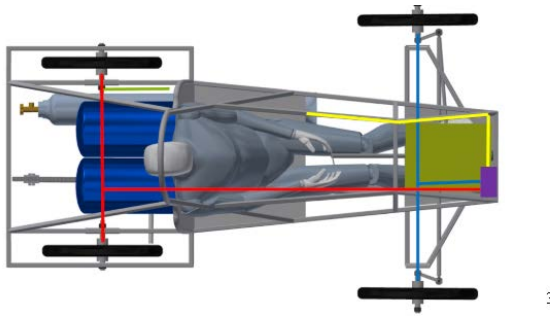

Fig. 1 Brake Circuit

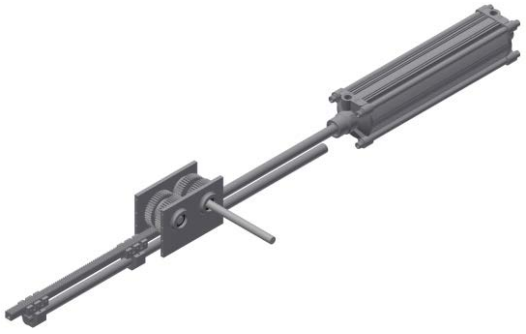

Fig. 2 Motor Unit

The double acting cylinder gets the feed pressure trough a 5/2 routing valve controlling the linear movement's direction. Before this valve we have a 5/3 valve which can close the feed and choose between the normal or puffer feed circle. The relays controlling the valves are controlled by an Arduino Mega microcontroller.

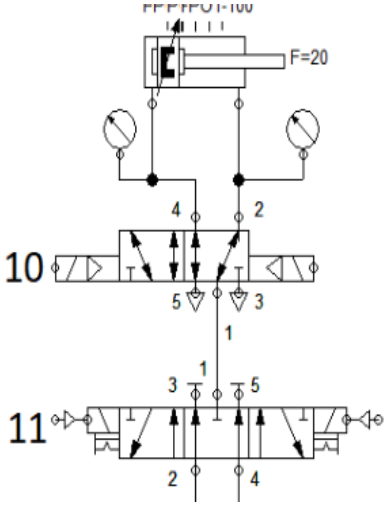

Fig. 3 Pneumatic circuit

Our braking system is from four mechanical disc brakes in two braking circle and the breaking force is created by a pedal operated by the driver.

2. MECHANICAL SYSTEM

On the engine we won't have any changes , only the feed pressure will be reduced to 4 bars in order to avoid problems from too much acceleration which could not be compensated by the later mentioned servos and to have enough time for the control system to response .

The first problem we have to solve is steering our vehicle. Normally the driver creates the steering torque trough the steering wheel. In our case we need to create this torque some other ways.

Our solution for this is a 12-24 V operating voltage 380 Kgcm toque servo motor preassembled with a gear unit and a control circuit. The motor will be placed in the original legroom of the car and it would be removable in order to be convertible between autonomous and human driver mode.

Fi. 4 Selected Servo unit

The torque generated by the motor (red in the model) will be transferred trough a 3 joint mechanism (blue in the model) to the steering mechanism. The last joint will be the original bearing of the steering column, of course this will be replaced by this alternative mechanism.

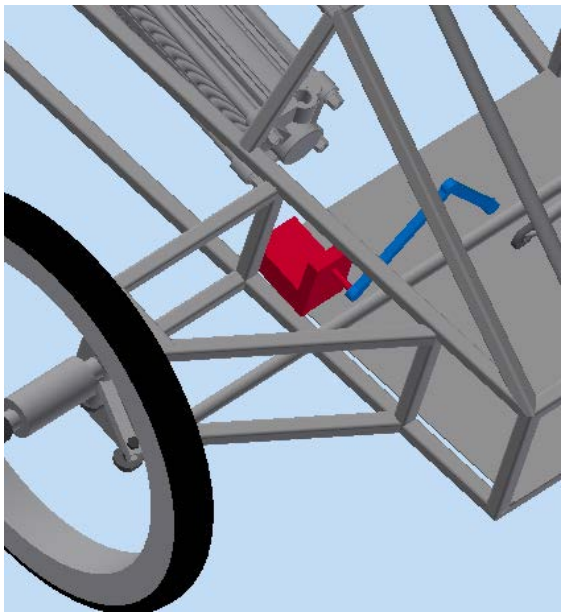

Fig. 5 Steering Servo Unit

The other problem we have to solve is the braking. Originally the driver applies the break force which will be replaced with the same motor and mechanism we used in the steering. The only change here will be that the last bearing of the mechanism will be fixed to the brake pedal. For safety the spring returning the pedal to original position will close the break circuit in original position, so if the servo won't be operable the break circuit closes and the vehicle stops.

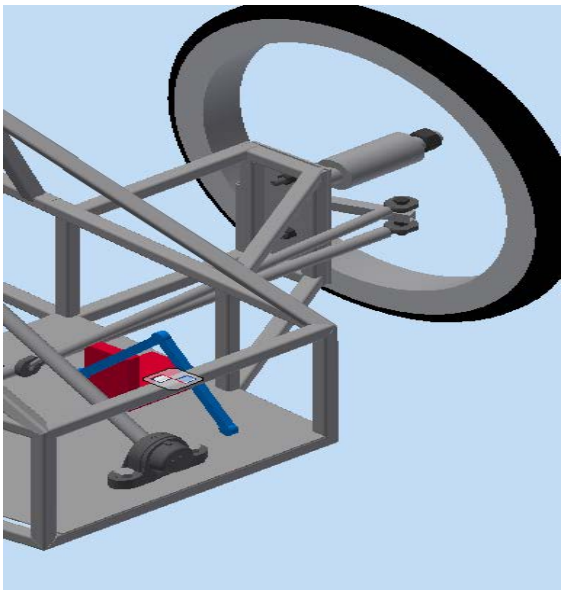

Fig. 6 Position of Brake Servo Unit

3. ELECTRICAL SYSTEM

The first change we will need in our electrical circuit is an additional 24 V battery so we could separate the steering and braking servos feed from the original control systems feed which is for the valve controlling relays. It's necessary because the high torque motors current need is much higher than the valve relays.

The servos are assembled with control units so no additional motor driver is needed. The control units will be used in pulse width modulation mode so for controlling them we will use an additional arguing Uno besides the original for the relay control.

We will use four LED/LDR pair in order to give line following abilities to our car. The resistivity change generated by the LDRs could be captured by the radio's analog inputs. The four LED/LDR pairs will be placed in a square in the front of the car. The logic behind the use of these sensors is that from black line in the floor the sensors will give feedback whether the car is on track or not.

Also we will use two ultrasound sensors in order to detect objects in front of the car. The radio's ability to use the same pins for input and output makes it possible to use only one digital pin per sensor.

Also an MMA 7455 three axis acceleration sensor in order to have acceleration data available for our decision making process.

For giving gas signal to the car the original arduino for relay control will be used with the original code, the only change will be that the gas signal sensor won't be attached to the button on the wheel where the driver can give the signal but will be replaced by a wire from the arduino responsible for autonomous control.

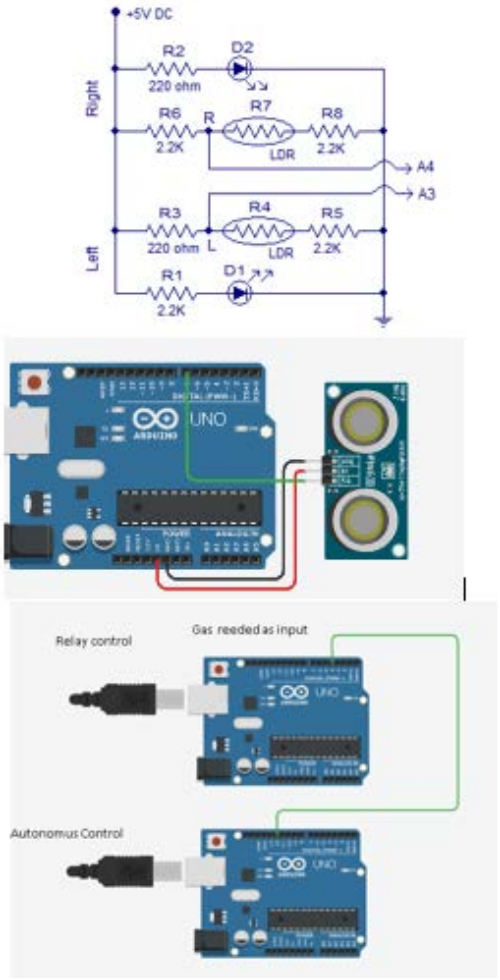

Fig. 7 LED/LDR

Also a radio module will be part of the system in order to be able to give outside user control opportunity. This is necessary for giving emergency control signals in case of an unwanted autonomous behavior and also it's very useful for testing the servo motors behavior before giving the control to the system. Of course this module will have a pair attached to another microcontroller also attached serially to a personal computer which controls it over a program. Some buttons and a joystick controller will be attached to the microcontroller in order to be able to give commands. With the help of this intervention to the control system will be available for a human user.

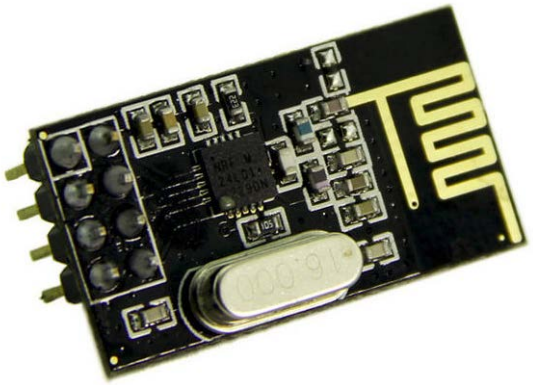

Fig. 8 Radio Module

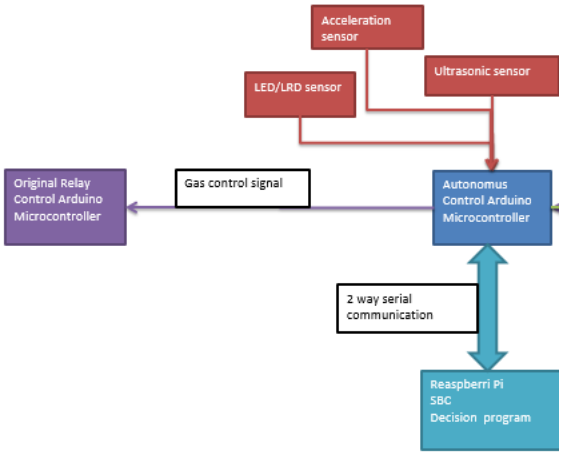

Fig. 9 System Architecture: Part1

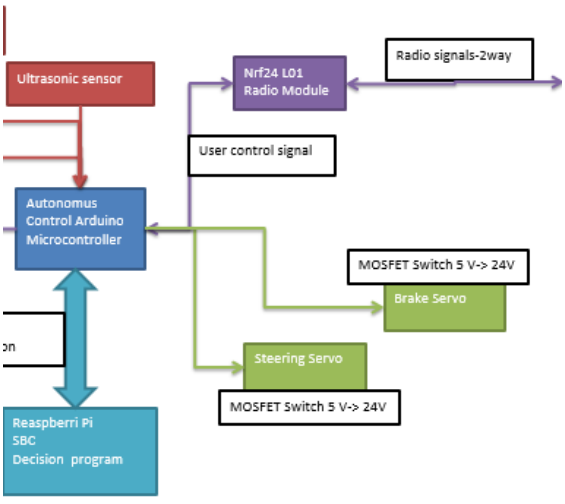

Fig. 10 System Architecture: Part2

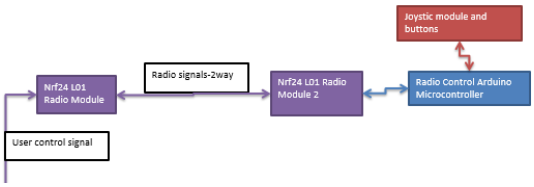

Fig. 11 System Architecture: Part3

The electrical architecture of the whole system can be observed in the pictures above.

4. CONTROL SYSTEM

The control loop would be out of two threads with some interaction between them: one responsible for the steering servo, the other responsible for the braking and gas control.

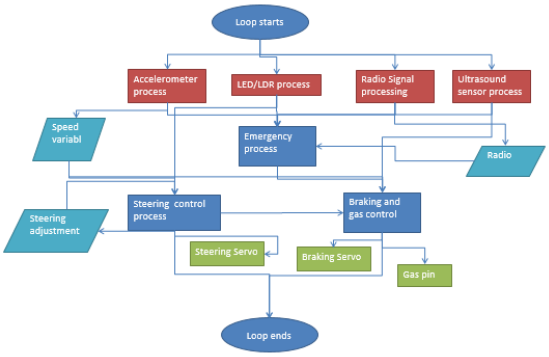

Fig. 12. Control Loop

The steering thread would start with an on track decision making process. This process takes the LED/LRD sensors as input and outputs a value which gives information about the car's position according to the line. A speed control process which takes the accelerometer as an input trough all control loops gives a value about the car's speed. The last servo position command from the previous loop will be used in a memory variable. With the help of these three preprocesses a steering adjustment control process will use these variables and makes a decision how much rotation of the servo is needed for the steering servo. Also this process gives a feedback for the servo position memory and sends the adjustment value also to the braking and gas control process.

The braking and gas control process takes the ultrasound sensor as an input variable which gives value of an object's distance before the car. The previously mentioned speed control process using the accelerometer is used as an input here also. The value of steering adjustment from the other process is used here as an input. From these inputs the program calculates the need of braking or acceleration and according to this gives command to the brake servo exclusive or the gas pin.

Of course at the cases of some events the braking control automatically activates the breaking servo at full adjustment. These events are the following: the radio module lost contact with the control radio module for more than a half second, no sensor data from the ultrasound sensors, no sensor data from the LED/LDR sensors, stop signal received through the radio module. Also if take control command is received through the radio module the autonomous control loop switches to the user control loop

The architecture of the control loop could be found on the next picture.

5. FURTHER POSSIBILITIES

This system only gives an ability to the car to follow one predefined line. To further expand it's abilities we need more sensors and control methods to take full advantage of this system.

First of all a raspberry pi single board computer (SBC) could be implemented with serial connection to the autonomous control microcontroller taking the decision making loop from it and act as the "brain" of the system. With this SBC we will be able to speed up the decision making loop much faster and some image recognition cameras could be attached too. With these abilities the computer could run artificial neural network processes gaining the ability of machine learning. The opportunities would be nearly endless, because in this way the car would not need a line drawn into the floor to follow, but it could be used to follow a route with some signs only predefined for the image processing and also could solve some traffic problems such as avoidance of objects, traffic sign recognition and so on.

The modified electronic architecture is in the picture below.

REFERENCES

[1] Edgar Sánchez-Sinencio Clifford Lau *; Artificial neural networks* ;;ISBN:0-87942-289-0

[2] *Arduino Wireless Communication* – NRF24L01 Tutorial;https://howtomechatronics.com/tutorials/arduino/arduino-wireless-communication-nrf24l01-tutorial/

[3] *Line Follower Robot using Arduino* – DIY Guide to Build Your Project; http://www.circuitstoday.com/line-follower-robot-using-arduino

[4] K Nonami,M Kartidjo, KJ Yoon, A Budiyono(2013);*Autonomus Control Systems and Veichles*, ISBN 978-4-431-54276-6